

Dear Hubertus,

We have strongly revised the manuscript by addressing all comments of the reviewers as mentioned in the online version and in the attached file.

We also have tried to take into account your comments in the best way.

As for paleoclimatic implications, we have mentioned some of them in the conclusion (yellow highlights). We would prefer not to add much more in order to avoid speculations using this approach which has still not been checked by any experimental set-ups at low temperature.

As for the dust influence, we have included a discussion as mentioned in our previous letter to you in February. A sensitivity test D has been included for showing the effect of “re-parameterizing” the activation energies after implementation of the impurity effects (Figures 7 and 8, Table 3 and associated discussion). In addition, we have detailed how a modification of the Freitag parameterization can improve the modelled $\delta^{15}\text{N}$ on the different polar sites over the last deglaciation compared to the current parameterization (Supplementary Text S2 and Figure S10).

Finally, we have noted that one reviewer finds the paper “lengthy” and we basically agree. One suggestion would be to move in the supplementary materials the section associated with sensitivity tests A, B, C and D as well as the associated Figures 7 and 8 and Table 3. This modification has not been done yet. We are waiting for your advice on this proposition.

You will find in the file “answer to reviewers” the detailed answers to all comments as well as the new manuscript and supplementary materials with modifications highlighted in yellow.

With best regards,

Camille Bréant and the co-authors.

For the text below, the color are used as follows:

- Black: original comments from reviewers
- Red: answer from authors in the online version
- Green: additional precisions for the submission of the revised manuscript

Interactive comment on “Modelling the firn thickness evolution during the last deglaciation: constrains on sensitivity to temperature and impurities” by Camille Bréant et al.

Answer to Anonymous Referee #1

Bréant et al. address an important outstanding problem in ice core research, namely the model-data mismatch of $\delta^{15}\text{N}-\text{N}_2$ as a proxy for firn thickness during the last deglaciation. They offer an interesting new solution to this problem, by proposing a temperature-dependent effective activation energy for firn sintering. In their framework, this can be understood as the effect of three separate firn densification mechanisms working in parallel, each with its own activation energy. Their modified firn densification model provides an improved fit to the deglacial $\delta^{15}\text{N}$ evolution at cold interior sites, while still being able to fit relatively warm sites that were already modeled well by existing models.

I would ask the authors to consider the following points in a revised manuscript:

We thank the reviewer 1 for his detailed comments and took them into account as detailed below.

- The $\delta^{15}\text{N}$ model-data mismatch has a long history in ice core research, and is described most clearly by Landais et al. 2006. Several solutions have been proposed for this problem. Without explicitly stating so, the present manuscript takes as the starting assumption that the temperature sensitivity of the densification model must be the problem, due to the absence of a modern analog. I'll refer to this as the “no-analog solution” to the LGM $\delta^{15}\text{N}$ problem.

I think it would be important to introduce the LGM $\delta^{15}\text{N}$ problem better, and outline some of the other proposed solutions. For example, Landais et al. (2006) concluded that reconstruction of past accumulation rates was the most likely solution.

Why was that explanation abandoned in favor of the no-analog explanation?

It is unclear to me what the main objective is of the present paper. Is the purpose to simply test whether the LGM $\delta^{15}\text{N}$ problem can be solved using a different activation energy scheme? Or is the purpose to present a new model that will replace the Goujon model in future research at LGGE? Both models fit present day data equally well, so whether the new model is an improvement relies solely on whether you believe the no-analog solution to be the correct one.

Finally, did they solve the problem? From the conclusion section it is not exactly clear whether or not the no-analog and dust mechanisms fully solve the LGM $\delta^{15}\text{N}$ problem. It seems like the dust mechanism is insufficient by itself, given that it makes sites the fit to sites like GISP2, NGRIP and WAIS Divide worse. The no-analog solution seems to do a better job, yet it requires an unknown process with very low activation energy (see below). Moreover, EDML remains confusing to me. It's warm enough during the LGM to have modern analog sites, yet it does

show the $\delta^{15}\text{N}$ model-data mismatch in traditional firn models. I would appreciate some added discussion on whether the LGM $\delta^{15}\text{N}$ problem has now been solved satisfactorily, and whether we can forget about other proposed solutions.

The purpose of this paper is to evaluate the LGGE model of firn densification by comparison with data in modern and past climate conditions, with a focus on the major problem of the too small densification rate during the glacial in East Antarctica highlighted in Capron et al. (2013) and earlier studies. We will also state more clearly in the motivation for this study (introduction) that the modelled lock-in depth and associated Δage were too large at Dome C / Vostok during the last glacial maximum with the old model.

Line 132-136: “The differences in modelled and measured $\delta^{15}\text{N}$ for glacial period in cold sites of the East-Antarctic plateau have important consequences for the Δage estimate and hence the ice core chronology: using the firn densification models, the modelled Δage for glacial period at Vostok and Dome C is too large by several centuries (Loulergue et al., 2007; Parrenin et al., 2012). “

Indeed, Landais et al. (2006) have suggested that the forcing scenario can explain the model-data mismatch for sites like Law Dome and Kohnen (still, they needed a convective zone of 10 m during the LGM at Kohnen to reconcile $\delta^{15}\text{N}$ and firn model run with the low estimate of accumulation rate) but it is not realistic to reconcile $\delta^{15}\text{N}$ and model outputs in lower accumulation rate sites like Vostok and Dome C. Such model – data discrepancy was largely discussed in Capron et al. (2013) and we wanted to go one step further.

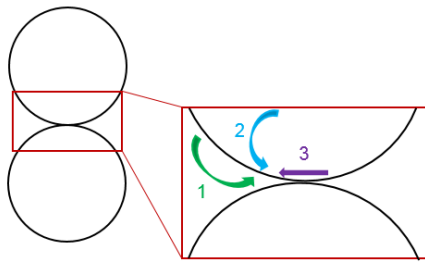
We did not perform a major revision of the model but tested the effect of relatively simple model changes (e.g. the dependence of activation energy to temperature and dust tests that can easily be adapted to other models). We agree that if the new model provides some ideas to solve the model – data mismatch at low temperature through modification of the activation energy, the problem is clearly not solved and this will be stated clearly and in a coherent manner in both conclusion and abstract. In the revised manuscript, we will thus clarify the fact that the association of three activation energies with three precise physical mechanisms is not proved.

Line 24-32 (Abstract): “We show that both the new temperature parameterization and the influence of impurities contribute to the increased agreement between modelled and measured $\delta^{15}\text{N}$ evolution during the last deglaciation at sites with low temperature and low accumulation rate, such as Dome C or Vostok. We find that a very low sensitivity of the densification rate to temperature has to be used in coldest conditions. The inclusion of impurities effects improves the agreement between modelled and measured $\delta^{15}\text{N}$ at cold East Antarctic sites during the last deglaciation, but deteriorates the agreement between modelled and measured $\delta^{15}\text{N}$ evolution in Greenland and Antarctic sites with high accumulation unless threshold effects are taken into account. “

Line 333-349: Following these arguments and despite the lack of experimental constraints to test this assumption, we propose a new parameterization of the activation energy in the LGGE firn densification model which increases the firn densification rate at low temperatures. We have thus enabled introduction of three adjusted activation energies as proposed in Table 1 and Figure 2. We have replaced the creep parameter in Equation (3) by:

$$A = A_0 \times \left(a_1 \times e^{\frac{-Q_1}{RT}} + a_2 \times e^{\frac{-Q_2}{RT}} + a_3 \times e^{\frac{-Q_3}{RT}} \right) \quad (7)$$

We have chosen a minimal number of mechanisms (3) for simplicity in the following but the conclusions of our work would not be affected by a choice of more mechanisms.



- Close to melting temperature: mass transfer by diffusion (potential mechanism for high temperature)
(1) mechanism 1 associated with activation energy Q_1
- Low temperature: lattice diffusion (classical mechanism)
(2) mechanism 2 associated with activation energy Q_2
- Very low temperature : boundary diffusion from grain boundary (potential mechanism for low temperature)
(3) mechanism 3 associated with activation energy Q_3

Figure 2: Different sintering mechanisms of snow for different temperatures proposed by analogy with the hot ceramic sintering (inspired by Figure 1 in Ashby, 1974). Note that more sintering mechanisms can be found in the literature and the attributions of 3 different mechanisms for the firn densification model is only a working hypothesis here.

Line 953-963 (conclusion): “First, laboratory or field studies of firn densification at very cold controlled conditions are needed to check the predominance of one mechanism over another at low temperature such as the predominance of the boundary diffusion over grain boundary mechanism around -60°C ; this is a real challenge because of the slow speed of deformation. Second, we have suggested that the current parameterization of impurity on firn softening should be revised, especially for very high impurity load (Greenland) using for example thresholds on impurity concentrations. Third, the separate effects of impurities and temperature on firn densification and hence $\delta^{15}\text{N}$ evolution should be tested on periods other than the last deglaciation. Sequences of events associated with non-synchronous changes in surface temperature, accumulation rate and impurity content would be particularly valuable for this objective.”

We will also introduce better the $\delta^{15}\text{N}$ problem referring to previous works (Landais et al., 2006; Capron et al., 2013; ...) and summarizing the associated results and other options to solve the problem (e.g. convective zone, thermal effect).

Line 137-153 (Introduction): “Several hypotheses have already been evoked to explain the $\delta^{15}\text{N}$ model-data mismatch in Antarctica as detailed in Landais et al. (2006), Dreyfus et al. (2010) and Capron et al. (2013). First, the firnification models have been developed and tuned for reproducing present-day density profiles and it is questionable to apply them to glacial climate conditions in Antarctica for which no present-day analogues are available. Second, increasing impurity concentration has been suggested to fasten firn densification during glacial period (Freitag et al., 2013; Hörhold et al., 2012). Third, a ~ 20 m deep convective zone has been evidenced in the megadunes region in Antarctica (Severinghaus et al., 2006) hence suggesting that deep convective zones can develop in glacial periods in Antarctica and explain the mismatch between firn densification model and $\delta^{15}\text{N}$ data (Caillon et al., 2003). This hypothesis can explain the mismatch between modelled and measured $\delta^{15}\text{N}$ at EDML during glacial period by invoking a 10 m convective zone (Landais et al., 2006). However, it has been ruled out for explaining the strong mismatch between model and $\delta^{15}\text{N}$ data at EDC for the last glacial period (Parrenin et al., 2012). Fourth, firn densification is very sensitive to changes in temperature and accumulation rate so that uncertainties in the surface climate parameters can lead to biased value of the modelled LID and hence $\delta^{15}\text{N}$. Fifth, a significant thermal fractionation signal can affect the total $\delta^{15}\text{N}$ signal. However, this hypothesis has been ruled out by Dreyfus et al. (2010) based on $\delta^{15}\text{N}$ and $\delta^{40}\text{Ar}$ data on the last deglaciation at EDC.”

In the conclusion and perspectives, we will also mention the possibility to improve the constraints on firn modeling through the use of cross-dating on new ice cores with high resolution signals as already used by Parrenin et al. (2012).

Line 974-976: “Finally, additional constraints on the firn modelling can also be obtained through the use of cross-dating on new ice core with high resolution signals as already used by Parrenin et al. (2012). »

- To get the densification rate to increase meaningfully at low temperatures, the authors have to introduce a densification process with an extremely low activation energy of $Q_3=1.5$ kJ/mol (low enough to be essentially temperature-insensitive).

They suggest this process to be surface diffusion. However, experimental studies suggest the activation energy for ice surface diffusion is on the order of 14 to 38 kJ/mol (e.g. Jung et al., doi: 10.1063/1.1770518, Nie et al., doi: 10.1103/Phys-RevLett.102.136101, and references therein). The value used by Bréant et al.

seems an order of magnitude too small to be surface diffusion. Therefore, they are essentially invoking densification by an unknown process with very small Q . The authors should acknowledge that the values they use for Q_3 seems unrealistically low. In my view, this is an important piece of evidence that the “no-analog assumption” by itself may be insufficient to solve the LGM $\delta^{15}\text{N}$ problem – the authors may not share this view.

At the other end, their high- Q process (suggested to be vapor diffusion) has a value that seems too high at $Q_1=110$ kJ/mol. Vapor diffusion scales with the vapor pressure, and the enthalpy of sublimation in ice is only 51 kJ/mol.

We thank the Referee for providing references for the activation energy of ice surface diffusion. We will include a test of a 15 kJ/mol in replacement of our previous “test C” in the revised manuscript. Using 15 kJ/mol leads to intermediate results between the “old” and “new” model results.

Test C is included in Figure 7, Figure 8 and Table 3.

Corresponding discussion in lines 825-831: “Test C has been designed so that the activation energy at low temperature corresponds to estimates of activation energy for ice surface diffusion (Jung et al., 2004; Nie et al., 2009), a mechanism that is expected to be important at low temperature (Ashby, 1974). Using such a parameterization leads to a fair agreement between the modelled and the measured $\delta^{15}\text{N}$ change over the last deglaciation for the different sites. At Dome C, the correct sign for the $\delta^{15}\text{N}$ evolution between LGM and the Holocene is predicted by the model. However, the modelled $\delta^{15}\text{N}$ increase is still too small compared to the data and the $\delta^{15}\text{N}$ calculated by the “new model”.”

Actually, the only way to reconcile our model with $\delta^{15}\text{N}$ data by invoking a change of activation energy with temperature is to have a negligible influence of temperature on the densification rate below -50°C . We agree that the values are surprisingly low for activation energy at low temperature in order to fit the $\delta^{15}\text{N}$ data. There is a clear limitation of our approach which is empirical, and cannot isolate mechanisms, but it calls for further lab and field studies. The effect of temperature could also be misrepresented in our model (and in other densification models) by other ways than the value of activation energy.

The need for experimental check is stated in the conclusion.

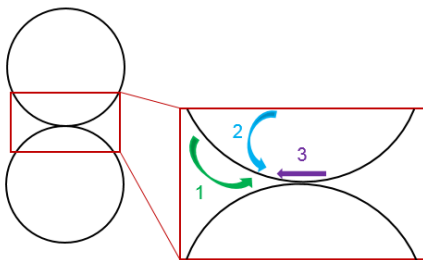
Lines 964-968: “First, laboratory or field studies of firn densification at very cold controlled conditions are needed to check the predominance of one mechanism over another at low temperature such as the predominance of the boundary diffusion over grain boundary mechanism around -60°C; this is a real challenge because of the slow speed of deformation.”

As written above, we will make clear that the association of our three activation energies with three precise physical mechanisms is not proved. Indeed, while several mechanisms have been highlighted for the densification of ice over several temperature ranges, there is no unambiguous attribution of a particular mechanism to a particular temperature. The determination of the activation energies for our model has an empirical basis as for previous studies. We will further emphasize this aspect in the revised version, especially when discussing Figure 2.

cf line 333-349: “Following these arguments and despite the lack of experimental constraints to test this assumption, we propose a new parameterization of the activation energy in the LGGE firn densification model which increases the firn densification rate at low temperatures. We have thus enabled introduction of three adjusted activation energies as proposed in Table 1 and Figure 2. We have replaced the creep parameter in Equation (3) by:

$$A = A_0 \times \left(a_1 \times e^{\frac{-Q_1}{RT}} + a_2 \times e^{\frac{-Q_2}{RT}} + a_3 \times e^{\frac{-Q_3}{RT}} \right) \quad (7)$$

We have chosen a minimal number of mechanisms (3) for simplicity in the following but the conclusions of our work would not be affected by a choice of more mechanisms.



- Close to melting temperature: mass transfer by diffusion (potential mechanism for high temperature)
(1) mechanism 1 associated with activation energy Q_1
- Low temperature: lattice diffusion (classical mechanism)
(2) mechanism 2 associated with activation energy Q_2
- Very low temperature : boundary diffusion from grain boundary (potential mechanism for low temperature)
(3) mechanism 3 associated with activation energy Q_3

Figure 2: Different sintering mechanisms of snow for different temperatures proposed by analogy with the hot ceramic sintering (inspired by Figure 1 in Ashby, 1974). Note that more sintering mechanisms can be found in the literature and the attributions of 3 different mechanisms for the firn densification model is only a working hypothesis here.”

Despite some empirical approach, it should be noted that although not necessarily linked to vapor diffusion, high values of activation energy have indeed been measured at high temperatures: values of Q_1 derived from ice creep tests (Jacka and Li 1994, Morgan 1991) can be up to 170 kJ/mol. Note also that the exact value of Q_1 does not influence the result of our study since we are working at low temperature where the effect of Q_1 is minor.

Line 323-325: an activation energy significantly higher than 60 kJ/mol could be favoured (up to 177 kJ/mol between -1 and -5°C [Jacka and Li, 1994]) in order to best fit density profiles with firn densification models (Arthern et al., 2010; Barnes et al., 1971; Jacka and Li, 1994, Morgan, 1991).”

Finally, note that the range of effective activation energies that we use (Q_{eq} see supplementary figure S4) and allows to correctly simulate the observed densification rates is much smaller than the range of the Q_1 , Q_2 , Q_3 values. Above -25°C , Q_{eq} ranges between 58 and 60 kJ/mol.

- Ultimately the goal of firn modelling is to predict Δage , and therefore I was surprised that no Δage results are shown. How does the new activation energy scheme change the simulated Δage ? In Greenland we have direct constraints on Δage via the thermal $\delta^{15}\text{N}$ signals. How well does the model capture those? Likewise, in evaluating the model performance on page 18, the authors test only how well the model predicts the LID (i.e. $\delta^{15}\text{N}$). The more important metric, in my mind, is how well the model predicts Δage . This can be evaluated via the integrated density from the surface to the LID (because Δage is essentially the mass of overlying snow divided by the accumulation rate).

The following table will be inserted in the supplement (together with supplementary table S1) for the comparison of Δage at the bottom of the firn for the different sites studied here. Even if the comparison based on Δage or on modeled density profiles does not lead to exactly the same conclusion for each site, the main features already observed for the comparison of the standard deviation between modeled and measured density profiles are also observed here. This is the case for the worsened agreement between model and data at Talos and Mizuho when using the new parameterization or the improved model vs data agreement at low temperature and low accumulation sites of the bottom of the table (B32, EDML, South Pole, Dôme C, Vostok, Dome A).

Δage	Data	Old	New	New + dust
Dye 3	78	68.4	61.8	-
DE08	35.5	36.8	31.3	-
km105	104.4	111.7	106.4	-
Site2	112.2	109.2	103.3	-
Siple Dome	329	287.9	296.9	284.9
D-47	152	145.3	141.7	-
Byrd	238.9	225	226.9	-
NEEM	209.4	187.4	191.9	187.4
Crete	156.1	150	145.7	-
km200	137.9	156.7	152.6	-
WAIS divide	225	206.5	206.5	233.3
North GRIP	248.4	226.2	236.5	224.5
GRIP	209.9	205.7	205.7	200
B29	270.3	251	264.7	252.9
Mizuho	483.7	518.4	557	-
Talos	554.1	592.6	637.7	656.4
B32	896.8	816.1	889.9	978.4
EDML	874.5	787.3	852.9	899.7
SP	1160.9	965.2	1002.8	1068.7
DC	2639.1	2473	2461	2557
Vostok	2814.3	2960.4	2810.4	2919.5
Dome A	2812.7	3024.8	2764	-

This table and associated caption is included in the supplement, Supplementary Table S2

For paleo application, we think that it is better to compare model outputs to $\delta^{15}\text{N}$ profiles because we do not have direct indication of the Δage (it necessary depends on the timescale). The only way to compare Δage model output with data is actually on the abrupt warming recorded very clearly both in the $\delta^{18}\text{O}$ in the ice phase and $\delta^{15}\text{N}$ in the gas phase on the NGRIP ice core because we have an accurate associated timescale (GICC05). This is the reason why we will present a table in the supplement showing the Δage outputs for the different model parameterizations and a comparison with data estimates based on $\delta^{18}\text{O}$ and $\delta^{15}\text{N}$ records of the abrupt warming in the ice and in the gas phases. The agreement between data and model is slightly better when using the new version but the addition of dust leads to a strong deterioration as observed on the $\delta^{15}\text{N}$ profiles.

NGRIP	Δage (old version)	Δage (new version)	Δage (new version + dust)	DATA
Bolling /Allerod	870 years	920 years	740 years	1040±100 years
End of Younger Dryas	760 years	820 years	640 years	800±100 years

NB: the uncertainty on the Δage from the data is mainly linked to the resolution of the $\delta^{15}\text{N}$ signal.

This table is included in the supplement, Supplementary Table S5

- On lines 624-625 the authors conclude that uncertainties in the climate forcing cannot explain the LGM $\delta^{15}\text{N}$ problem. However, to solve the $\delta^{15}\text{N}$ problem one would need to make the LGM warmer, not colder! For some reason the temperature uncertainties in Fig. S9 are applied very asymmetrically, such that the LGM is always very cold.

The uncertainties for the LGM temperature estimate on the Antarctic plateau are given in Jouzel et al. (2003) as cited in the manuscript in discussion. In this study, the authors have gathered all available constraints for the amplitude of temperature change between the LGM and the Holocene mainly at the Vostok and Dome C sites. The main conclusion is that temperature uncertainty for the amplitude of the last deglaciation is estimated to -10% to +30% in Antarctica. The reason for such asymmetry is mainly linked to outputs of atmospheric general circulation models equipped with water isotopes. These models suggest that the present day spatial slope between $\delta^{18}\text{O}$ and temperature most probably underestimate the amplitude of the temperature change between glacial and interglacial period. We have followed this estimate of asymmetric uncertainty on the amplitude of temperature change during deglaciation and this is the reason why the scenario with warmer LGM is not very different from the control scenario. We do not have references suggesting a much warmer LGM for Antarctica than the classical estimate from water isotopes. More recent studies focusing on the validity of the isotopes vs temperature relationship in Antarctica have also suggested that this relationship can be applied with confidence for glacial temperature reconstruction (Cauquoin et al., 2015) why one should be cautious for past interglacial temperature reconstruction (Sime et al., 2009). Finally, a recent estimate of the deglacial temperature increase based on $\delta^{15}\text{N}$ measurements at WAIS (Cuffey et al., PNAS, 2016) led to a 11.3°C temperature increase over the last deglaciation (1°C warming to be attributed to change in elevation), larger than the temperature increase reconstructed in East Antarctica from water isotopes by 2-4°C. This last estimate is against not in favour of a “warm” LGM.

Still, it should be noted that the uncertainty of 20% on LGM accumulation rate on central sites as given by DATICE in the AICC2012 construction is probably overestimated. Indeed, deglaciation occurs around 500 m depth at Dome C, hence with small uncertainty on the thinning function. Dating tie points can thus constraint quite tightly the accumulation rate.

Summarizing, we believe that the uncertainties given in our manuscript correspond to up to date uncertainties on temperature and accumulation for the last glacial maximum and do not underestimate the possible range of temperature and accumulation rate values for the LGM.

We will complete our manuscript with some explanations given above.

Line 643-669: “The reason for such asymmetry is mainly linked to outputs of atmospheric general circulation models equipped with water isotopes. These models suggest that the present day spatial slope between $\delta^{18}\text{O}$ and temperature most probably underestimate the amplitude of the temperature change between glacial and interglacial period. We have followed this estimate of asymmetric uncertainty on the amplitude of temperature change during deglaciation in our study. Recent studies have also suggested that the relationships between water isotopes and temperature and between water isotopes and accumulation rate can be applied with confidence in Antarctica for glacial temperature reconstruction (Cauquoin et al., 2015) while one should be cautious for interglacial temperature reconstruction with warmer conditions than today (Sime et al., 2009). Finally, a recent estimate of the deglacial temperature increase based on $\delta^{15}\text{N}$ measurements at WAIS (Cuffey et al., 2016) led to a 11.3°C temperature increase over the last deglaciation (1°C warming to be attributed to change in elevation). This is larger than the temperature increase reconstructed in East Antarctica from water isotopes by 2-4°C and again not in favour of a “warm” LGM.

In the construction of the AICC2012 chronology (Bazin et al., 2013; Veres et al., 2013), the first order estimate of accumulation rate from water isotopes for EDML, Talos Dome, Vostok and Dome C has been modified by incorporating dating constraints or stratigraphic tie points between ice cores (Bazin et al., 2013; Veres et al., 2013). The modification of the accumulation rate profiles over the last deglaciation for these 4 sites is less than 20% and the uncertainty of accumulation rate generated by the DATICE model used to build AICC 2012 from background errors (thinning history, accumulation rate, LID) and chronological constraints is 30% for the LGM (Bazin et al., 2013; Frieler et al., 2015; Veres et al., 2013). Still, it should be noted that the uncertainty of 20% on LGM accumulation rate on central sites as given in the AICC2012 construction is probably overestimated. Indeed, deglaciation occurs around 500 m depth at Dome C, hence with small uncertainty on the thinning function and on the accumulation rate. These values are consistent with previous estimates of accumulation rate uncertainties over the last deglaciation ($\pm 10\%$ for Dome C (Parrenin et al., 2007) and $\pm 30\%$ in EDML (Loulergue et al., 2007)).”

- It is not very clear how the parameters in Table 1 were selected. How was the model calibrated? Did the authors minimize some cost function? The authors do give three representative examples in Table 3, but no criteria for choosing the best model.

In their preferred model (Table 1), process 1 ($Q_1 = 110$ kJ/mol) doesn't do much. At all relevant temperatures, process 2 is at least an order of magnitude larger.

The values for the prefactors a_1 , a_2 and a_3 have been chosen to best reproduce the $\delta^{15}\text{N}$ variations over deglaciation at Dome C or Vostok while keeping a good agreement (at least not deteriorating the model-data agreement obtained with the old LGGE model) for (1) the deglacial $\delta^{15}\text{N}$ variations at higher accumulation rate sites and (2) the density profiles for present-day firn. Hundreds of

sensitivity tests have been performed using a strategy based on dichotomy to reduce the mismatch between modeled and measured $\delta^{15}\text{N}$ change over the last deglaciation at low accumulation rate sites. The constraint of keeping a correct agreement of model results with present day density profiles and for the last deglaciation at warm sites strongly reduces the possible choices of a_i and Q_i . This is illustrated by the small range of Q_{eq} values on supplementary Figure S4.

This will be better explained in the new manuscript.

Line 358-363: “Hundreds of sensitivity tests have been performed using a strategy based on dichotomy to reduce the mismatch between modeled and data. The constraint of keeping a correct agreement of model results with present day density profiles and for the last deglaciation at warm sites strongly reduces the possible choices of a_i and Q_i (Section 3). The best value obtained for Q_3 is lower than published values for surface or boundary diffusion but is necessary to reproduce the deglaciation at cold East Antarctic Sites. Sensitivity test C will illustrate the effect of using a higher value.”

- The authors claim that the new model provides a better fit to modern data than the old model. The LID prediction improves by 1.2 ± 6 meter. That hardly seems like a statistically significant improvement. Using as Student's t-test it should be trivial to show whether the null hypothesis (both models perform equally well) can be rejected.

As mentioned earlier, I would encourage the authors to not only compare the predicted LID to the fitted data, but also to compare the integrated density in the simulations to the integrated density of the fit. The latter metric is more representative of Δ_{age} .

We agree that the new model is not significantly better than the old one for density fit as well as LID and Δ_{age} predictions. This will be written more clearly in the new manuscript. As explained above, our main aim is to preserve the good agreement (no deterioration) between modeled and measured firn density profile while improving the $\delta^{15}\text{N}$ model- data agreement over the last deglaciation on the East Antarctic plateau.

Line 548-553: “Still, looking at all different firn profiles, the general agreement between modeled and measured firn density profiles is preserved. The agreement between measured and modeled firn density is increased for some sites at (1) low accumulation rate and temperature in Antarctica (Dome A, Vostok and Dome C but not South Pole) and at (2) relatively high temperature and accumulation rate (Dye 3, Siple Dome, NEEM). In parallel, a larger disagreement between model and data is observed for some other sites particularly in coastal Antarctica (DE08, Km 200, WAIS Divide).”

Line 564-578: “The introduction of three different activation energies for different temperature ranges leads to changes of the modeled density profiles at high densities (above about 800 kg/m^3). A clear improvement is obtained for example at South Pole (Supplementary Figure S6), although the overall impact of using three activation energies remains small.”

The incorporation of the impurity effect following the Freitag et al. (2013) parameterization in our model slightly deteriorates the model-data agreement because no specific re-adjustment of model parameters was performed. However the model prediction of the density profiles remains correct although the impurity effect parameterization was developed for a different purpose: simulating

density layering (Freitag et al., 2013). This encouraged us to test this simple parameterization in glacial climate conditions.

Overall, in terms of $\sigma_{\text{model-fit}}$, only an insignificant improvement (about 3%) is obtained by using the modified model (3 activation energies and implementation of impurity effect) rather than the former Goujon et al. (2003) mechanical scheme. However a systematic improvement is obtained at the six coldest sites.”

Δ age calculation for present-day firn will be provided in the supplement.

This result is displayed in supplementary Table S2

- The closest analog to LGM conditions in East Antarctica is the Dome A site, with mean annual temperatures below 58°C. The old LGGE model provided a reasonable fit to density at this site (Cunde et al., 2008). Why is this site not included in the calibration data set?

Dome A will be included in our revised manuscript as Dr Cunde kindly provided us the necessary data. Recent estimates of the accumulation rate at Dome A lead to a value of 2.3 cm w.eq. / yr (close to the values at Vostok and Dome C). With this accumulation rate, the model – data agreement is improved in the “new” simulations (see e.g. Δ age values in the above table).

Dome A has been included in the different figures and tables in the main text and the supplement corresponding to section 3.1.

- The MS does not give many technical details about the running of the models. What time and spatial step size are used? What is the lower model boundary? What geothermal heat flux is used? The latter is important in the stagnant firn columns of the LGM.

The model spatial grids and lower boundary condition were not changed compared to the former model (Goujon et al. (2003), and the time step (site dependent) was chosen to lead to stable results. A section will be added in the Supplement to complete the description of the model running conditions.

The details are given now in supplementary Text S1

- The authors test the dust softening hypothesis of Johannes Freitag and Maria Hörhold. It is important to note that this model of Freitag et al (2013) was designed to simulate layering, rather than bulk density as it is used here. How were Ca data averaged in the model runs? How does the Ca data resolution compare to the model resolution? Please discuss some of the caveats regarding dust. From talking to Johannes Freitag, I get the impression he believes layering to be more relevant than bulk density in this regard. What do the authors recommend? Should future users incorporate dust or not?

Our main intention is to show that the Freitag et al. (2013) parameterization leads to interesting results and that the dust effect deserves further attention in future studies. When transposed to our model, it provides a reasonable fit of the data at all modern sites. Then, we acknowledge that

the implementation of Ca effect in addition to the effect of temperature influence on the activation energy Q is not optimal since the parameterization of Q_1 , Q_2 , Q_3 and associated a_1 , a_2 , a_3 has been adjusted without Ca effect implementation. The implementation of Ca hence necessarily slightly deteriorates the model – data agreement.

As for the layering and its effect on the LID, it cannot be simply implemented in our firn densification model. This is the reason why the dust has been implemented through its influence on the bulk density which is indeed different from the simulations of Freitag et al. (2013). We will clarify the fact that we do not expect the Freitag et al. (2013) parameterization to be properly tuned for simulating the variations of firn thickness or Δ age as it was not designed for this purpose.

Line 408-413: “The values of a_i and Q_i were not readjusted after the implementation of impurity effects to avoid adding tuning parameters. Still, because the large range of calcium concentrations encountered in past climate conditions has a strong impact on model results, this may be a solution to reduce the model-data mismatch. This is explored in Section 3 through a sensitivity test D. In the same section, we will also propose a modification of the Freitag parameterization using thresholds to reduce the model-data mismatch.”

We expect that the dust influence on bulk density or individual layer density is quite similar. Indeed, from a physics point of view, the density of a given layer is not directly dependent of the density of the surrounding layers as the load pressure on a layer is only controlled by the weight of the layers above (which depends on the precipitation rate but not their density). Thus the impurity effects on the bulk density and on individual layers density should be similar. This probably explains why the comparison is rather good between the polynomial fit of the measured density profiles (hence excluding layering) and modeled firn density profiles with dust influences according to Freitag et al. (2013).

For modern simulations, a single average calcium concentration is used (the value in Table S1). In past climate simulations, the calcium concentration data used were directly taken from the source data file available for each ice core. The temporal variations in Calcium concentrations are then simply interpolated at each model time step. The details on the temporal resolution will be given in the supplement together with the parameters used to run the model. The caveats regarding dust (e.g. using calcium as a diagnostics of dust content and the intention of the Freitag et al. (2013) parameterization) will be better introduced.

Supplementary Text S1 and line 406-407: “We use raw data of the calcium concentration for all the sites when available even if question may arise on calcium concentration being the best diagnostic for dust content.”

- I do not understand the rationale behind the LID parameterization of Equation 10. The authors use a very complicated way to define the LID, namely the depth where the modelled $\delta^{15}\text{N}$ in the open pores matches the $\delta^{15}\text{N}$ in the mature ice. This approach involves simulating the bubble trapping process, which is very (!!) poorly understood. The depth range of bubble trapping is completely unknown at most sites, unless measurements of closed porosity are available (which is not the case at most sites). Also, trapping depends strongly on density layering, as early work at Law Dome and more recent work by Rachael Rhodes and others have shown.

We agree with the Referee on the fact that gas trapping is insufficiently understood. However, the same uncertainties apply when using $\delta^{15}\text{N}$ measurements in ice (after this trapping) in past climate conditions to evaluate our model results. The intention of our definition referring to $\delta^{15}\text{N}$ in the mature ice is to get closer to what is used for past climate conditions. Systematic measurements of $\delta^{15}\text{N}$ in recent ice would be very helpful in the future to improve an LID definition relevant for ice-core interpretation. This will be mentioned in the revised manuscript.

The section 2.4 on the LID has been fully rewritten

The lock-in depth is very clearly visible in firn air sampling data, as an abrupt change in the concentration slope of many tracers. Why not use this commonly used and simple metric, which can be directly derived from data? I fear that modelling something as complicated as bubble trapping could easily lead to errors. How does the fit of Figure S5 look when using the common definition of the lock-in depth?

Different thresholds based on trace gas data in the open porosity of the firn were tested in Table 2 of Witrant et al. (2012). Unfortunately, different definitions (based on greenhouse gas concentration slope change, the $\delta^{15}\text{N}$ plateau, etc.) lead to fairly large differences especially at the most arid sites of the central Antarctic plateau which are a major focus of this study. In particular, as no $\delta^{15}\text{N}$ plateau is observed at these sites, the progressive bubble trapping should lead to less fractionated $\delta^{15}\text{N}$ values in mature ice than in deep firn at these sites. Only fairly small density variations are allowed by our LID parameterization. They will be further discussed in the revised manuscript. Our major conclusion is that the LID definition does not explain the mismatch between model results and $\delta^{15}\text{N}$ data during deglaciations.

The whole section 2.4 has been rewritten

- One of the important achievements of this work is to compile a large database of reliable firn density measurements. This would be an extremely valuable resource to the firn research community if it were publicly available in a format that is easy to use. I would like to kindly ask the authors to make this database publicly available as a supplement to the manuscript, as is also strongly encouraged by the data policy of the journal (Climate of the Past).

The manuscript does not have a statement of data availability yet, which will need to be added as per the editorial guidelines of CP.

We made our best to document the nature and sources of the density data that we used. We are not the owner of the data in most cases, this is why we will provide the polynomial fits of the data rather than the datasets.

We have gathered all polynomial fits in a document to be posted as the Supplementary material

- throughout the paper the authors refer to “snow” as everything above the critical density, and “firn” as everything below. This is not common usage, and should be specified.

We use the same words as Goujon et al. (2003). This will be explained in the new manuscript.

Line 185-186: “The first stage, named “snow densification” as in Goujon et al. (2003),”

Some minor comments and typos:

L2: “constrains” should be “constraints” ok

L23: “to” should be “on” ok

L24: “existence”. Maybe “dominance” would be better? ok

L35: “depict”. What about “reconstruct”? ok

L61: The close relationship between A and T seems to be mostly an assumption. See e.g. Monnin (2004), Fudge (2016) or Van Ommen (2004).

This is indeed true but we focus better on site from the Antarctic plateau where the link should be true at least qualitatively. Moreover, we expect a certain correlation between change in accumulation rate and change in temperature when considering long term averages (several thousands of years for the LGM) while a certain decoupling between accumulation and temperature is expected at short scale because of the different possible snow accumulation processes. This will be explained in the new manuscript.

Line 61-70: “On glacial – interglacial timescales, increasing temperature is associated with increasing snow accumulation. Indeed, the thermodynamic effect dominates when dealing with long term averages (several thousands of years), even if accumulation and temperature are not always correlated on millennial and centennial timescale in polar regions, especially in coastal areas (e.g. Fudge et al., 2016; Altnau et al., 2014). As a consequence, when comparing LGM and Holocene averages, we observe for all available ice cores covering the last deglaciation increases in both accumulation and temperature. In the firn densification model, both effects partially compensate each other, with the temperature effect being dominant in the current densification models for the LID simulation over glacial – interglacial transitions in deep drilling sites of the East Antarctic plateau, hence leading to the modelled LID decrease.”

L65: in HL the “change” in pore space is proportional to the increase in weight.

Yes, this is the meaning of our sentence, accumulation rate being directly linked with weight.

Line 75: “the weight of the overlying snow, hence the accumulation rate.”

L89: Better write: “In the absence of thermal gradients”, the $\delta^{15}\text{N}$ trapped : : :.. The geothermal heat flux matters also ok

L101-102. Thermal fractionation does not only occur in Greenland, but anytime there is a thermal gradient.

This is true but in order to have a strong thermal fractionation, we need abrupt temperature changes at the surface. We have thus added “strong” before “thermal fractionation”

L105: what is Ω ?

This will be explained in the new manuscript (Grachev et Severinghaus, 2003)

Line 117: “where Ω is the thermal fractionation coefficient”

L106: What does this statement mean? Can thermal fractionation not exceed 0.15 permil? Or is this the maximum observed value?

This will be explained in the new manuscript

Line 119: “(the $\delta^{15}\text{N}_{\text{therm}}$ observed is in most cases lower than 0.15‰).”

Section 2: It may be more useful to identify the different stages of densification via their density range, rather than their depth range.

Yes, we are agree, this will be changed in the new manuscript.

Done.

L158-160: likely all three stages are blurred in reality, with the densification mechanisms overlapping, see e.g. Hörhold et al. (2011).

We agree with this comment, we will precise it in the new version.

Line 192-193: “In reality, the adjacent densification mechanisms likely coexist at intermediate densities.”

L213: remove “s” in “equals” ok

L236: I thought that was just an ad-hoc scaling factor to make things fit. Does Y have a real meaning, and does it correspond to some physical process?

Equations (4) and (5) in our manuscript show the relationship between γ used in Goujon et al., 2003 and the parameters in Alley, 1987 : $\gamma = (2/15)(\lambda/\nu)(R/r^2)$ where λ is the bond thickness, ν the bond viscosity, R the grain radius and r the bond radius. Alley (1987) then calculates and discusses the activation energy for viscosity. On the other hand Goujon et al. (2003) simply used an adjusted value of γ , as explained in our manuscript text following Equation 5. We replace γ in Equation 4 by $\gamma' \exp(-Q/RT)$ in Eq. 6 and evaluate that $Q = -49.5$ kJ/mol. As γ' is still adjusted in the model, using γ or $\gamma' \exp(-Q/RT)$ does not change the model results.

In the modified manuscript, we will remind the relationship between Y and the physical parameters in Alley (1987) at line 236.

Line 265-272: “Alley (1987) calculated a viscosity (ν) related activation energy of 41 kJ/mol, consistent with recommended values for grain-boundary diffusion (42 kJ/mol) or measured from grain growth rate (Alley, 1987 and references therein). In Goujon et al. (2003), no explicit temperature effect is used but the parameter γ varies by several orders of magnitude from site to

site. The parameter γ is calculated to maintain a continuous densification rate between the first and second stages at a chosen critical density. We translate the variations of $\gamma = (2 \lambda R) / (15 \nu r^2)$ from site to site into $\gamma = \gamma' \exp(-Q/RT)$, and calculate the activation energy Q using a classical logarithmic plot as a function of $1000/T$ (see e.g. Herron and Langway, 1980)."

L248: Please add a multiplication signs (0:5 _ 109) ok

L295: note that seasonally sensitive densification rates (as from Arthern et al.) cannot be compared to mean annual densification rates.

The large values up to 100-130kJ/mol are originally from Morgan et al, 1991, and Jacka and Li 1994 and their values are not related to seasonal thermal gradients, which are not taken into account in this study. Also note that the equivalent effective activation energy in our model (Q_{eq}) remains lower than 60 kJ/mol (see supplementary Figure S4 and answer to second general comment).

L328: Note that Arthern does not attribute his high activation energies to vapor diffusion. Vapor diffusion should have an activation energy of 51 kJ/mol, i.e. the enthalpy of sublimation. Again, please be careful not to conflate activation energies of models that do and do not resolve the seasonal temperature signal.

We removed the attribution to a specific mechanism and simply note: "At warm temperature, empirical determinations of Q_1 lead to values of the order of 100-130 kJ/mol (Arthern et al., 2010; Barnes et al., 1971; Zwally and Li, 2002)."

Line 322-325: "Actually, it has been observed that, at warm temperature, an activation energy significantly higher than 60 kJ/mol could be favoured (up to 177 kJ/mol between -1 and -5°C [Jacka and Li, 1994]) in order to best fit density profiles with firn densification models (Arthern et al., 2010; Barnes et al., 1971; Jacka and Li, 1994, Morgan, 1991)."

These high values are actually not linked to a seasonal temperature signal: Jacka and Li (1994) made isothermal laboratory measurements to determine them.

L357-358: This assumption is probably not valid for vapor diffusion?

This is indeed correct. We will specify it. It should still be noted that this does not have any significant influence for the relatively cold sites studied here.

Line 388-392: "We have implemented this parameterization in our model with the simple assumption that the impurity effect is the same for all mechanisms. It allows us to keep the number of tunable parameters to a minimum, even though this assumption is probably not correct for the vapor diffusion process. Note however that this will not affect the applications discussed below since vapor diffusion is only important for warm sites."

Section 2.2.3:

please specify at what resolution you allow Ca to vary. Do you smooth/average the records in some way?

No, the records are not smoothed (cf answer on dust data above). This will be specified in the new manuscript.

cf Supplementary Text S1

L376-377: This is an odd definition of the close-off depth. Isn't the pressure in (closed) bubbles is always higher than that of the atmosphere? What about: the density at which the total pore volume, at the atmospheric pressure of the site, equals the air content of mature ice. (or similar)

We use the same definition of the close-off density as in Goujon et al. (2003). It defines the boundary between the second (firn) and third (ice) mechanical formulations in the model. As no model change was performed, the phrasing will be simplified in the revised manuscript.

Line 416-418: "As in Goujon et al. (2003), the final densification stage begins at the close-off density derived from air content measurements in mature ice. Further porosity reduction results in an air pressure increase in the bubbles"

L395: polar firn study "sites", : : : ok

L398 "trapping density" should be "lock-in density" ok

L403: where does the $\ln(1/A_c)$ functional form come from? Is this inspired by theory?

No, this is just an ad-hoc adjustment. In the previous model version (Goujon et al., 2003), the LID definition was related to a value of the closed/total porosity ratio adjusted for each drilling site but time independent (see lines 387-389). This dependency on the geographic location with independence from climate is not completely self-consistent. This is why we tested another LID definition.

The description of our LID definition and tests will be modified following the comments from both Referees.

Section 2.4

L405: : : better agreement "between" the modelled LID "and" $\delta^{15}\text{N}$: : : ok

L405: is the $\delta^{15}\text{N}$ measured on firn samples or ice samples?

Line 4

Yes, they are measured in firn samples, we will replace « measured at the available firn sampling sites » by « measured in firn samples at available sites »

L413-414: In fact, it makes it worse. ok

L458 and L490. The limits of the summation are listed the wrong way around; $i = 1$ should be printed below N_{max} ok

L490: why compare the model to the fit, and not just to the data as was done in Eq. 11? That way you compare apples to apples in Figure 5.

There is no simple way to compare model results and density data in a multi-site consistent way due to the strong site to site differences in the data (measurement techniques, sample size, number of

samples, depth dependent resolution, etc.). Model results are compared to the fit in order to better characterize:

- bulk density (as opposed to density variability) which we aim at predicting with the model
- site to site variations in the quality of the model prediction of the bulk density profile. The regular depth resolution used leads to an integrative diagnostics somewhat comparable to delta-age. The manuscript section between lines 492 and 511 will be revised.

Line 513-523: “Note that we compare here the model to the fit of the data and not directly to data because of the strong site to site differences in the data (e.g. data resolution, sample size). Figure 5 and Supplementary Table S1 display the $\sigma_{\text{model-fit}}$ for the 22 different sites before and after modifications detailed in Section 2.”

3.1.1. Data – model comparisons using the old model

Comparing our model results to density data is not trivial due to the diversity in measurement techniques and samplings discussed above, as well as the natural variability in density that we do not capture with a simplified model aiming at simulating very long time scales. A rough indication is given by comparing $\sigma_{\text{model-fit}}$ and $\sigma_{\text{fit-data}}$.”

L493-494: is this improvement statistically significant? Please provide t-test significance or similar. No, it is not, this will be mentioned in the revised manuscript

Line 548-553: “Still, looking at all different firm profiles, the general agreement between modeled and measured firm density profiles is preserved. The agreement between measured and modeled firm density is increased for some sites at (1) low accumulation rate and temperature in Antarctica (Dome A, Vostok and Dome C but not South Pole) and at (2) relatively high temperature and accumulation rate (Dye 3, Siple Dome, NEEM). In parallel, a larger disagreement between model and data is observed for some other sites particularly in coastal Antarctica (DE08, Km 200, WAIS Divide).”

Line 564-578: “The introduction of three different activation energies for different temperature ranges leads to changes of the modeled density profiles at high densities (above about 800 kg/m³). A clear improvement is obtained for example at South Pole (Supplementary Figure S6), although the overall impact of using three activation energies remains small.”

The incorporation of the impurity effect following the Freitag et al. (2013) parameterization in our model slightly deteriorates the model-data agreement because no specific re-adjustment of model parameters was performed. However the model prediction of the density profiles remains correct although the impurity effect parameterization was developed for a different purpose: simulating density layering (Freitag et al., 2013). This encouraged us to test this simple parameterization in glacial climate conditions.

Overall, in terms of $\sigma_{\text{model-fit}}$, only an insignificant improvement (about 3%) is obtained by using the modified model (3 activation energies and implementation of impurity effect) rather than the former Goujon et al. (2003) mechanical scheme. However a systematic improvement is obtained at the six coldest sites.”

L505-506: I think this is somewhat of a uneven comparison, you should be comparing $\sigma_{\text{model-data}}$ to $\sigma_{\text{fit-data}}$. $\sigma_{\text{model-fit}}$ could in theory be smaller than $\sigma_{\text{fit-data}}$, as the data has some inherent scatter and layering.

We agree on the fact that the sentences at lines 505-507 are too much of a shortcut. On the other hand, the polynomial fit to the data is close to the bulk density profile that we aim at modelling. The manuscript section between lines 492 and 511 will be revised.

cf change of text corresponding to answer to the problem line 490

L513-514: first stage is important in getting the correct Δ age, though.

A Table with Δ age results (see above) will be included in the Supplement and briefly commented in the manuscript.

The supplementary Table S2 gives the Δ age values and comparisons

L541: Do you make a correction for the convective zone? yes, 2 m (L.580)

L544-546: Do you include the geothermal heat flux? Yes, the geothermal heat flux is included in the model and hence implemented for the calculation of $\delta^{15}\text{N}$ from the temperature profile.

L552-553: How do you include the borehole calibration from Dahl-Jensen et al (1998)?
This is not clear

The scenario for temperature evolution in NorthGRIP includes the borehole calibration from Dahl-Jensen et al., (1998) by imposing a 23°C temperature change between LGM and present-day. This corresponds to a temporal slope for the relationship between $\delta^{18}\text{O}$ and temperature of 0.3 permil.°C⁻¹ over the deglaciation. This slope is thus applied for reconstructing the temperature evolution for the last deglaciation at NorthGRIP in this study. Then, the temperature amplitude for B/A and Y/D is adjusted on the $\delta^{15}\text{N}$ data obtained by Kindler et al. (2014) on the NorthGRIP core.

A paragraph explaining the temperature scenario will be added in the supplement.

Some explanation are given in the caption of Supplementary Table S3

Also, in the main text, we added a few words on lines 633-636: "In Greenland (NGRIP, GISP2), the temperature is reconstructed using the $\delta^{18}\text{O}_{\text{ice}}$ profiles together with indication from borehole temperature measurements (Dahl-Jensen, 1998) and $\delta^{15}\text{N}$ data for NGRIP (Kindler et al., 2014) for the quantitative amplitude of abrupt temperature changes."

L592-593: How well do the different models fit the exact timing of the $\delta^{15}\text{N}$ increase?

This is set by Δ age, so an important test for the models.

Indeed, the different models do not lead to the same calculated Δ age as shown in the new table that we will insert in the supplementary materials. We will hence also comment this aspect on Figure 6.

Supplementary Table S4 provide the new table that we were referring to.

A text had also been added on lines 780-784: "Some differences are also observed for the timing of the $\delta^{15}\text{N}$ peaks for Bølling-Allerød and end of Younger Dryas at NGRIP when using the different model versions reflecting variations in the simulated Δ age (cf Supplementary Table S5); the general agreement with the measured profile is preserved with even a slight improvement of the modelled Δ age with $\delta^{15}\text{N}$ constraints with the modified model."

L639-642: Again, I think the link between Accumulation and temperature is not as strong as you suggest here, particularly near the margins where most accumulation is delivered by storms.

We agree that the link between accumulation and temperature is not always so strong and we will nuance this sentence in the revised manuscript. Indeed, near the margin, the link between accumulation and temperature is not straightforward as discussed for example at Law Dome in Landais et al. (QSR, 2006). However, here, we mainly deal with sites that are on the East Antarctic plateau and there is no simple way how we could explain a different evolution for temperature and accumulation rate at Dome C on the long timescale (i.e. on the difference between LGM and present-day).

Line 61-70: "On glacial – interglacial timescales, increasing temperature is associated with increasing snow accumulation. Indeed, the thermodynamic effect dominates when dealing with long term averages (several thousands of years), even if accumulation and temperature are not always correlated on millennial and centennial timescale in polar regions, especially in coastal areas (e.g. Fudge et al., 2016; Altnau et al., 2014). As a consequence, when comparing LGM and Holocene averages, we observe for all available ice cores covering the last deglaciation increases in both accumulation and temperature. In the firn densification model, both effects partially compensate each other, with the temperature effect being dominant in the current densification models for the LID simulation over glacial – interglacial transitions in deep drilling sites of the East Antarctic plateau, hence leading to the modelled LID decrease."

L666: "densification rates" (add "s") ok

L682: compatible with the data "except at Talos Dome". Table 3: please be more clear what all the numbers are. I assume these are Q1, Q2, Q3 etc, but this is not very clear. ok

L706-710: Please rewrite this sentence, it is really hard to follow.

When using the parameterization of Table 1 ("new model"), Figure 7 shows strong improvement of the simulation of the $\delta^{15}\text{N}$ difference between EH and LGM. Indeed, the modeled EH-LGM difference now has the correct sign at very cold sites of East Antarctica (Figure 7) when compared to $\delta^{15}\text{N}$ measurements.

This sentence was inserted in the new text

L725: change "less good" to "worse" ok

L734-736: Could this be because the uncertainty in the input temperature does not include the possibility that the LGM was much warmer than the optimal scenario?

This is unfortunately not sufficient to explain the mismatch. Even if significantly higher LGM temperature (-6°C instead of -9°C) without any change in accumulation rate would decrease the $\delta^{15}\text{N}$ at LGM at EDML down to the level of the accu_minus scenario (Figure S9). This is unfortunately not enough to reconcile model and data on the amplitude of the change of $\delta^{15}\text{N}$ between the LGM and present-day. Moreover, note that such lack of correlation between temperature and accumulation rate changes can be observed in coastal sites but is again very unlikely in the East Antarctic plateau.

L756-757: Ca from volcanic events?

We do not know if the very fast peaks observed on the calcium concentrations correspond to volcanic eruptions, on the other hand we know that they do not affect the $\delta^{15}\text{N}$ profiles.

L817: Is your new modeled EDC Δ age consistent with the work of Parrenin et al. (2013)?

Yes, our study is in line with the work of Parrenin et al. (2012 and 2013). This will be specified in the new manuscript and was actually one of the aims of the tuning of activation energy values to temperature.

Line 955-963 (conclusion): “Our finding is however associated with several limitations so that this new model does not propose a definite re-evaluation of the formulation of the activation energy but better proposes some ways to be further tested and explored to improve firn densification models especially for applications on paleoclimate reconstructions. Our approach remains empirical and we could not identify separately the different mechanisms involved. The problem of $\delta^{15}\text{N}$ data-model mismatch in low temperature and accumulation rate sites of East Antarctica is thus not definitively solved. Still, we showed that revising the temperature and impurity dependence of firn densification rate can potentially strongly reduce the $\delta^{15}\text{N}$ data-model mismatch and proposed preliminary parameterizations easy to implement in any firn densification model.”

Anonymous Referee #2

Received and published: 23 November 2016

We thank the reviewer for the comments that are indeed helpful to convey a comprehensive message. We have tried to take into account all comments as detailed below.

General:

The authors state that they have improved the LGGE firn densification model based on physical mechanisms. They argue with a better agreement between modelled and measured $\delta^{15}\text{N}$ data. But the physical arguments stand on shaky ground and the better agreement for some sites are opposed by significant lesser agreement of the model data at other sites. A general comment of caution regarding the physical approach: Though the concept of Arzt, based on monosized spheres, which deviates substantially from the physical reality, produces reasonable firn density profiles, they are not really better than those of empirical parametric models. The reason is the rigidity of the 'physical' model and it is not surprising that an empirical approach with more free parameters, as e.g. in the Pimienta-model, may even better catch the reality! The authors now introduce rather arbitrarily two additional Arrhenius-type mechanisms. Thereby they can readily simulate a higher densification rate at very low temperatures. A corroboration of the new model by the better agreement with a small glacial delta age (or delta depth, i.e. shallower glacial firn depth) by Parrenin (2012) is unjustified because this agreement was exactly the purpose of tuning the model.

The purpose of this paper is to evaluate the LGGE model of firn densification by comparison with data in modern and past climate conditions, with a focus on the major problem of the too small densification rate at very low temperature in East Antarctica highlighted in Capron et al. (2013) and earlier studies. We did not perform a major revision of the model but tested the effect of relatively simple model changes (e.g. the activation energy and dust tests can easily be adapted to other models).

We agree that our parameterization has been chosen to better match the $\delta^{15}\text{N}$ data and hence the Δage estimate by Parrenin et al. (2012) at Dome C. This was already present in the previous manuscript and will be highlighted more clearly in the revised version. Our new parameterization should also not affect too much the agreement observed between model and data in higher temperature and accumulation rate conditions which is not trivial. We thus investigated to which extent the firnification model invoking different mechanism for firn densification is able to reproduce the $\delta^{15}\text{N}$ evolution over deglaciations in low accumulation rate sites of East Antarctica without degrading the good agreement observed with the old version of the model between measured and modeled firn density profiles and between modeled and measured $\delta^{15}\text{N}$ evolution over the last deglaciation at sites with higher accumulation rates.

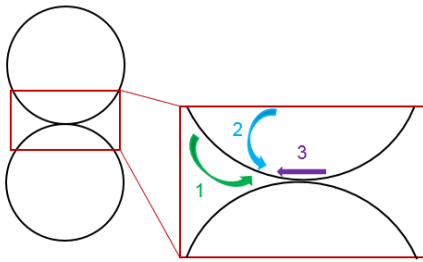
The only way to reconcile our model with $\delta^{15}\text{N}$ data by invoking a change of activation energy with temperature is to have a negligible influence of temperature on the densification rate below -50°C . Several reasons for this effect can be invoked. We proposed here an interpretation with different activation energies for firn densification based on previous studies showing different densification mechanisms over different temperatures. Still, our proposed interpretation is not definitive for explaining firn densification over a large range of temperature. In the revised manuscript, we will make clear that the association of our three activation energies with three precise physical

mechanisms is not proved. Indeed, while several mechanisms have been highlighted for the densification of ice over several temperature ranges, there is no unambiguous attribution of a particular mechanism to a particular temperature. The determination of the activation energies for our model has an empirical basis as for previous studies. We will further emphasize this aspect in the revised version, especially when discussing Figure 2. We will also state that the effect of temperature could be misrepresented in our model by other ways than the value of activation energy opening the ways to other studies.

Line 333-349: “Following these arguments and despite the lack of experimental constraints to test this assumption, we propose a new parameterization of the activation energy in the LGGE firn densification model which increases the firn densification rate at low temperatures. We have thus enabled introduction of three adjusted activation energies as proposed in Table 1 and Figure 2. We have replaced the creep parameter in Equation (3) by:

$$A = A_0 \times \left(a_1 \times e^{\frac{-Q_1}{RT}} + a_2 \times e^{\frac{-Q_2}{RT}} + a_3 \times e^{\frac{-Q_3}{RT}} \right) \quad (7)$$

We have chosen a minimal number of mechanisms (3) for simplicity in the following but the conclusions of our work would not be affected by a choice of more mechanisms.



- Close to melting temperature: mass transfer by diffusion (potential mechanism for high temperature)
(1) mechanism 1 associated with activation energy Q_1
- Low temperature: lattice diffusion (classical mechanism)
(2) mechanism 2 associated with activation energy Q_2
- Very low temperature : boundary diffusion from grain boundary (potential mechanism for low temperature)
(3) mechanism 3 associated with activation energy Q_3

Figure 2: Different sintering mechanisms of snow for different temperatures proposed by analogy with the hot ceramic sintering (inspired by Figure 1 in Ashby, 1974). Note that more sintering mechanisms can be found in the literature and the attributions of 3 different mechanisms for the firn densification model is only a working hypothesis here.”

In addition, several sentences have been removed all along Section 2.2

The approach regarding other transport mechanisms involved in sintering is not convincing. Why should surface diffusion explain the higher densification rates at low temperatures? First, surface diffusion itself does not lead to densification and second also indirect effects will most likely not favor densification. Surface diffusion increases neck diameters and thus decreases pressure at contact area, which decreases creep and in addition it increases curvature radii that decrease the generation of lattice vacancies, and thus decreasing lattice diffusion. Q_3 , the activation energy applied for surface diffusion seems unrealistically low. Higher values, between 30 and 50 kJ, have been reported.

We agree with the referee on the fact that surface diffusion does not directly lead to densification. We went back to Ashby 1974 (Acta Metallurgica, vol.22, pp.275-289) and actually the dominant mechanism at low temperature should rather be boundary diffusion from grain boundaries which is a mechanism enabling densification. We are not aware of activation energy values associated with

this mechanism in firn. As stated above, we will make clear that the association of our three activation energies with three precise physical mechanisms is not proved.

Lines 329-330 have been modified “lattice diffusion from the surface of the grains and/or boundary diffusion from grain boundaries should be favoured (Ashby, 1974).”

Figure 2 has also been modified for the very low temperature mechanism proposed.

As for the measured values of activation energy, Anonymous Referee#1 provided two references for the activation energy of surface diffusion in the range 14-38 kJ/mol and we will include in the revised manuscript a test showing that using 15kJ/mol leads to intermediate results between the “old” and “new” model results.

Test C is included in Figure 7, Figure 8 and Table 3.

In the main text, discussion on lines 825-832 has been inserted: “Test C has been designed so that the activation energy at low temperature corresponds to estimates of activation energy for ice surface diffusion (Jung et al., 2004; Nie et al., 2009), a mechanism that is expected to be important at low temperature (Ashby, 1974). Using such a parameterization leads to a fair agreement between the modelled and the measured $\delta^{15}\text{N}$ change over the last deglaciation for the different sites. At Dome C, the correct sign for the $\delta^{15}\text{N}$ evolution between LGM and the Holocene is predicted by the model. However, the modelled $\delta^{15}\text{N}$ increase is still too small compared to the data and the $\delta^{15}\text{N}$ calculated by the “new model”. This is probably due to a too high creep parameter at low temperature.”

Considering the influence of dust on densification is interesting but does not substantially contribute to solving the discrepancy between model and data, because the densification enhancement by dust leads for too many sites to a deterioration of the modelled densities.

The tuning of Q1, Q2, Q3 and associated a1, a2, a3 has been done without dust influence. As a conclusion and as noted by Referee 2 (comment on lines 483+497), the implementation of dust necessarily slightly deteriorates the model – data agreement. This will be clarified in the revised version when discussing the dust influence addition.

We will also clarify the fact that we do not expect the Freitag et al. (2013) parameterization to be properly tuned for simulating the variations of firn thickness as it was not designed for this purpose. One way to improve the constraints on the problem (how does dust influence the glacial firn depth?) is to study other deglaciations, where the dust increase and the temperature increase are not synchronous.

Line 408-413: “The values of a_i and Q_i were not readjusted after the implementation of impurity effects to avoid adding tuning parameters. Still, because the large range of calcium concentrations encountered in past climate conditions has a strong impact on model results, this may be a solution to reduce the model-data mismatch. This is explored in Section 3 through a sensitivity test D. In the same section, we will also propose a modification of the Freitag parameterization using thresholds to reduce the model-data mismatch.”

To further explore the dust influence for paleoclimate studies, we have implemented of Test D (Figure 7 and Table 3) + discussion line 874-887: “The model – data mismatch observed when

incorporating the dust effect may be partially due to the fact that we did not readjust a_i and Q_i after implementation of the impurity effect. To explore this possibility, sensitivity test D has been designed with a re-parameterization of the a_i and Q_i values after implementation of the impurity effect. To do so, we calculated the optimal creep parameter A for each mean EH and LGM condition at each site, and adjusted sequentially a_3 , a_2 , a_1 , Q_3 , Q_2 , and Q_1 to minimize the model-data mismatch. Only a_3 , a_2 and Q_3 needed adjustments, and their values can be found in Table 3. We did not perform the adjustment on modern density profiles, because these are only weakly sensitive to the dust parameterization, Ca^{2+} concentrations being low.

Impurity concentration is very high at NGRIP during the glacial period. As a consequence, even if our new parameterization of a_i and Q_i (new model) properly reproduces the Greenland $\delta^{15}N$ level at LGM, this glacial modelled Greenland $\delta^{15}N$ level is too low when including the impurity effect. The re-parameterization of a_i and Q_i proposed as sensitivity test D enables an improvement of the agreement between model and data for glacial $\delta^{15}N$ at WAIS-Divide, maintain the results at Dome-C and EDML, but can still not produce reasonable results at NGRIP (Figure 7)."

We have also proposed a revised parameterization of the Freitag parameterization including additional threshold effects (Supplementary Figure S10 and Supplementary Text S2) and corresponding discussion on lines 895-897 +:

"To further improve the model – data agreement with the dust parameterization, a possibility is to add simple thresholds on a minimum and maximum effect of calcium as proposed in supplementary material (Supplementary Text S2 and Figure S10)."

The mentioned possibility of saturation of the densification enhancement by dust at high concentration would only work for Greenland but not for WAIS divide.

Indeed, the « dust saturation hypothesis » cannot reconcile the Holocene firn thickness at NGRIP and WAIS-Divide, which are nearly identical with 10 times more Ca at NGRIP compared to WDC. Another possibility is that the impact of dust depends on the densification mechanism, and is much more important at cold temperature.

cf previous answer

My criticism shall not disesteem the huge work accomplished for improving the calibration of the model for modern firn densities that is also presented in this paper. This calibration with new improved firn density profiles certainly leads on average to slight optimization of the model parameters.

However, a better fit to glacial firn depths has only been achieved by a direct tuning of the creep factor at low temperatures. This should be clearly communicated as such.

And as the authors mention in the supplement this can be achieved with any other of the common densification models.

As mentioned in the previous manuscript, the choice of the very low value for Q_3 is indeed designated for increasing firn densification at low temperature. This tuning of the creep factor will be stated more clearly earlier in the manuscript (section 2.2)

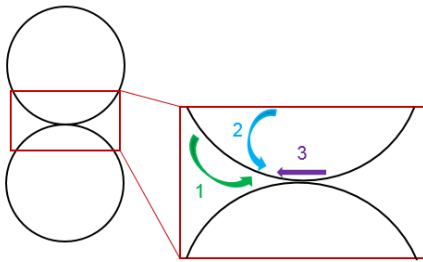
Line 22-23: "we apply a dependency of the creep factor on temperature and impurities in the firn densification rate calculation."

Line 24-27: “We show that both the new temperature parameterization and the influence of impurities contribute to the increased agreement between modelled and measured $\delta^{15}\text{N}$ evolution during the last deglaciation at sites with low temperature and low accumulation rate, such as Dome C or Vostok”

Line 333-363: “Following these arguments and despite the lack of experimental constraints to test this assumption, we propose a new parameterization of the activation energy in the LGGE firn densification model which increases the firn densification rate at low temperatures. We have thus enabled introduction of three adjusted activation energies as proposed in Table 1 and Figure 2. We have replaced the creep parameter in Equation (3) by:

$$A = A_0 \times \left(a_1 \times e^{\frac{-Q_1}{RT}} + a_2 \times e^{\frac{-Q_2}{RT}} + a_3 \times e^{\frac{-Q_3}{RT}} \right) \quad (7)$$

We have chosen a minimal number of mechanisms (3) for simplicity in the following but the conclusions of our work would not be affected by a choice of more mechanisms.



- Close to melting temperature: mass transfer by diffusion (potential mechanism for high temperature)
(1) mechanism 1 associated with activation energy Q_1
- Low temperature: lattice diffusion (classical mechanism)
(2) mechanism 2 associated with activation energy Q_2
- Very low temperature : boundary diffusion from grain boundary (potential mechanism for low temperature)
(3) mechanism 3 associated with activation energy Q_3

Figure 2: Different sintering mechanisms of snow for different temperatures proposed by analogy with the hot ceramic sintering (inspired by Figure 1 in Ashby, 1974). Note that more sintering mechanisms can be found in the literature and the attributions of 3 different mechanisms for the firn densification model is only a working hypothesis here.

When building the new parameterization of the activation energy (Equation 7), the determination of Q_1 , Q_2 and Q_3 on the one side and a_1 , a_2 and a_3 on the other side are not independent from each other. We first determine three temperature ranges corresponding to the dominant mechanisms, then we attribute values to the activation energies Q_1 , Q_2 and Q_3 . The coefficients a_1 , a_2 and a_3 are finally adjusted to produce the expected evolution of the creep parameter with temperature, to best reproduce $\delta^{15}\text{N}$ evolution over deglaciations (Section 3.2) and respect the firn density profiles available (Section 3.1).

Hundreds of sensitivity tests have been performed using a strategy based on dichotomy to reduce the mismatch between modeled and data. The constraint of keeping a correct agreement of model results with present day density profiles and for the last deglaciation at warm sites strongly reduces the possible choices of a_i and Q_i (Section 3). The best value obtained for Q_3 is lower than published values for surface or boundary diffusion but is necessary to reproduce the deglaciation at cold East Antarctic Sites. Sensitivity test C will illustrate the effect of using a higher value.”

Conclusion has also been largely revised in this direction

In my view, this lengthy paper clearly raises false expectations. The paper could be organized such that in a first part the improvement of the parameter calibration on modern density profiles are presented and in a second part one could investigate how the creep factor needs to be tuned in order to better simulate the glacial data for the different ice cores, with and without dust enhancement. The diverging results would readily show that so far no unified model can simulate the existing range of data.

>> We will implement a new (short) section 3.1 that present the agreement between modeled and measured firn density profiles using the revised version of the LGGE model with only one activation energy (i.e. corresponding to modifications depicted in section 2.1). To show the influence of this revisions compared to the old version, Figure 5 will display an additional vertical bar for each site.

Then, we will present our proposition that with a parameterization with three activation energies we are able to better fit $\delta^{15}\text{N}$ profiles at low accumulation sites in Antarctica. The limitations of this assumption presented at the beginning of the answer to Ref 2 will be clearly stated. We will then show that the implementation of 3 activation energies does not significantly deteriorate the agreement between modeled and measured firn density profiles but that some divergences persist for paleoclimatic simulations especially when adding the dust influence which call for future studies for investigating the influence of both temperature and dust on firn densification and lock-in depth prediction.

The whole Section 3 has been reorganized following the suggestion of the reviewer.

Some specific comments:

L. 2: title "constrains" -> constraints ok

L. 23: " we introduce a dependency of the activation energy to temperature and impurities in the firn densification rate calculation". It is rather a temperature dependent creep factor. The authors 'apply' the impurity dependence, it was 'introduced' by Freitag et al.

Yes, this will be rewritten in the manuscript.

Line 22-24: "we apply a dependency of the creep factor on temperature and impurities in the firn densification rate calculation. The temperature influence intends to reflect the dominance of different mechanisms for firn compaction at different temperatures."

L. 79: " questionable when used outside of its range of calibration". Not only then as in case of EDML.

>> It is true that EDML is difficult to reconcile with the model. We have shown in Landais et al. (2006) that it can be reconciled with the model only if accounting for large uncertainties in past accumulation rate and a reasonable convective zone (10 m) (Landais et al., 2006). This will be specified in the revised manuscript.

Line 146-147: "This hypothesis can explain the mismatch between modelled and measured $\delta^{15}\text{N}$ at EDML during glacial period by invoking a 10 m convective zone (Landais et al., 2006)."

L. 186: Is A0 a constant? Value?

Yes, $A_0 = 7.89 \times 10^{-15} \text{ Pa}^{-3} \cdot \text{s}^{-1}$, this is specified in the new manuscript. It is the same value as in Equation A5 of Goujon et al. (2003)

L. 210-228: This 'bending into shape' demonstrates again that a more parametric approach can be closer to reality than a 'pure physical' one.

True, but aiming to use physical formulation is perhaps safer when we venture out of the calibrated range. Still, our approach is very much empirical at this stage, since the creep constant and other model parameters such as D_0 have been calibrated empirically. We will make clearer the fact that our approach is not a 'pure physical' one: we will add a sentence at line 86 clarifying the fact that the simplified physical mechanisms in our model include adjusted parameters.

The section 2.2 has been rewritten (cf also comments above)

L. 245 (eq. 6) Is 0.1 bar the pressure at 2 m depth (L. 213)? This should be clarified in the text..

0.1 bar is a rough approximation of the pressure at two to three meters depth, which depends on the density profile of the overlying snow.

The sentence at lines 211-213 will be replaced with:

Indeed, since the model is not able to represent the metamorphism in the first two meters, we impose a constant pressure of 0.1 bar (see Equation 6), which is an approximation of the pressure at 2-3 meters depth. It results in a nearly constant densification rate in the top 2-3 meters rather than a constant density in the top 2 meters.

Line 245-247: "we impose a constant pressure of 0.1 Bar (see Equation 6), which is an approximation of the pressure at 2-3 m depth. It results in a nearly constant densification rate in the top 2-3 m rather than a constant density in the top 2 meters."

L. 305: "three different mechanisms highlighted above" There are more than 3 mechanisms mentioned above. Table 1, Fig. 2 may not be above.

Replaced by "three different mechanisms highlighted in Table 1 and Figure 2"

L. 321, 824: "surface lattice diffusion" Is this term correct for 'surface diffusion'?

This has been changed to "boundary diffusion from grain boundary" following Ashby (1974)

L. 358: "assuming that the impurity effect is the same for all mechanisms". This seems very unlikely!

Line 390-392: "even though this assumption is probably not correct for the vapor diffusion process. Note however that this will not affect the applications discussed below since vapor diffusion is only important for warm sites."

L. 362,3: "f1" subscript 1 ok

L. 403: "A subscript c" is a strange notation for accumulation rate. Define abbreviation

in text. This parameterization is surprising. Of course temperature and accumulation rate are strongly correlated, so we expect an corresponding correlation with accumulation rate. But for two sites with equal accumulation rate but different temperature we don't expect the same LID as densification is strongly temperature dependent. So this parameterization may be justified for most conditions but one must be careful applying it in general and during glacial conditions.

"A subscript c" A is more commonly used but here, we wish to avoid confusion with A_i and a_i used in Equation 7 and Section 2.2. We will use "Ac" instead of " A_c " in the revised manuscript. In the previous model version (Goujon et al., 2003), the LID definition was related to a value of the closed/total porosity ratio adjusted for each drilling site but time independent (see lines 387-389). This dependency on the geographic location with independence from climate is not self-consistent. This is why we tested another LID definition. Note that we do not directly parameterize the lock-in depth but only allow moderate variations of the lock-in density. This will be clarified in the revised manuscript by using the notation " ρ_{LI} " instead of " ρ_{LID} " and concluding on the small impact of the definition change.

This is done in the new version

L. 427: Degree of polynomial fit?

It is site dependent primarily because the number of density measurements is highly site dependent. The polynomial fits used will be provided in the supplement of the revised manuscript.

L. 405,6: "This parameterization leads to a much better agreement of the modelled LID with $\delta^{15}N$ measured at the available firn sampling sites than when using the outputs of the old model" This has nothing do with the model. It is just a different parameterization. The better agreement would apply for the old model as well.

This will be corrected in the revised manuscript.

Line 454-456: "This parameterization leads to ρ_{LI} variations in the range 780-840 kg/m^3 (Supplementary Figure S5) and a much better agreement between the modelled LID and $\delta^{15}N$ measured in firn samples at available sites than when using a fixed closed / total porosity ratio."

L. 456: "rough indicator of data quality" This seems a daring assumption, as natural variability might be in the same order of magnitude.

>> Completed as "rough indicator of data quality or estimate of natural variability"

L. 471: explain "traction constraint"

In the long term, mechanical strain conditions result in different crystal orientations in ice cores drilled near dome summits (where uniaxial compression along the vertical direction dominates) and along flow lines with a component of horizontal tension (see e.g. Montagnat et al., 2014, www.the-cryosphere.net/8/1129/2014/, and references therein). Moreover Vostok is located above a lake and the basal gliding results in a low shear stress, thus the crystal orientations likely results from a deformation in tension along the horizontal (Lipenkov et al., 1989). In the manuscript, we will replace "traction constraint" with "horizontal tension".

Line 529-531: "One possible reason is the very different flow regimes of the two sites, one being at a Dome summit, and the other on a flow line and subject to a horizontal tension (Lipenkov et al., 1989)."

L. 483 + 497: ?? " the original parameterization of Freitag et al. (2013) always remain in reasonable agreement with the data the incorporation of the impurity effects following the Freitag et al. (2013) parameterization in our model most often deteriorates the model-data agreement".

This is a good point, thanks. As some model tuning is performed prior to the incorporation of the impurity effect but not after, an overall slight but not significant degradation of the model results is obtained when adding the Freitag et al. (2013) parameterization. The inconsistency will be corrected in the revised manuscript.

Line 568-573: "The incorporation of the impurity effect following the Freitag et al. (2013) parameterization in our model slightly deteriorates the model-data agreement because no specific re-adjustment of model parameters was performed. However the model prediction of the density profiles remains correct although the impurity effect parameterization was developed for a different purpose: simulating density layering (Freitag et al., 2013). This encouraged us to test this simple parameterization in glacial climate conditions."

L. 509: "This effect is due to a densification rate that is too high in the first stage, and this formulation is not affected by the new temperature sensitivity." If this is a general feature, why is it not accounted for correctly?

Figure 3 in Alley (1987) indicates that the modeled densification rates tend to be somewhat too low at low densities and somewhat too high at higher densities. This induces an "S" shape of the density profile that is also visible in our model results. Correcting this bias would require an in-depth revision of the Alley (1987) mechanism. As we say at lines 513-514, the first stage of densification is not crucial for predicting the LID: the modifications of the Alley (1987) mechanism did not improve significantly the model results. In the revised manuscript, Figure 5 will include results with the "new model" and a single value of activation energy. This will further illustrate the small impact of the modifications in the first stage of densification.

Figure 5 has been modified

L. 613: "This observation questions the possible presence of a convective zone and/or .." Is the presence questioned or the constancy of the convective zone?

>> The **presence** of a significant convective zone is questioned for the LGM -> We will precise that it is clearly the presence of the convective zone at LGM that is questioned.

done

L. 689: "Evolution" It is not 'evolution' but 'dependence'. Fig. 8b: Vertical axis title: not Log(A) is shown but A on a log-scale. Fig. 8 could be probably presented in one single graph with A on a log-scale facilitating the comparison between the different temperature ranges.

The caption of Fig. 8 and axis of Fig.8b will be modified.

We think that it is important to keep the 3 figures. They are useful to see the different scenarios for the different temperatures and especially the addition of figure 8c (by comparison with only figure 8b) permits to observe the intersection points between the different scenarios.

We have tried different representations but did not find a better way to present the results and the associated discussion.

L. 709: "an inversion of the $\delta^{15}\text{N}$ difference" probably better: "a correct sign of the $\delta^{15}\text{N}$ difference". ok

L. 711: I strongly question the value of tests A to C. The chosen parameters are very arbitrary. I don't see what the authors want to show us, except that some parameters are better here and worse there, which is rather trivial.

>> We agree that test C was not very useful in the previous manuscript., We propose to replace the original test C by a sensitivity test run with $Q_3=15\text{kJ/mol}$ a value close to the lower bound of the observed range for activation energies (Jung et al., 2004, reference provided by Referee#1). Using 15 kJ/mol leads to intermediate results between the "old" and "new" model results. The only way to reconcile our model with $\delta^{15}\text{N}$ data by invoking a change of activation energy with temperature is to have a negligible influence of temperature on the densification rate below -50°C and hence to decrease Q_3 largely below 15 kJ/mol (1.5 kJ/mol). This will be discussed in the revised manuscript.

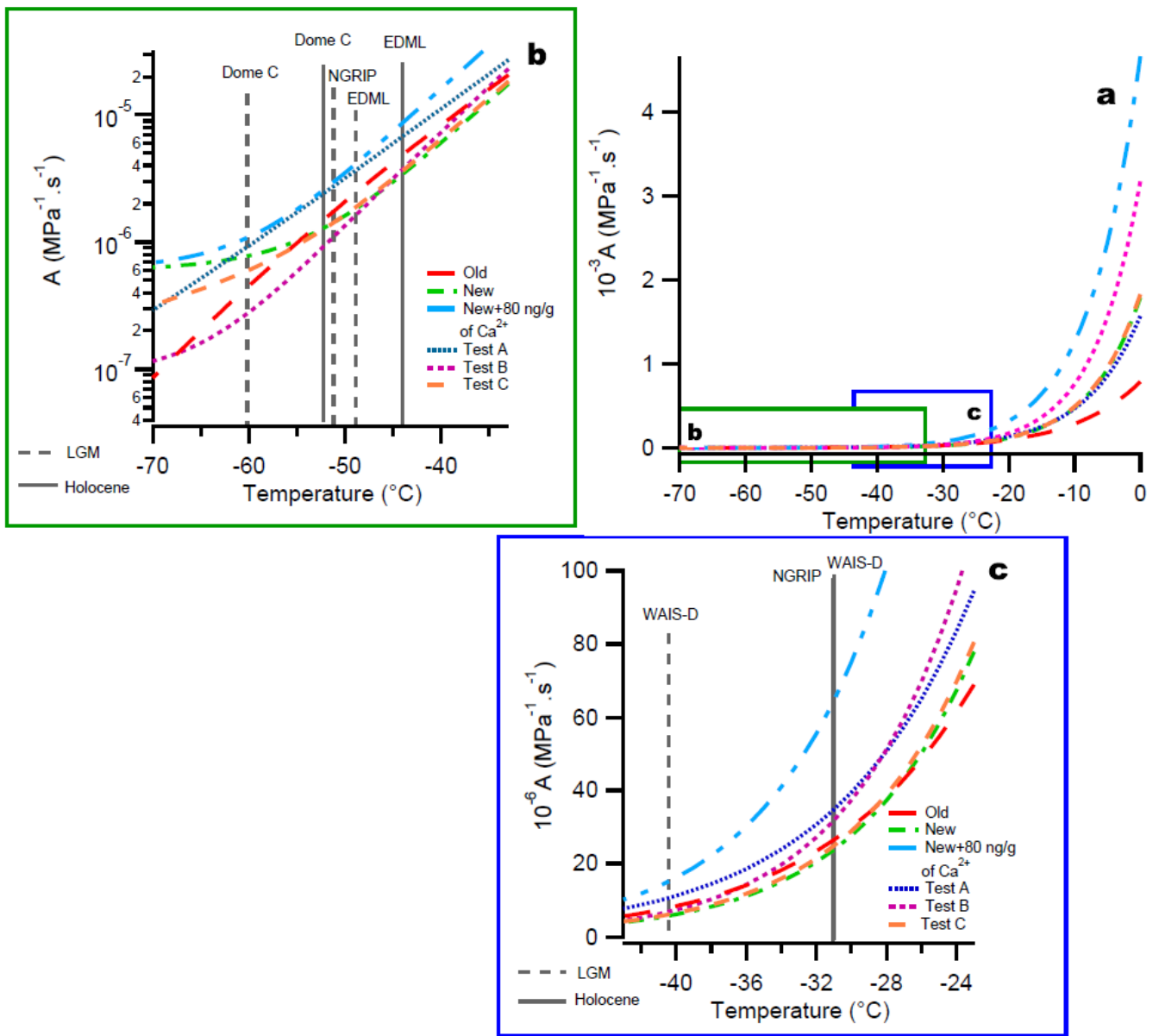


Figure 8 has been changed as well as the associated discussion. See for example the implementation of test C (based on experimental values for the activation energy as provided by reviewer 1) on lines 825-835: “Test C has been designed so that the activation energy at low temperature corresponds to estimates of activation energy for ice surface diffusion (Jung et al., 2004; Nie et al., 2009), a mechanism that is expected to be important at low temperature (Ashby, 1974). Using such a parameterization leads to a fair agreement between the modelled and the measured $\delta^{15}\text{N}$ change over the last deglaciation for the different sites. At Dome C, the correct sign for the $\delta^{15}\text{N}$ evolution between LGM and the Holocene is predicted by the model. However, the modelled $\delta^{15}\text{N}$ increase is still too small compared to the data and the $\delta^{15}\text{N}$ calculated by the “new model”. This is probably due to a too high creep parameter at low temperature. Summarizing, the best agreement between data and model for Dome C is obtained for the parameters given on Table 1: the creep parameter of “new model” flattens below -50°C and is thus not very different for the LGM or the EH at Dome C.”

L. 765: “.. instead of the Herron and Langway model..” -> instead of the parameters for the Herron and Langway model. ok

L. 781: "may act on deformation in opposite way" Why? Please explain.

>> "In particular, the solubility of dust particles, and their position inside or at the grain boundaries may act on deformation in opposite way" – the sentence is indeed not clear

It has been modified as:

"Dust particles do not always influence densification on the same way: dissolved particles soften firn and ice while the softening or hardening effect of non-dissolved impurities is less clear (Fujita et al., 2016; Alley et al., 1987)"

L. 797: " an up-to-date version " This is an empty phrase.

The phrasing will be modified

Line 924: "In this study, we have presented a revision of the LGGE firn densification model."

L. 787: " the new parameterization of the creep parameter preserves good agreement between the old model outputs and data at sites that were already well simulated"

Because the creep parameter is kept +- the same, so it is trivial.

The phrasing will be modified

Line 913-915: "To sum up, the new parameterization of the creep parameter has been designed to preserve good agreement between the old model outputs and data at sites that were already well simulated (WAIS-Divide, NGRIP, Talos Dome)."

L. 815: " This result is in agreement with the recent low delta age estimate by Parrenin et al. (2012) over the deglaciation at Dome C". No surprise, because it has been forced to agree.

>> This is true and will be specified in the conclusion

"The latest results are in good agreement with the recent determination of Δage within the AICC2012 timescale: 3920 years for EDC 21 ka and 5100 years for Vostok 21 ka. This is not unexpected since the EDC LID in the construction of the AICC2012 timescale is deduced from the EDC $\delta^{15}\text{N}$ scenario".

L. 850: "Ore" -> Core ok

Modelling the firn thickness evolution during the last deglaciation: constraints on sensitivity to temperature and impurities

Camille Bréant ^{1,2}, Patricia Martinerie ², Anaïs Orsi ¹, Laurent Arnaud ² and Amaëlle Landais ¹

¹Laboratoire des Sciences du Climat et de l'Environnement, UMR8212, CEA-CNRS-UPS/IPSL, Gif-sur-Yvette, France

²Univ. Grenoble Alpes, CNRS, IRD, IGE, UMR5001, Grenoble, F-38000, France

The transformation of snow into ice is a complex phenomenon difficult to model. Depending on surface temperature and accumulation rate, it may take several decades to millennia for air to be entrapped in ice. The air is thus always younger than the surrounding ice. The resulting gas-ice age difference is essential to document the phasing between CO₂ and temperature changes especially during deglaciations. The air trapping depth can be inferred in the past using a firn densification model, or using $\delta^{15}\text{N}$ of air measured in ice cores.

All firn densification models applied to deglaciations show a large disagreement with $\delta^{15}\text{N}$ measurements in several sites of East Antarctica, predicting larger firn thickness during the Last Glacial Maximum, whereas $\delta^{15}\text{N}$ suggests a reduced firn thickness compared to the Holocene. We present here modifications of the LGGE firn densification model, which significantly reduce the model-data mismatch for the gas trapping depth evolution over the last deglaciation at cold sites of East Antarctica, while preserving the good agreement between measured and modelled modern firn density profiles. In particular, we apply a dependency of the creep factor on temperature and impurities in the firn densification rate calculation. The temperature influence intends to reflect the dominance of different mechanisms for firn compaction at different temperatures. We show that both the new temperature parameterization and the influence of impurities contribute to the increased agreement between modelled and measured $\delta^{15}\text{N}$ evolution during the last deglaciation at sites with low temperature and low accumulation rate, such as Dome C or Vostok. We find that a very low sensitivity of the densification rate to temperature has to be used in coldest conditions. The inclusion of impurities effects improves the agreement between modelled and measured $\delta^{15}\text{N}$ at cold East Antarctic sites during the last deglaciation, but deteriorates the agreement between modelled and measured $\delta^{15}\text{N}$ evolution in Greenland and Antarctic sites with high accumulation unless threshold effects are taken into account.

1. Introduction

Ice cores are important tools to decipher the influence of different forcings on climate evolution. They are particularly useful to reconstruct the past variations of polar temperature and greenhouse gases. The longest record covers 8 last glacial – interglacial cycles (EPICA community members, 2004; Jouzel et al., 2007; Loulergue et al., 2008; Lüthi et al., 2008) and very high resolution climate records can be retrieved from ice cores drilled in high accumulation regions (Marcott et al., 2014; Rhodes et al., 2015; WAIS Divide Project Members, 2013, 2015).

Polar ice is a porous medium, and contains bubbles filled with ancient atmospheric air, allowing the reconstruction of the atmospheric composition in the past. The air is trapped at about 100 m under the ice sheet surface. Above that depth, the interstitial air in firn pores remains in contact with the atmosphere. Consequently, the air is always younger than the surrounding ice and this age difference, Δ_{age} , can reach several millennia at the low temperature and accumulation rate sites of East Antarctica.

A precise determination of Δ_{age} is essential to quantify the link between temperature changes recorded in the water isotopic measurements on the ice phase and greenhouse gas concentrations recorded in the gas phase. Still, quantifying the temporal relationship between changes in greenhouse gas concentrations in air bubbles and changes in polar temperature recorded in the isotopic composition of the ice is not straightforward. One way to address this question goes through the development of firn densification models that depict the progressive densification of snow to ice, and the associated decrease of porosity. Below a certain threshold density, the pores seal off and the air is trapped. The firn densification models thus calculate the Lock-in Depth (hereafter LID) according to surface climatic conditions. A higher temperature accelerates the firn metamorphism and leads to a lower LID. On the other hand, a higher snow accumulation at the surface will have the effect of increasing the firn sinking speed and hence the LID.

On glacial – interglacial timescales, increasing temperature is associated with increasing snow accumulation. Indeed, the thermodynamic effect dominates when dealing with long term averages (several thousands of years), even if accumulation and temperature are not always correlated on millennial and centennial timescale in polar regions, especially in coastal areas (e.g. Fudge et al., 2016; Altnau et al., 2014). As a consequence, when comparing LGM and Holocene averages, we observe for all available ice cores covering the last deglaciation increases in both accumulation and temperature. In the firn densification model, both effects partially compensate each other, with the temperature effect being dominant in the current densification models for the LID simulation over

glacial – interglacial transitions in deep drilling sites of the East Antarctic plateau, hence leading to the modelled LID decrease.

A first class of densification models is based on an empirical approach to link accumulation rate and temperature at different polar sites to densification rates (allowing the match between the modelled and the measured density profiles) (e.g. Herron and Langway, 1980). The Herron and Langway (1980) model assumes that the porosity (air space in the firn) variations directly relate to the weight of the overlying snow, hence the accumulation rate. A temperature dependence following an Arrhenius law is also implemented to account for a more rapid compaction at higher temperature. Finally, the exact model sensitivity to temperature and accumulation rate is adjusted empirically in order to simulate observed density profiles. Measured density profiles exhibit different densification rates above and below 550 kg/m^3 so that different empirical laws are used for densities above and below this threshold. Indeed, 550 kg/m^3 corresponds to the observed maximum packing density of snow (e. g. Anderson and Benson, 1963), hence to a change in the driving mechanism of firnification.

Despite its simple empirical description, and although more sophisticated empirical models have been developed (Arthern et al., 2010; Helsen et al., 2008; e.g. Li and Zwally, 2004; Ligtenberg et al., 2015), the Herron and Langway (1980) firn model often provides good quality results and is still used in a number of ice core studies (e.g. Buizert et al., 2015; Overly et al., 2015, Lundin et al., 2017). However, its validity is questionable when used outside of its range of calibration, such as glacial periods at cold sites of the East Antarctic plateau for which no present-day analogue exists. As a consequence firn models including a more physical description of densification have been developed (e.g. Arnaud et al., 2000; Salamatin et al., 2009). The model developed over the past 30 years at LGGE (Arnaud et al., 2000; Barnola et al., 1991; Goujon et al., 2003; Pimienta, 1987) aims at using a physical approach which remains sufficiently simple to be used on very long time scales (covering the ice core record length). More complex models, explicitly representing the material micro-structure have been developed but require a lot more computing time (Hagenmuller et al., 2015; Miller et al., 2003). Still, the simplified physical mechanisms in our model include parameters adjusted through comparison of modelled and measured present-day firn density profiles which may induce biased results outside the range of calibration.

In parallel to firn densification modelling, past firn LID can also be determined using the $\delta^{15}\text{N}$ measurements in the air trapped in ice cores. Indeed, in the absence of transient thermal gradients,

the $\delta^{15}\text{N}$ trapped at the bottom of the firn is mainly related to the diffusive column height (DCH). This is due to gravitational settling in the firn following the steady state barometric equation (Craig et al., 1988; Schwander, 1989; Sowers et al., 1989):

$$\delta^{15}\text{N}_{grav} = \left[\exp\left(\frac{\Delta mgz}{RT_{mean}}\right) - 1 \right] 1000 \approx \frac{gz}{RT_{mean}} \Delta m \times 1000 (\text{‰}) \quad (1)$$

Where Δm is the mass difference (kg/mol) between ^{15}N and ^{14}N , g is the gravitational acceleration (9.8 m/s²), R is the gas constant (8.314 J/mol/K), T_{mean} is the mean firn temperature (K), and z is the diffusive column height (m) noted (DCH). In the absence of convection at the top of the firn, the firn LID is equal to the DCH.

In Greenland ice cores, where strong and abrupt surface temperature changes occurred during the last glacial period and deglaciation, $\delta^{15}\text{N}$ is also affected by **strong** thermal fractionation. An abrupt warming (on the order of 10°C in less than 50 years) indeed induces a transient temperature gradient in the firn of a few degrees (Severinghaus et al., 1998; Guillevic et al., 2013; Kindler et al., 2014). $\delta^{15}\text{N}$ is thus modified as $\delta^{15}\text{N}_{therm} = \Omega \cdot \Delta T$, where Ω is the thermal fractionation coefficient (Grachev and Severinghaus, 2003) and this thermal signal is superimposed on the gravitational one (the $\delta^{15}\text{N}_{therm}$ observed is in most cases lower than 0.15‰).

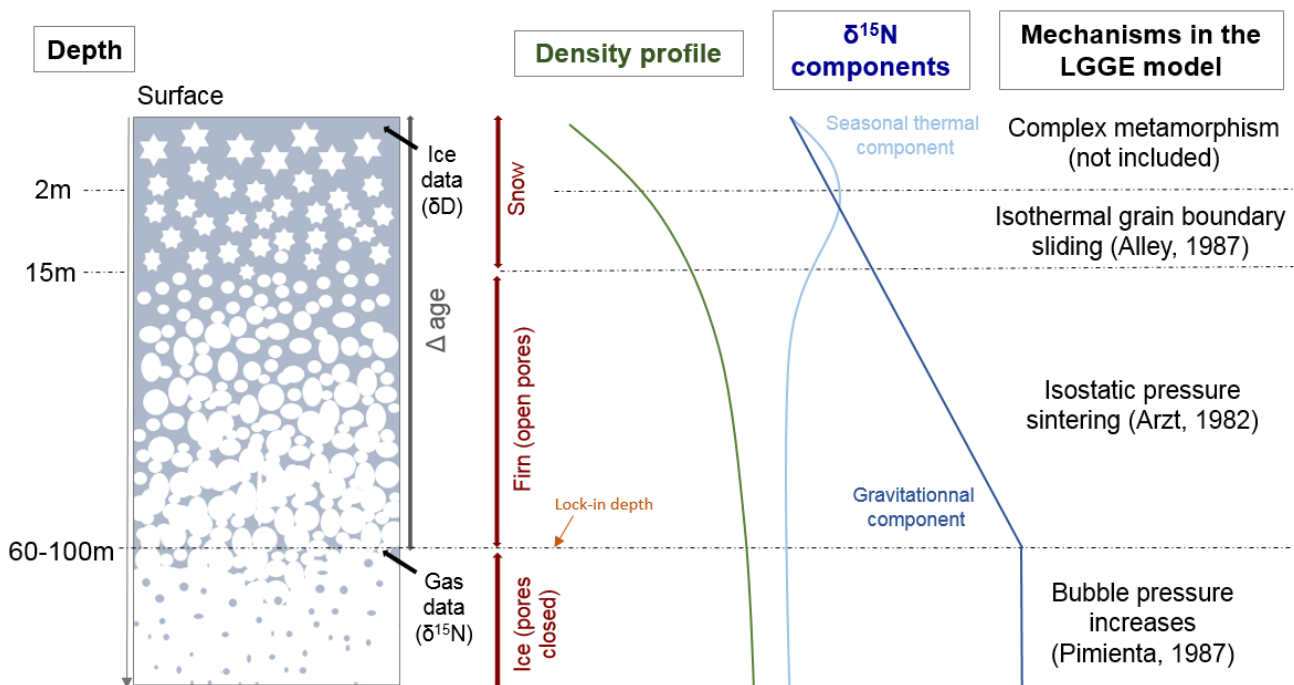


Figure 1: Overview of snow densification and influence on the $\delta^{15}\text{N}$ profile in the absence of any significant convective zone as observed in most present-day $\delta^{15}\text{N}$ profiles (Landais et al., 2006; Witrant et al., 2012).

While models can reproduce the observed $\delta^{15}\text{N}$ at Greenland sites over the last climatic cycle, a strong mismatch is observed for cold Antarctic sites, especially on the East-Antarctic plateau (Dreyfus et al., 2010). In particular, both the empirical and physical models predict a decrease of the LID during glacial to interglacial transitions (Goujon et al., 2003; Sowers et al., 1992) while the $\delta^{15}\text{N}$ evolution indicates an increase of the LID (Capron et al., 2013; Sowers et al., 1992). The decrease in the LID in the models is caused by the increase in temperature during the deglaciation, which has a stronger impact than the increase in the accumulation rate. The differences in modelled and measured $\delta^{15}\text{N}$ for glacial period in cold sites of the East-Antarctic plateau have important consequences for the Δage estimate and hence the ice core chronology: using the firn densification models, the modelled Δage for glacial period at Vostok and Dome C is too large by several centuries (Loulergue et al., 2007; Parrenin et al., 2012).

Several hypotheses have already been evoked to explain the $\delta^{15}\text{N}$ model-data mismatch in Antarctica as detailed in Landais et al. (2006), Dreyfus et al. (2010) and Capron et al. (2013). First, the firnification models have been developed and tuned for reproducing present-day density profiles and it is questionable to apply them to glacial climate conditions in Antarctica for which no present-day analogues are available. Second, increasing impurity concentration has been suggested to fasten firn densification during glacial period (Freitag et al., 2013; Hörhold et al., 2012). Third, a ~ 20 m deep convective zone has been evidenced in the megadunes region in Antarctica (Severinghaus et al., 2006) hence suggesting that deep convective zones can develop in glacial periods in Antarctica and explain the mismatch between firn densification model and $\delta^{15}\text{N}$ data (Caillon et al., 2003). This hypothesis can explain the mismatch between modelled and measured $\delta^{15}\text{N}$ at EDML during glacial period by invoking a 10 m convective zone (Landais et al., 2006). However, it has been ruled out for explaining the strong mismatch between model and $\delta^{15}\text{N}$ data at EDC for the last glacial period (Parrenin et al., 2012). Fourth, firn densification is very sensitive to changes in temperature and accumulation rate so that uncertainties in the surface climate parameters can lead to biased value of the modelled LID and hence $\delta^{15}\text{N}$. Fifth, a significant thermal fractionation signal can affect the total $\delta^{15}\text{N}$ signal. However, this hypothesis has been ruled out by Dreyfus et al. (2010) based on $\delta^{15}\text{N}$ and $\delta^{40}\text{Ar}$ data on the last deglaciation at EDC.

In this study, we test whether simple modifications of the LGGE model can reduce the model-data mismatch for the LID evolution over the last deglaciation in sites on the East Antarctic plateau. In particular, it has been suggested by Capron et al. (2013) that the firn densification rate is

underestimated at very low temperature. We also examine the possible influence of impurity concentration in the LGGE model following the approach by (Freitag et al., 2013; Hörhold et al., 2012). The manuscript is organized as follows. In the next (second) section we present the physical model with a focus on recent modifications. In a third section, we confront the model outputs to present-day observed firn density profiles and $\delta^{15}\text{N}$ data over the last deglaciation at different polar sites from Greenland and Antarctica. Section 4 summarizes our conclusions.

2. Densification model description and improvements

An in-depth description of the LGGE firn densification model is provided in Goujon et al. (2003). Here we first briefly summarize its content, and then detail the modifications introduced in this study. The main inputs to the model are temperature and snow accumulation rate (Supplementary Text S1). During climatic transitions occurring at similar or shorter time scales than firnification, the propagation of the atmospheric temperature signal into the firn has to be taken into account (Schwander et al., 1997). The thermo-mechanical model comprises four modules. A simple ice sheet flow module calculates the vertical speed in a 1D firn and ice column. This vertical speed is used in the thermal module to calculate heat advection. The thermal module solves the heat transfer equation, which combines heat advection and heat diffusion across the whole ice-sheet thickness. Using the resulting temperature profile in the firn, the mechanical module evaluates the densification rates resulting from three successive mechanisms detailed below. Finally, a gas-age module keeps track of snow layers sinking in a Lagrangian mode and uses a gas trapping criterion in order to evaluate the gas trapping depth and the ice age – gas age difference (Δage).

The model does not take into account the complex mechanisms associated with snow metamorphisms under the influence of strong temperature gradients, wind and sublimation/re-condensation (Colbeck, 1983; Kojima, 1967; Mellor, 1964). This kind of metamorphism affects the 1-3 meters at the top of the firn and has a minor role on the modelled LID.

Below this depth, the densification of snow into ice has been divided in three stages (e.g. Maeno and Ebinuma, 1983 and references therein; Figure 1). The first stage, named “snow densification” as in Goujon et al. (2003), corresponds to a rearrangement and packing of snow grains until approaching the maximum compaction at a density of about 550 kg/m^3 (or 0.6 on a unitless scale relative to the density of pure ice) defined as the critical density. The second stage represents the “firn densification” by sintering associated with visco-plastic deformation. Finally, when the bubbles are closed (at a relative density of about 0.9), the ice densification is driven by the difference in

pressure between air trapped in bubbles and the solid ice matrix subject to the weight of the overlying firn structure. In reality, the adjacent densification mechanisms likely coexist at intermediate densities. Below we further describe the mechanical structure of the model with a focus on recent modifications and proposed parameterizations. We refer to Arnaud et al. (2000) and Goujon et al. (2003) for more details.

The model uses macroscopic (simplified) mechanical laws, which link the densification speed (dD_{rel}/dt , in terms of relative density ($D_{rel} = \frac{\rho}{\rho_{ice}}$)) to its main driving force: the overburden pressure of overlying snow. It is important to note that in our model, the accumulation rate influences firn densification only through the overburden pressure:

$$P(h) = g \int_0^h \rho dz \quad (2)$$

where g is the gravity constant and ρ is the density in kg/m^3 . This differs from the Herron and Langway (1980) model where the effect of accumulation rate is adjusted and expressed with a different power law for snow and firn densification rates. In porous materials, the overburden pressure P is transmitted through contact areas between grains rather than the entire surface of the material. This is expressed by replacing P with an effective pressure P_{eff} in mechanical stress-strain laws. The relationship between P and P_{eff} depends on the material geometry (e.g. Equation A4 in Goujon et al., 2003). A higher temperature (T) facilitates the deformation of materials, and this effect is commonly represented by an Arrhenius law: $e^{\left(\frac{-Q}{RT}\right)}$ where R is the gas constant and Q an activation energy. The value of the activation energy depends on the underlying physical mechanism of ice and snow deformation but Arrhenius expressions cannot represent deformation effects linked to ice melting. The relationships between densification speed and overburden pressure take the following general form:

$$\frac{dD_{rel}}{dt} = A_0 \times e^{\left(\frac{-Q}{RT}\right)} \times (P_{eff})^n \quad (3)$$

where $A_0 = 7.89 \times 10^{-15} \text{ Pa}^{-3} \cdot \text{s}^{-1}$ (Goujon et al., 2003, Eq. A5). A_0 represents the dependency of the deformation speed on the material geometry change and n is the stress exponent. In the rest of the manuscript, we will refer to $A = A_0 \times e^{\left(\frac{-Q}{RT}\right)}$ as the creep parameter.

2.1 Densification of snow

During the first stage, the dominant snow densification mechanism is assumed to be isothermal

boundary sliding and the model of Alley (1987) is used (Figure 1). The geometrical approximation used to build the model is to represent snow as equal size spheres with a number of contacts between neighbours increasing with density. In the LGGE model, the Alley mechanism is implemented as Equation A1 in Goujon et al. (2003):

$$\frac{dD_{rel}}{dt} = \gamma \left(\frac{P}{D_{rel}^2} \right) \left(1 - \frac{5}{3} \times D_{rel} \right) \quad (4)$$

It directly relates to Equation (5) in Alley (1987):

$$\frac{dD_{rel}}{dt} = \frac{2}{15} \times \frac{\lambda}{\nu} \times \frac{R}{r^2} \times \left(1 - \frac{5}{3} * D_{rel} \right) \times \frac{P}{D_{rel}^2} \quad (5)$$

where λ is the bond thickness, ν the bond viscosity, R the grain radius and r the bond radius. P is expressed as a function of accumulation and gravity (Equation 2).

The important simplification in the LGGE model is the replacement of geometry dependent parameters, not available for past conditions, with a variable γ , adjusted in order to obtain a continuous densification rate at the boundary between the first and the second stage of densification.

A first modification in this module consists of extending the Alley (1987) scheme to the upper two meters of the firn rather than using a constant density value. Indeed, since the model is not able to represent the metamorphism of the first two meters, we impose a constant pressure of 0.1 Bar (see Equation 6), which is an approximation of the pressure at 2-3 m depth. It results in a nearly constant densification rate in the top 2-3 m rather than a constant density in the top 2 meters.

The second modification concerns the transition between the snow and firn densification stages at the relative density of 0.6. In Equation (4), the term $\left(1 - \frac{5}{3} \times D_{rel} \right)$ implies that the densification speed drops to zero at $D_{rel} = \frac{3}{5}$ (i.e. 0.6 the maximal compaction density). The second stage of densification (firn densification) is driven by an important overburden pressure on the contact area hence associated with a high densification speed. The transition between the sharp decrease of the densification speed for D_{rel} values close to 0.6 in the snow densification stage and the high densification speed at the beginning of the firn densification (i.e. in the same range of value for D_{rel}) causes some model instabilities especially at sites with high temperature and accumulation rate. In order to improve the model stability, we go back to the definition of the term $\left(1 - \frac{5}{3} \times D_{rel} \right)$ in the initial formulation of Alley (1987). This term relies on a correlation between the coordination number (N) and relative density: $D_{rel} = 10 N$. We slightly modified this relationship and imposes $D_{rel} =$

10 N - 0.5 which better matches the data on Figure 1 of Alley (1987). This results in replacing the term $\left(1 - \frac{5}{3} \times D_{rel}\right)$ in Equation (4) with $\left(1 + \frac{0.5}{6} - \frac{5}{3} \times D_{rel}\right)$. This modification shifts the density at which the densification rate becomes relative zero from 0.6 to 0.65 and suppresses the model instability.

We also examine the effect of temperature on the first-stage densification mechanism and on the critical density. Alley (1987) calculated a viscosity (ν) related activation energy of 41 kJ/mol, consistent with recommended values for grain-boundary diffusion (42 kJ/mol) or measured from grain growth rate (Alley, 1987 and references therein). In Goujon et al. (2003), no explicit temperature effect is used but the parameter γ varies by several orders of magnitude from site to site. The parameter γ is calculated to maintain a continuous densification rate between the first and second stages at a chosen critical density. We translate the variations of $\gamma = (2 \lambda R) / (15 \nu r^2)$ from site to site into $\gamma = \gamma' \exp(-Q/RT)$, and calculate the activation energy Q using a classical logarithmic plot as a function of 1000/T (see e.g. Herron and Langway, 1980). We obtain a value of 48 kJ/mol. Using the revised temperature dependency for the firm densification mechanism (see next section), a slightly higher value of Q = 49.5 kJ/mol is calculated (Supplementary Figure S1). This is fairly similar to the values in Alley (1987) but much higher than the value in the upper firm of the Herron and Langway (1980) model: 10.16 kJ/mol. Incorporating this explicit temperature dependency term, we obtain our new final expression for the upper firm densification rate:

$$\frac{dD_{rel}}{dt} = \gamma' \left(\frac{\max(P, 0.1 \text{ bar})}{D_{rel}^2} \right) \left(1 + \frac{0.5}{6} - \frac{5}{3} \times D_{rel} \right) \times e^{\left(\frac{-Q}{RT} \right)} \quad (6)$$

where $\gamma' \times e^{\left(\frac{-Q}{RT} \right)}$ is equivalent to γ in Equation (4). However γ varies by two orders of magnitude as a function of temperature whereas γ' remains in the range from 0.5×10^9 to 2×10^9 bar⁻¹.

Finally, the temperature dependency of the critical density, which defines the boundary between the first and second stage densification mechanisms, is also re-evaluated. According to Benson (1960) and Arnaud (1997; 2000), this critical density increases with temperature. However the slope change in density profiles associated with the critical density may be difficult to locate and the Benson (1960) and Arnaud (1997) parameterizations are based on only few observation sites. We evaluate the critical density values which allow the best match of density data by our model results at 22 sites and do not find any correlation between critical density and temperature or accumulation rate (Supplementary Figure S2). We thus remove this dependency with temperature included in the

old version of the LGGE model and use a mean relative critical density of 0.56 at the boundary between the first and second stage of densification in the new version of the model. The effect of surface density was also tested and does not have a strong impact on the model results (Supplementary Figure S3).

2.2 Densification of firn

At this stage, the observation of density profiles with depth suggests that the densification rate is controlled by a classical power law creep as used for ice deformation (Arzt et al., 1983; Maeno and Ebinuma, 1983; Wilkinson and Ashby, 1975). Arzt (1982) proposed a pressure sintering mechanism for firn densification following a power law creep and taking into account the progressive increase of the coordination number. He solved the geometrical problem of compressing a random dense packing of monosized spheres with associated deformation of each sphere into irregular polyhedra. Equation (23) of Arzt (1982) is directly used in the firn densification model.

2.2.1 Revised temperature sensitivity of the firn densification rate

A strong assumption in the firn densification module is the constant activation energy corresponding to self-diffusion of ice (60 kJ/mol). This choice corresponds to a unique mechanism supposed to drive densification. Densification is thus assumed to be driven by dislocation creep (Ebinuma and Maeno, 1987) in which the associated mechanism is lattice diffusion or self-diffusion. At the grain scale, we can describe the lattice diffusion processes associated with dislocation as diffusion within the grain volume of a water molecule from a dislocation site in the ice lattice to the grain neck in order to decrease the energy associated with grain boundaries (Blackford, 2007). Typically, an activation energy of 60 to 75 kJ/mol is associated with this mechanism (Arthern et al., 2010; Barnes et al., 1971; Pimienta and Duval, 1987; Ramseier, 1967 and references therein).

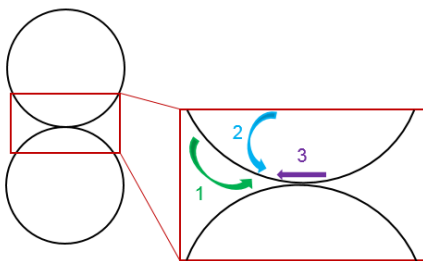
However, multiple studies have already shown that several (6 or more) mechanisms can act together for firn or ceramic sintering (Ashby, 1974; Blackford, 2007; Maeno and Ebinuma, 1983; Wilkinson and Ashby, 1975): lattice diffusion from dislocations, grain surfaces or grain boundaries; vapor transport; surface and boundary diffusions. In order to properly take these different mechanisms into account, different activation energies (one activation energy per mechanism) should ideally be introduced in the firn densification model. Actually, it has been observed that, at warm temperature, an activation energy significantly higher than 60 kJ/mol could be favoured (up to 177 kJ/mol between -1 and -5°C [Jacka and Li, 1994]) in order to best fit density

profiles with firn densification models (Arthern et al., 2010; Barnes et al., 1971; Jacka and Li, 1994, Morgan, 1991). This suggests that a mechanism different from lattice diffusion is dominant for grain compaction at high temperature (i.e. higher than -10°C). At low temperature (-50°C), by analogy with ceramic sintering, lattice diffusion from the surface of the grains and/or boundary diffusion from grain boundaries should be favoured (Ashby, 1974). The activation energy for surface diffusion is estimated to be in the range 14-38 kJ/mol (Jung et al., 2004; Nie et al., 2009).

Following these arguments and despite the lack of experimental constraints to test this assumption, we propose a new parameterization of the activation energy in the LGGE firn densification model which increases the firn densification rate at low temperatures. We have thus enabled introduction of three adjusted activation energies as proposed in Table 1 and Figure 2. We have replaced the creep parameter in Equation (3) by:

$$A = A_0 \times \left(a_1 \times e^{\frac{-Q_1}{RT}} + a_2 \times e^{\frac{-Q_2}{RT}} + a_3 \times e^{\frac{-Q_3}{RT}} \right) \quad (7)$$

We have chosen a minimal number of mechanisms (3) for simplicity in the following but the conclusions of our work would not be affected by a choice of more mechanisms.



- Close to melting temperature: mass transfer by diffusion (potential mechanism for high temperature)
(1) mechanism 1 associated with activation energy Q_1
- Low temperature: lattice diffusion (classical mechanism)
(2) mechanism 2 associated with activation energy Q_2
- Very low temperature : boundary diffusion from grain boundary (potential mechanism for low temperature)
(3) mechanism 3 associated with activation energy Q_3

Figure 2: Different sintering mechanisms of snow for different temperatures proposed by analogy with the hot ceramic sintering (inspired by Figure 1 in Ashby, 1974). Note that more sintering mechanisms can be found in the literature and the attributions of 3 different mechanisms for the firn densification model is only a working hypothesis here.

When building the new parameterization of the activation energy (Equation 7), the determination of Q_1 , Q_2 and Q_3 on the one side and a_1 , a_2 and a_3 on the other side are not independent from each other. We first determine three temperature ranges corresponding to the dominant mechanisms, then we attribute values to the activation energies Q_1 , Q_2 and Q_3 . The coefficients a_1 , a_2 and a_3 are finally adjusted to produce the expected evolution of the creep parameter with temperature, to best reproduce $\delta^{15}\text{N}$ evolution over deglaciations (Section 3.2) and respect the firn density profiles available (Section 3.1).

Hundreds of sensitivity tests have been performed using a strategy based on dichotomy to reduce the mismatch between modeled and data. The constraint of keeping a correct agreement of model results with present day density profiles and for the last deglaciation at warm sites strongly reduces the possible choices of a_i and Q_i (Section 3). The best value obtained for Q_3 is lower than published values for surface or boundary diffusion but is necessary to reproduce the deglaciation at cold East Antarctic Sites. Sensitivity test C will illustrate the effect of using a higher value.

The resulting expression for the creep parameter A (Equation 7), does not strongly differ from using simply $A = A_0 \times e^{\left(-\frac{60000}{RT}\right)}$, as used in the original model. To illustrate this point, we calculated an equivalent activation energy, Q_{eq} , such that $A = A_0 \times e^{\left(-\frac{Q_{eq}(T)}{RT}\right)}$, and found Q_{eq} varying between 54 and 61 kJ/mol (Supplementary Figure S4). Thus only moderate changes to the densification equation are needed to improve the behaviour of the model at cold temperature. In addition, only moderate changes in Q_{eq} are allowed to preserve the consistency between model results and present-day density profiles.

Activation Energy (J/mol)	Coefficient
$Q_1 = 110000$	$a_1 = 1.05 \cdot 10^9$
$Q_2 = 75000$	$a_2 = 1400$
$Q_3 = 1500$	$a_3 = 6.0 \cdot 10^{-15}$

Table 1: Preferred set of values for the three activation energies and associated pre-exponential constants

2.2.2 Sensitivity of the firn densification rate to impurities

Firn densification can be influenced by impurity content in snow. Alley (1987) already suggested that grain growth is influenced by impurities dissolved in ice, and that impurities in the grain boundaries affect the relative movement of snow grains. More recently, Hörhold et al. (2012) observed a correlation between the small scale variability of density and calcium concentration in Greenland and Antarctic firn cores. Based on

this observation, Freitag et al. (2013) proposed that the densification rate depends on the impurity content. They implemented an impurity parameterization in two widely used densification models (Herron and Langway, 1980; Barnola et al., 1991), and were able to reproduce the density variability in two firn cores from Greenland and Antarctica.

We have implemented this parameterization in our model with the simple assumption that the impurity effect is the same for all mechanisms. It allows us to keep the number of tunable parameters to a minimum, even though this assumption is probably not correct for the vapor diffusion process. Note however that this will not affect the applications discussed below since vapor diffusion is only important for warm sites. Concretely, we start again from the evolution of the creep parameter with respect to temperature given in Equation (7) and add a dependency to calcium concentration such as:

$$\text{if } [Ca^{2+}] > [Ca^{2+}]_{crit} : Q' = f_1 \times \left[1 - \beta \ln \left(\frac{[Ca^{2+}]}{[Ca^{2+}]_{crit}} \right) \right] \times Q \quad (8)$$

$$\text{if } [Ca^{2+}] < [Ca^{2+}]_{crit} : Q' = f_1 \times Q \quad (9)$$

With, $[Ca^{2+}]_{crit} = 0.5 \text{ ng/g}$ (the detection limit of continuous flow analysis). Q' represents the new activation energy calculated as a function of the calcium concentration for each site. Our main simulations are performed with the f_1 and β calculated by Freitag et al. (2013) for application within the Herron and Langway model: $f_1 = 1.025$, $\beta = 0.01$. Using the values for application within the Pimienta-Barnola model ($f_1 = 1.015$, $\beta = 0.0105$) leads to similar results (Section 3.2). For a first evaluation of the impurity effect in our model, both the temperature and impurity effects are combined through the application of Equations (8) and (9) to each of the three different activation energies Q_1 , Q_2 and Q_3 . We use raw data of the calcium concentration for all the sites when available even if question may arise on calcium concentration being the best diagnostic for dust content.

The values of a_i and Q_i were not readjusted after the implementation of impurity effects to avoid adding tuning parameters. Still, because the large range of calcium concentrations encountered in past climate conditions has a strong impact on model results, this may be a solution to reduce the model-data mismatch. This is explored in Section 3 through a sensitivity test D. In the same section, we will also propose a modification of the Freitag parameterization using thresholds to reduce the model-data mismatch.

2.3 Densification of ice

As in Goujon et al. (2003), the final densification stage begins at the close-off density derived from

air content measurements in mature ice. Further porosity reduction results in an air pressure increase in the bubbles (Martinerie et al., 1992, Appendix 1). This density is calculated using the temperature dependent close-off pore volume given by Martinerie et al. (1994). Further densification of this bubbly ice is driven by the pressure difference between ice matrix and the air in bubbles (Maeno and Ebinuma, 1983; Pimienta, 1987). The densification rate strongly decreases with depth as these two opposite pressures tend to balance each other (Goujon et al., 2003). This stage is not essential for this study since $\delta^{15}\text{N}$ entrapped in air bubbles does not evolve anymore.

2.4 Lock-in depth

In the previous version of the model, the LID was computed as a fixed closed to total porosity ratio. The ratio value used has been adjusted for each drilling site, for example it is 21% for Vostok and 13% at Summit in Goujon et al. (2003), but it was time independent and thus insensitive to climate. We revised the LID definition in order to relate its present day geographic variations to climatic parameters.

Ideally, $\delta^{15}\text{N}$ profiles in the open porosity of the firn follow the barometric slope in the diffusive zone, and show no variations in the lock-in zone. However $\delta^{15}\text{N}$ data can deviate from this behaviour, especially at the very low accumulation rate sites such as Dome C, Vostok or Dome Fuji, where no $\delta^{15}\text{N}$ plateau is observed in the lock-in zone (Bender et al., 1994; Kawamura et al., 2006; Landais et al., 2006). Moreover, as we aim at comparing our model results with $\delta^{15}\text{N}$ data in deep ice cores, the most consistent LID definition should refer to $\delta^{15}\text{N}$ data in mature ice but very few measurements are available for recent ice. Systematic $\delta^{15}\text{N}$ measurements in the closed porosity of the deep firn or recently formed mature ice would be very helpful to better constrain the LID in the future. We take advantage of recent advances in gas transport modelling (Witrant et al., 2012) that allowed correct simulation of the $\delta^{15}\text{N}$ behaviour in deep firn. Observations of modern firn air profiles show that the thickness of the lock-in zone (the zone in the deep firn with constant $\delta^{15}\text{N}$) increases when the snow accumulation rate increases (Witrant et al., 2012). We estimate $\delta^{15}\text{N}$ in ice, i.e. after complete bubble closure, at 12 firn air pumping sites with the Witrant et al. (2012) model. For each site, the lock-in density (ρ_{LI}) is then defined as the density at which the modelled $\delta^{15}\text{N}$ value in the open porosity of the firn equals the modelled $\delta^{15}\text{N}$ in ice. The resulting lock-in density is strongly related to the accumulation rate (Supplementary Figure S5). As a result, we parameterized the lock-in density (ρ_{LI}) as a function of the accumulation rate, following:

$$\rho_{\text{LI}} = 1.43 \times 10^{-2} \times \ln(1/A_c) + 0.783 \quad (10)$$

This parameterization leads to ρ_{LI} variations in the range 780-840 kg/m³ (Supplementary Figure S5) and a much better agreement between the modelled LID and $\delta^{15}N$ measured in firn samples at available sites than when using a fixed closed / total porosity ratio. However, when used for simulating the LID during glacial periods with extremely low accumulation rate, it can predict a lock-in density that is higher than the close-off density, which is unrealistic. We thus also added a threshold in our new definition of the lock-in density: when ρ_{LI} exceeds the close-off density (ρ_{CO} , Section 2.3), we impose ρ_{LI} to be equal to ρ_{CO} .

3. Results

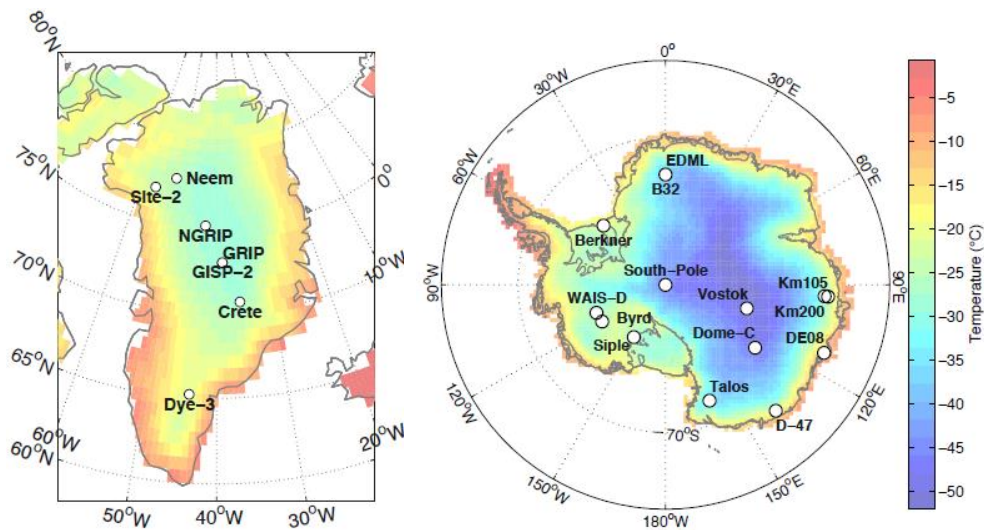


Figure 3: Maps of Greenland and Antarctica showing field sites and mean annual temperature from ERA interim (Dee et al., 2011)

3.1 Firn density profiles

We assessed the behaviour of the model by comparing measured and modelled firn density profiles from 22 sites from Greenland and Antarctica (Figure 3). Figure 4 shows this comparison at Byrd, NEEM, Dome C and Vostok, and other sites are displayed in the supplement (Supplementary Figure S6). A polynomial fit was adjusted to the density data in order to facilitate the comparison with model results. The data dispersion around the fit can be due natural density variations and/or measurement uncertainties.

A comparison of snow density measurement methodologies concluded that uncertainties are about 10 % (Proksch et al., 2016). Moreover, although firn density profiles are often used, the measurement technique is not always well documented. Efforts were made in this study to mention the methodology when available (Supplementary Table S1). At high densities (below bubble closure depth), the hydrostatic weighing technique is expected to be about 10 times more precise than simple volume and mass measurements (Gow, 1968) but rarely used, although it is important to correctly evaluate the fairly small density difference with pure ice density. We should note that the agreement between our model results and data is good at high densities for the three sites where hydrostatic weighing technique was used: Site 2 and D-47 (Supplementary Figure S6) as well as Byrd (Figure 4).

High-resolution measurements on small samples often aim at documenting the natural variability of density. Our model only simulates bulk density, and to illustrate a meaningful comparison, the highest resolution data (at DE08, B29, B32 and Dome C) were averaged over 0.25 m windows before being plotted. At some sites, a similar averaging was already performed before data publication (e.g. 1 m averaging at Byrd and Site 2, 0.5 m averaging at Mizuho). At a large number of sites, especially deep ice core drilling sites, measurements were performed on large volume samples. Still, it should be noted that at NEEM, although large volume samples were used, the data dispersion is higher than for Byrd (Figure 4) and part of the discrepancy between the model and data may be due to the uncertainty in the data.

For our study we have gathered density data covering the whole firn depth range, for which we had confidence in the data quality and the major site characteristics (temperature, accumulation). Although the effects of uncertainties on the data and natural density variability cannot be completely separated, we evaluate the data dispersion around the polynomial fit:

$$\sigma_{fit-data} = \sqrt{\left[\frac{\sum_{i=1}^{N_{max}} (\rho_{fit}^i - \rho_{measured}^i)^2}{N_{max}} \right]} \quad (11)$$

where N_{max} is the number of steps of data points, ρ_{fit} represents the regression of the density profile and $\rho_{measured}$ the measured density averaged on a 0.25 m window. $\sigma_{fit-data}$ generally lies below 10.0 kg/m³ (Figure 5).

In order to visualize the model data comparison with the different versions of the model on the 22 selected sites, we calculate the following deviation in parallel to the $\sigma_{fit-data}$ above (Equation 11):

$$\sigma_{model-fit} = \sqrt{\left[\sum_{i=1}^{N_{max}} \frac{(\rho_{model}^i - \rho_{fit}^i)^2}{N_{max}} \right]} \quad (12)$$

Note that we compare here the model to the fit of the data and not directly to data because of the strong site to site differences in the data (e.g. data resolution, sample size). Figure 5 and Supplementary Table S1 display the $\sigma_{model-fit}$ for the 22 different sites before and after modifications detailed in Section 2.

3.1.1. Data – model comparisons using the old model

Comparing our model results to density data is not trivial due to the diversity in measurement techniques and samplings discussed above, as well as the natural variability in density that we do not capture with a simplified model aiming at simulating very long time scales. A rough indication is given by comparing $\sigma_{model-fit}$ and $\sigma_{fit-data}$. They are of the same order of magnitude although $\sigma_{fit-data}$ is always lower than $\sigma_{model-fit}$ (Figure 5), confirming that the old model is likely not able to fully represent the diversity of the density profiles at the 22 measurement sites.

The model-data agreement is variable among the different sites even for those with similar surface climatic conditions. The temperatures and accumulation rates at Dome C and Vostok being similar, model results at these sites are similar, but the density data have a clearly different shape. At Vostok, a high densification rate is observed well above the critical density of about 550 kg/m³. One possible reason is the very different flow regimes of the two sites, one being at a Dome summit, and the other on a flow line and subject to a horizontal tension (Lipenkov et al., 1989). This is not taken into account in our simplified 1D model. Some density data at other sites also show no densification rate change near the critical density, resulting in model-data mismatches (see Siple Dome, km 105, km 200, Mizuho on Supplementary Figure S6).

The main disagreement between the old model and data is observed at the transition between the first and

the second densification stage with too high modeled densities and an associated slope change in the density profile that is too strongly imprinted. This effect is due to a densification rate that is too high in the first stage.

3.1.2. Data – model comparisons using the new model with only one activation energy

The modifications of the first densification stage described in Section 2.1 mainly reduce the slope change at the transition between the Alley (1987) and Arzt (1982) mechanisms (not shown). It also suppresses an instability of the previous model version which could fail to find a continuous densification rate at the boundary between Alley (1987) and Arzt (1982) mechanisms.

However the new model still shows a tendency to overestimate the snow densification rate and then underestimate the densification rate in the firn, as shown for NEEM and Vostok on Figure 4.

Still, looking at all different firn profiles, the general agreement between modeled and measured firn density profiles is preserved. The agreement between measured and modeled firn density is increased for some sites at (1) low accumulation rate and temperature in Antarctica (Dome A, Vostok and Dome C but not South Pole) and at (2) relatively high temperature and accumulation rate (Dye 3, Siple Dome, NEEM). In parallel, a larger disagreement between model and data is observed for some other sites particularly in coastal Antarctica (DE08, Km 200, WAIS Divide). When introducing these modifications for simulating $\delta^{15}\text{N}$ evolutions over the last deglaciation, no significant changes are observed with respect to simulations run with the old LGGE model. This is not unexpected since most of the modifications concern the first stage of densification (top 10-15 m of the firn). The other modifications concern the LID definition, it only has a small impact on the model results for the glacial-interglacial transitions and slightly increases the model – data mismatch over deglaciations (Supplementary Figure S7).

3.1.3. Data-model comparisons using the new model with three activation energy and implementation of impurity effect

The introduction of three different activation energies for different temperature ranges leads to changes of the modeled density profiles at high densities (above about 800 kg/m^3). A clear improvement is obtained for example at South Pole (Supplementary Figure S6), although the overall impact of using three activation energies remains small.

The incorporation of the impurity effect following the Freitag et al. (2013) parameterization in our model slightly deteriorates the model-data agreement because no specific re-adjustment of model parameters was performed. However the model prediction of the density profiles remains correct

although the impurity effect parameterization was developed for a different purpose, simulating density layering (Freitag et al., 2013). This encouraged us to test this simple parameterization in glacial climate conditions.

Overall, in terms of $\sigma_{\text{model-fit}}$, only an insignificant improvement (about 3%) is obtained by using the modified model (3 activation energies and implementation of impurity effect) rather than the former Goujon et al. (2003) mechanical scheme. However a systematic improvement is obtained at the six coldest sites.

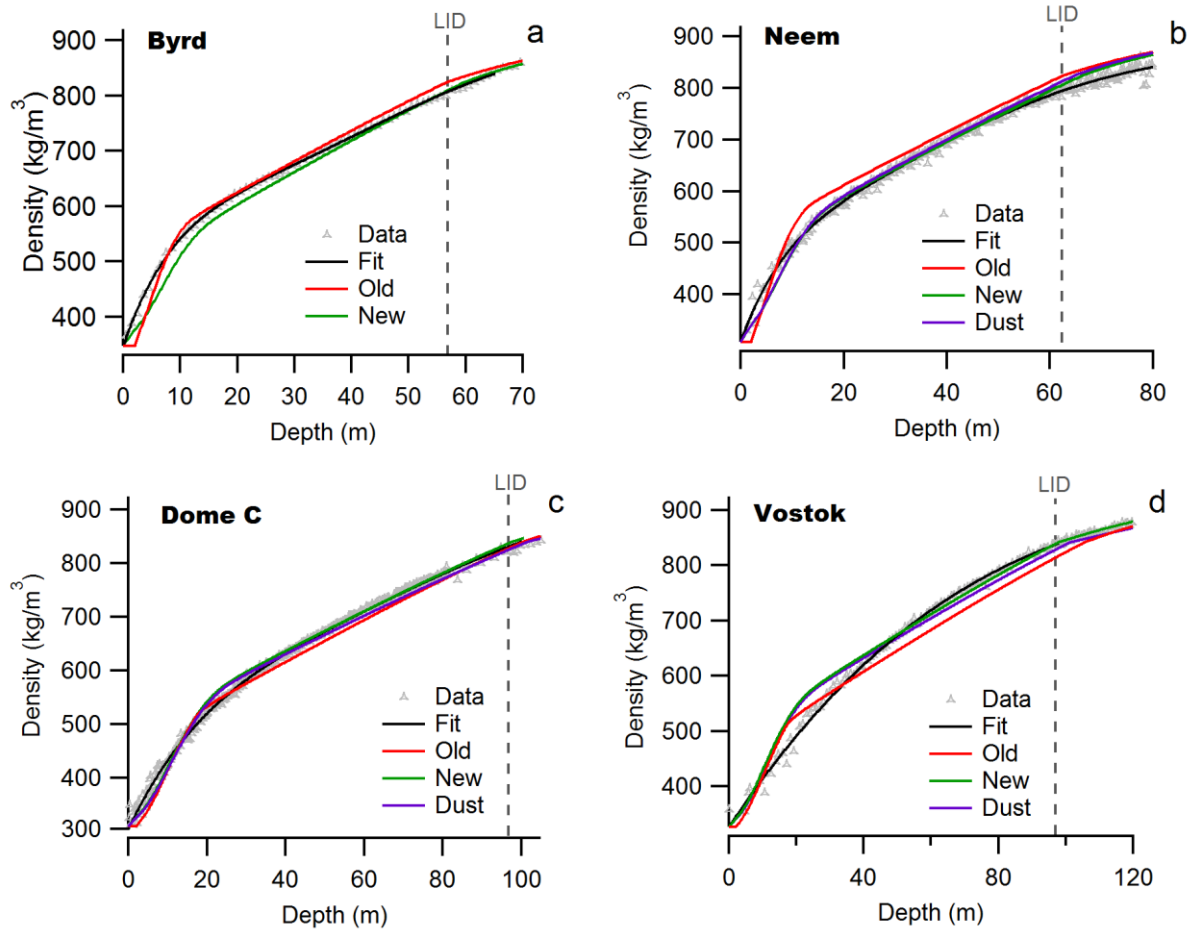


Figure 4: Density profiles of Byrd (a), NEEM (b), Dome C (c) and Vostok (d). The grey triangles correspond to the data. The black line corresponds to the polynomial fit, the red one to the old simulation, the green one to the new simulation and the purple one to the new simulation with impurity effect.

Finally, it should be noted that our main purpose is to improve the agreement between the modelled LID and the evolution of $\delta^{15}\text{N}$ over deglaciations in Antarctica. Thus, in addition to the above comparison of density profiles, we compared the depths at which the LID density, as defined by Equation (10), is reached in the polynomial fit to the data and in the new model results. In the old version of the model, the LID differences

between the model and data range between -17.9 m (at South Pole) and +8.6 m (at km 200) with a small mean value of -1.9 m and a standard deviation of 6 m. In the new version, the LID differences between the model and data are comparable, ranging between -14.1 m (at South Pole) and +12.8 m (at Talos Dome) with a small mean value of -0.7 m and a standard deviation of 6 m. Similar results are obtained for Δ_{age} (see Supplementary Table S2): the agreement with the data is similar for all model versions, and the new model leads to somewhat improved results for the coldest sites. We thus conclude from this section that the LGGE new firn densification model preserves the good agreement between (1) modelled and measured firn density profiles and (2) modelled and measured LID. We explore in the next section the performances of the new model for coldest and driest conditions by looking at the modelled LID and hence $\delta^{15}\text{N}$ evolution over glacial – interglacial transitions.

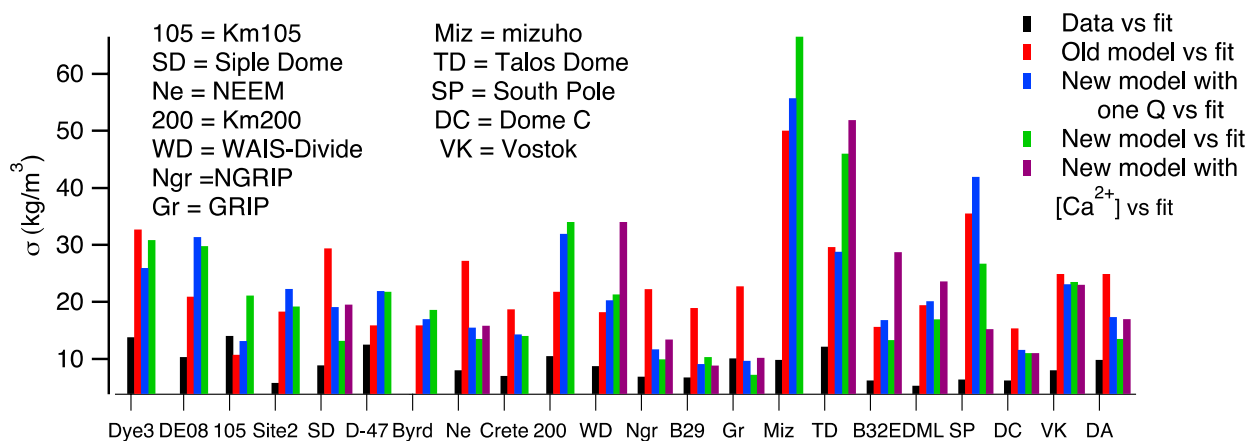


Figure 5: Representation of the $\sigma_{fit-data}$ in black and the $\sigma_{model-fit}$ (in red for the old model, in blue for the model with the new parameterization except the three activation energies, in green for the new model with three activation energy and in purple for the new model with the impurity effect) at 22 Greenland and Antarctic sites. The site characteristics are provided in Supplementary Table S1.

3.2 $\delta^{15}\text{N}$ glacial-interglacial profiles

In order to test the validity of the densification model in a transient mode, we model the time evolution of $\delta^{15}\text{N}$ over the last deglaciation, and compare it to measurements at 4 Antarctic and Greenland deep ice-core sites: Dome C (cold and low accumulation site in Antarctica with a strong mismatch observed between data and the old model), EDML (intermediate temperature and accumulation rate in Antarctica with a significant mismatch between data and the old model), WAIS-Divide (high temperature and accumulation rate site in Antarctica with a good model-data agreement) and NGRIP (Greenland site with a good agreement between model and data) (Figure 3).

The computation of $\delta^{15}\text{N}$ depends on the convective zone thickness, the LID and on the firn temperature profile. The gravitational $\delta^{15}\text{N}$ signal is indeed calculated from the LID and mean firn temperature according to the barometric equation (Equation 1). The thermal $\delta^{15}\text{N}$ depends on the temperature gradient between the surface and the LID. A small thermal signal exists in Antarctica because of geothermal heat flux (with an average change of about 0.02 ‰ during deglaciation) but no millennial variations are expected because the temperature variations are slow ($<2^\circ\text{C}/1000$ years) compared to abrupt climate changes observed in Greenland (e.g. NGRIP).

The model calculates *instantaneously* the diffusive column height and thermal fractionation. To take into account the smoothing due to gas diffusion in the open pores and progressive bubble close-off (Schwander et al., 1993), we smooth the $\delta^{15}\text{N}$ output with a log-normal distribution, of width $\Delta\text{age}/5$ and $\sigma=1$ (Kohler 2011, Orsi et al., 2014). This formulation of the smoothing takes into account the variations of the gas-age distribution with time.

3.2.1 Input scenarios

For the simulation of the $\delta^{15}\text{N}$ evolution over the last deglaciation, the firn densification model is forced by a scenario of surface temperature and accumulation rate deduced from ice core data (Supplementary Table S3). In Greenland (NGRIP, GISP2), the temperature is reconstructed using the $\delta^{18}\text{O}_{\text{ice}}$ profiles together with indication from borehole temperature measurements (Dahl-Jensen, 1998) and $\delta^{15}\text{N}$ data for NGRIP (Kindler et al., 2014) for the quantitative amplitude of abrupt temperature changes. Greenland accumulation rate is deduced from layer counting over the last deglaciation (e.g. Rasmussen et al., 2006). The uncertainty in the temperature reconstructions can be estimated to $\pm 3^\circ\text{C}$ over the last deglaciation in Greenland (Buizert et al., 2014). As for the Greenland accumulation rate, an uncertainty of 20% can be associated with the LGM value (Cuffey and Clow, 1997; Guillevic et al., 2013; Kapsner et al., 1995). In Antarctica, both temperature and accumulation rate are deduced from water isotopic records except for WAIS-Divide, where layer counting back to the last glacial period is possible (Buizert et al., 2015). Temperature uncertainty for the amplitude of the last deglaciation is estimated to -10% to +30% in Antarctica (Jouzel, 2003). The reason for such asymmetry is mainly linked to outputs of atmospheric general circulation models equipped with water isotopes. These models suggest that the present day spatial slope between $\delta^{18}\text{O}$ and temperature most probably underestimate the amplitude of the temperature change between glacial and interglacial period. We have followed this estimate of asymmetric uncertainty on the amplitude of temperature change during deglaciation in our study. Recent studies have also suggested that the relationships between water isotopes and temperature and between water isotopes and accumulation rate can be applied with confidence in Antarctica for glacial temperature reconstruction (Cauquoin et al., 2015) while one should be cautious for interglacial temperature reconstruction with warmer conditions than today (Sime et al., 2009). Finally, a recent estimate of the deglacial temperature increase based on $\delta^{15}\text{N}$ measurements at WAIS (Cuffey et al.,

2016) led to a 11.3°C temperature increase over the last deglaciation (1°C warming to be attributed to change in elevation). This is larger than the temperature increase reconstructed in East Antarctica from water isotopes by 2–4°C and again not in favour of a “warm” LGM.

In the construction of the AICC2012 chronology (Bazin et al., 2013; Veres et al., 2013), the first order estimate of accumulation rate from water isotopes for EDML, Talos Dome, Vostok and Dome C has been modified by incorporating dating constraints or stratigraphic tie points between ice cores (Bazin et al., 2013; Veres et al., 2013). The modification of the accumulation rate profiles over the last deglaciation for these 4 sites is less than 20% and the uncertainty of accumulation rate generated by the DATICE model used to build AICC 2012 from background errors (thinning history, accumulation rate, LID) and chronological constraints is 30% for the LGM (Bazin et al., 2013; Frieler et al., 2015; Veres et al., 2013). Still, it should be noted that the uncertainty of 20% on LGM accumulation rate on central sites as given in the AICC2012 construction is probably overestimated. Indeed, deglaciation occurs around 500 m depth at Dome C, hence with small uncertainty on the thinning function and on the accumulation rate. These values are consistent with previous estimates of accumulation rate uncertainties over the last deglaciation ($\pm 10\%$ for Dome C (Parrenin et al., 2007) and $\pm 30\%$ in EDML (Loulergue et al., 2007)).

We showed in Section 2.1 that surface density does not have a strong impact on the LID determination (Supplementary Figure S3). We do not have any indication of surface density in the past, so we impose a constant surface density of 0.35 for all sites at all times for transient runs. In order to convert the LID (deduced from density) to the diffusive column height measured by $\delta^{15}\text{N}$, we need an estimate of the convective zone in the past. We use a 2 m convective zone for all sites, except Vostok, where we use 13 m, in accordance with firn measurements (Bender et al., 2006). We assume that the convective zone did not evolve during the last deglaciation, consistently with dating constraints at Dome C and at Vostok during Termination 2 (Parrenin et al., 2012; Bazin et al., 2013; Veres et al., 2013; Landais et al., 2013).

3.2.2 Transient run with the old model

In this section, we focus on the $\delta^{15}\text{N}$ evolution over the deglaciation at different Greenland and Antarctic sites as obtained from the data and as modelled with the old version of the LGGE model. This comparison serves as a prerequisite for the comparison with outputs of the improved model over the same period for the same polar sites. The comparison between the old LGGE model and $\delta^{15}\text{N}$ data over the last deglaciation shows the same patterns already discussed in Capron et al. (2013). At Greenland sites, there is an excellent agreement between model and data showing both the decrease in the mean $\delta^{15}\text{N}$ level between the LGM and the Holocene and the $\sim 0.1\text{‰}$ peaks in $\delta^{15}\text{N}$ associated with the abrupt temperature changes (end of the Younger Dryas, Bølling-Allerød, Dansgaard-Oeschger 2, 3 and 4, Figure 6 and Supplementary Figure S8). On the other hand, the modelled and measured $\delta^{15}\text{N}$ over the last deglaciation show significant dissimilarities in

Antarctic $\delta^{15}\text{N}$ profiles displayed on Figure 6 and Supplementary Figure S8, except at the relatively high accumulation rate and temperature site of WAIS-Divide where the model simulates properly the $\delta^{15}\text{N}$ evolution in response to the change in accumulation and mean firn temperature estimated from water isotopic records and borehole temperature constraints (Buizert et al., 2015). Note that in Buizert et al. (2015), the modelled $\delta^{15}\text{N}$ was obtained from the Herron and Langway model. For the other Antarctic sites (Figure 6), we observe that model and data disagree on the $\delta^{15}\text{N}$ difference between the LGM and Holocene levels. At EDML, Dome C and Vostok, the model predicts a larger LID during the LGM, while $\delta^{15}\text{N}$ suggests a smaller LID compared to the Holocene (with the assumption of no change in convective zone during the deglaciation). In addition, the measured $\delta^{15}\text{N}$ profiles at Berkner Island, Dome C, EDML and Talos Dome display an additional short term variability, i.e. $\delta^{15}\text{N}$ variations of 0.05‰ in a few centuries during stable climatic periods. These variations can be explained by the ice quality (coexistence of bubbles and clathrates) at Dome C and EDML. Indeed, for pure clathrate ice from these two sites, such short term variability is not observed (e.g. Termination 2 at Dome C, Landais et al., 2013). At Berkner Island and Talos Dome, these variations cannot be explained by the quality of the measurements, by thermal effects nor by dust influence. They are also not present in the accumulation rate and temperature forcing scenarios deduced from water isotopes (Capron et al., 2013). **This observation questions the existence and variations of a convective zone and/or the accuracy of the reconstruction of past accumulation rate and temperature scenarios from water isotopes in Antarctica except at WAIS-Divide where layer counting is possible over the last deglaciation.** We thus explore further the influence of accumulation rate and temperature uncertainties on the $\delta^{15}\text{N}$ modelling.

The uncertainties in the changes of temperature and accumulation rates over the deglaciation significantly influences the simulated $\delta^{15}\text{N}$, as already shown in previous studies and this sensitivity of $\delta^{15}\text{N}$ has even been used to adjust temperature and/or accumulation rate scenarios (Buizert et al., 2013; Guillevic et al., 2013; Kindler et al., 2014; Landais et al., 2006). We tested the influence of the accumulation rate and temperature scenarios on the simulated $\delta^{15}\text{N}$ profiles for the last deglaciation, but even with large uncertainties in the input scenarios, it is not possible to reproduce the measured Antarctic $\delta^{15}\text{N}$ increase at Dome C and EDML with the old version of the LGGE model.

This result is illustrated on Figure 7 where we display a comparison between the amplitude of the measured $\delta^{15}\text{N}$ change and the amplitude of the modelled $\delta^{15}\text{N}$ change with the Goujon version over the last deglaciation. For this comparison, we calculated the Last Glacial Maximum (LGM) $\delta^{15}\text{N}$ average over the period 18-23 ka and the Early Holocene (EH) $\delta^{15}\text{N}$ average over the period 6-10 ka (or smaller, depending on available data, cf blue boxes on Figure 6). We estimated the uncertainty in the measured $\delta^{15}\text{N}$ change by calculating first the standard deviation of the $\delta^{15}\text{N}$ data over each of the two periods, LGM and EH as $\sigma_{15\text{N_data_EH}}$ and $\sigma_{15\text{N_data_LGM}}$ and then the resulting uncertainty on the $\delta^{15}\text{N}$ change as: $\sigma_{15\text{N_EH-LGM}} =$

$$\sqrt{\sigma_{15N_data_EH}^2 + \sigma_{15N_data_LGM}^2}$$

As for the modelled $\delta^{15}\text{N}$ change, associated error bars are deduced from the uncertainty on the temperature and accumulation input scenarios (shown on Supplementary Figure S9 for the improved model). The total error bar hence shows the difference between most extreme accumulation rate or temperature input scenarios. In these sensitivity tests, we assumed that it is not possible to have an underestimation of the temperature change with an overestimation of the accumulation rate (or the opposite) because changes in accumulation rate and temperature are linked, at least qualitatively when comparing LGM and Holocene mean values.

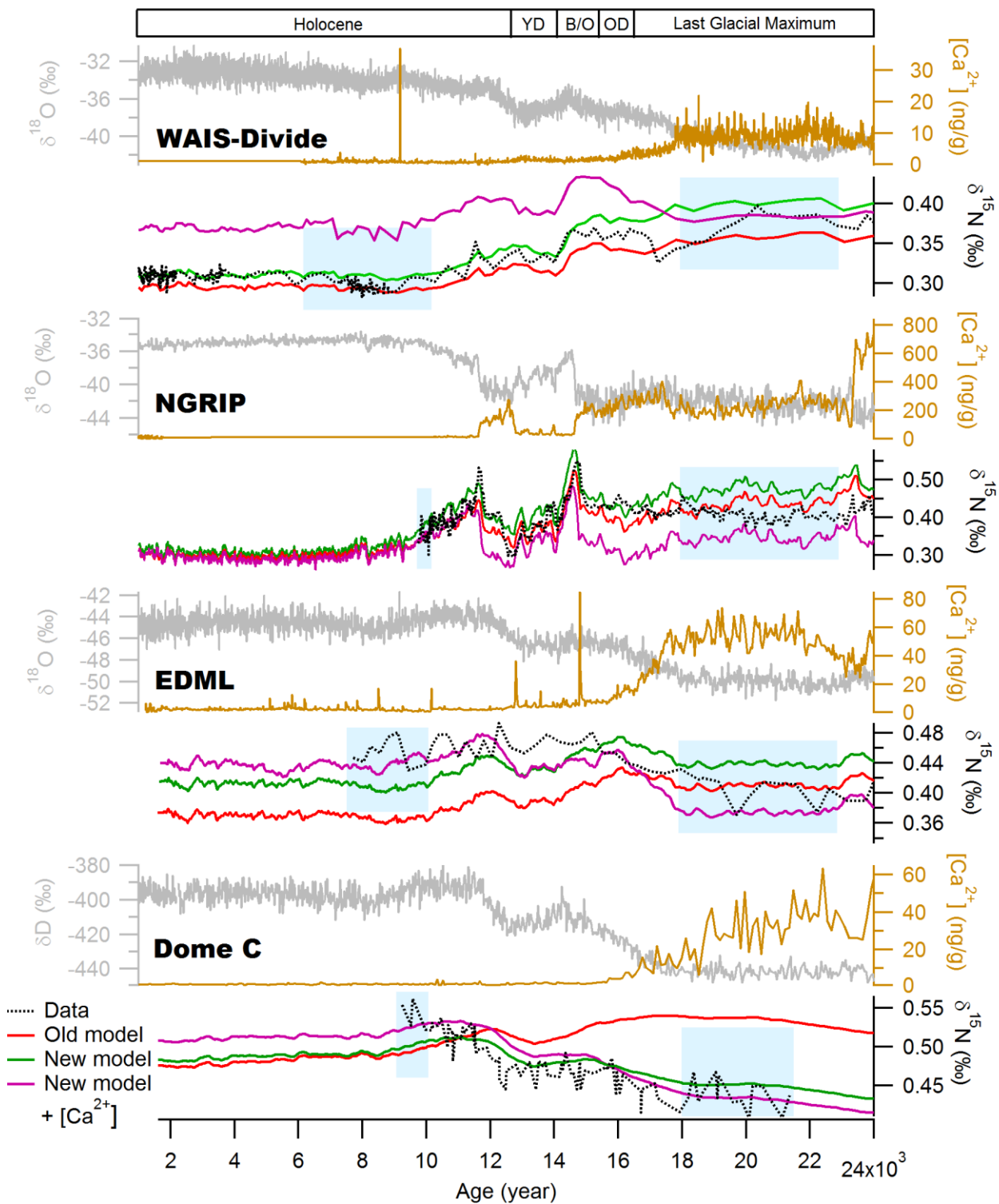


Figure 6: Comparison of the measured $\delta^{18}\text{O}$ or δD (grey), the calcium concentration (gold), the measured $\delta^{15}\text{N}$ (black) and the modelled $\delta^{15}\text{N}$ (old (red), new version (green) and new version with impurity (purple)) of the LGGE model for WAIS-Divide, NGRIP, EDML and Dome C. Blue boxes for each sites indicate the periods over which the $\delta^{15}\text{N}$ average for the LGM and EH have been estimated for the calculation of the amplitude of the $\delta^{15}\text{N}$ change over the deglaciation.

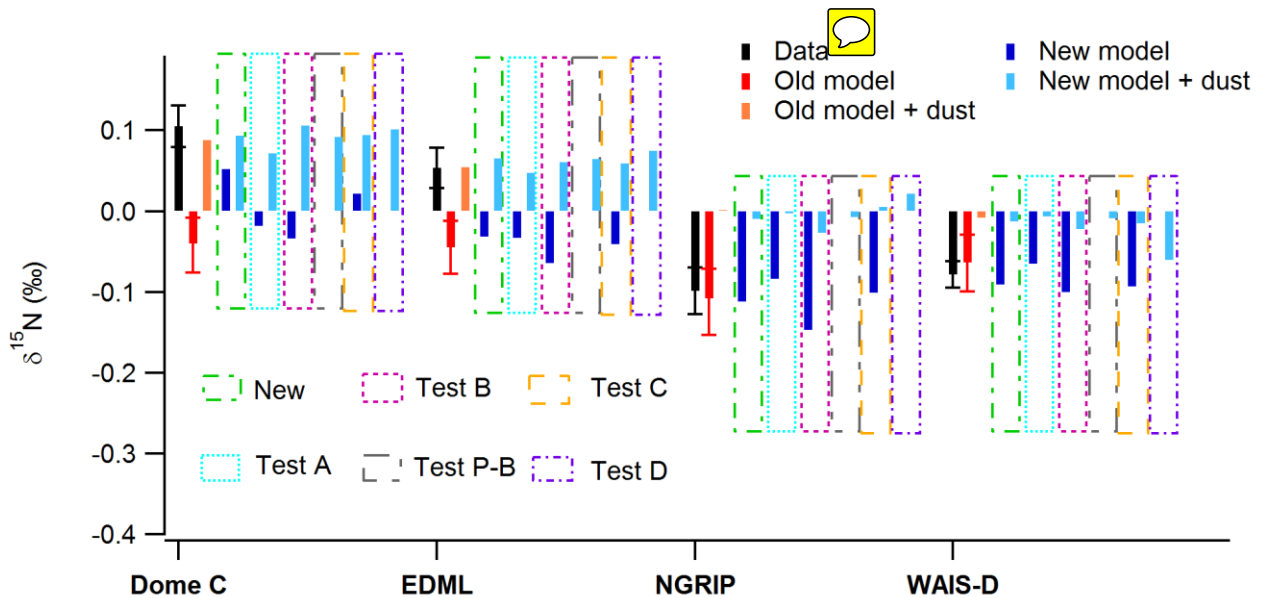


Figure 7: Difference between EH and LGM $\delta^{15}\text{N}$ at 4 different polar sites (raw data are given in Supplementary Table S4). The measured $\delta^{15}\text{N}$ difference is shown with a black bar. The modelled $\delta^{15}\text{N}$ difference is shown with colours: old version in red (orange with the impurity influence), new version in blue with different parameterizations. “New” corresponds to the parameterization of Table 1, sensitivity tests A, B, C and D are described in Table 3. When “+ dust” is mentioned, it corresponds to the addition of the impurity influence as parameterized by Freitag et al., (2013) (Equations 8 and 9). Test Pimienta-Barnola corresponds to a test with the Freitag parameterization adapted to the Pimienta-Barnola model instead of the Herron and Langway model used for the other sensitivity tests. **This test shows in light blue the result of the implementation of this parameterization combined with the “New” parameterization from Table 1. The same red error bars can be applied to all model outputs for each sites.**

3.2.3 Results with updated temperature parameterization

By construction, the new LGGE firn model with the temperature dependency of the firn densification module depicted on Section 2.2.1 is expected to improve the agreement between model and data for cold sites of East Antarctica over the last deglaciation by increasing densification **rates** at low temperature. This new parameterization modifies the densification rate through the creep parameter given in Equation (7). Figure 8 shows the evolution of the creep parameter with temperature for different choices of the three activation energies Q_1 , Q_2 and Q_3 . Compared to the old model, the densification rate is higher at low temperature, below -55°C (i.e. for LGM at Dome C and Vostok, Table 1). At higher temperature (between -55°C and -28°C corresponding to present-day temperature in most polar sites), the creep parameter is slightly lower than in the old model. The difference between the 2 curves is however not large so that densification rate is not strongly modified over this range. This is in agreement with comparable firn density profiles obtained for the different polar sites using the old or the improved LGGE model (Section 3.1, Figure 4).

In the improved model, the simulated profiles of $\delta^{15}\text{N}$ are comparable to $\delta^{15}\text{N}$ simulated with the old model at the sites that were already showing a good agreement between the old model outputs and data, for example NGRIP, GISP-2, Talos Dome and WAIS-Divide (Figure 6 and Supplementary Figure S8). This is expected since the corresponding densification rate is only slightly reduced in the temperature range of $-55^\circ\text{C}/-28^\circ\text{C}$ which corresponds to the temperature range encompassed over the last deglaciation at these sites. This results in a deeper LID and hence higher $\delta^{15}\text{N}$ level, which is in general compatible with the data (except at Talos Dome). Some differences are also observed for the timing of the $\delta^{15}\text{N}$ peaks for Bølling-Allerød and end of Younger Dryas at NGRIP when using the different model versions reflecting variations in the simulated Δage (cf Supplementary Table S5); the general agreement with the measured profile is preserved with even a slight improvement of the modelled Δage with $\delta^{15}\text{N}$ constraints with the modified model. At the coldest sites (Dome C, Vostok), the agreement between data and modelled profiles is largely improved with a modelled LGM $\delta^{15}\text{N}$ smaller than the modelled EH $\delta^{15}\text{N}$, but a perfect match cannot be found. At the intermediate EDML site, it is not possible to reproduce the sign of the slope during the deglaciation.

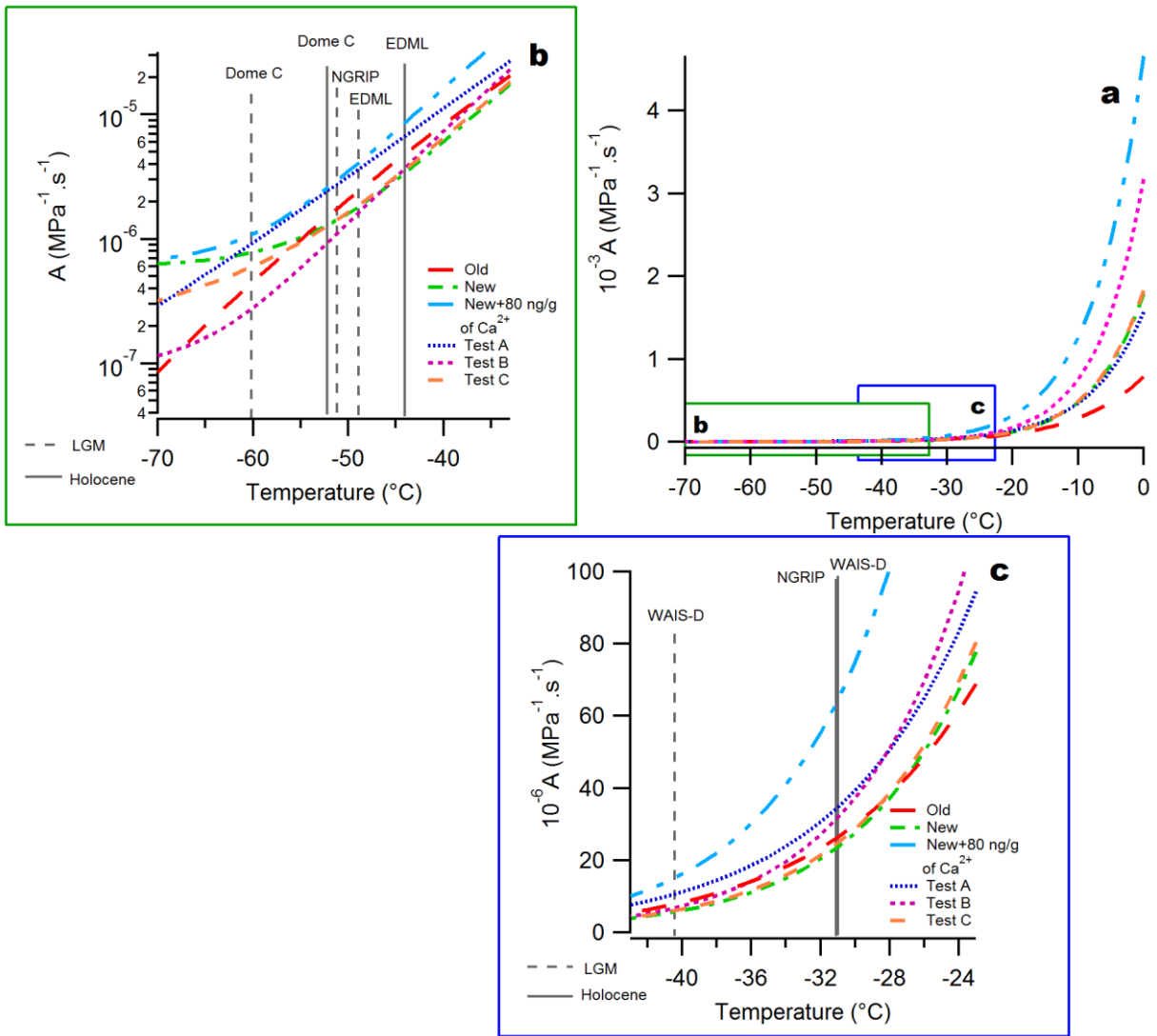


Figure 8: **Dependence of** the creep parameter (Equation 7) as a function of temperature for 6 different parameterizations. “Old” corresponds to the Goujon et al. (2003) version of the model; “New” corresponds to the improved LGGE model with parameterization described in Table 1; “New + 80 ng/g of Ca^{2+} ” corresponds to the parameterization of Table 1 with the addition of the impurity effect following Equation (8) and a $[Ca^{2+}]$ value of 80 ng/g; Tests A, B and C are sensitivity tests run with the values presented on Table 3. Figure 8a shows the creep parameter evolution for the whole temperature range, Figure 8b is a focus at very low temperature and Figure 8c is a focus at intermediate temperature. The grey vertical lines indicates the temperature for Early Holocene (EH, solid line) and LGM (dotted line) at the 4 study sites presented in Figures 6 and 7.

Test	Activation energy (J/mol)	Coefficient
Test A	$Q_1 = 90000$	$a_1 = 5.5 \cdot 10^5$
	$Q_2 = 60000$	$a_2 = 1.0$

	$Q_3 = 30000$	$a_3 = 4.5 \cdot 10^{-8}$
Test B	$Q_1 = 110000$	$a_1 = 5.5 \cdot 10^9$
	$Q_2 = 75000$	$a_2 = 1950.0$
	$Q_3 = 1500$	$a_3 = 9.0 \cdot 10^{-16}$
Test C	$Q_1 = 110000$	$a_1 = 1.05 \cdot 10^9$
	$Q_2 = 75000$	$a_2 = 1400$
	$Q_3 = 15000$	$a_3 = 8.7 \cdot 10^{-12}$
Test D	$Q_1 = 110000$	$a_1 = 1.05 \cdot 10^9$
	$Q_2 = 75000$	$a_2 = 980$
	$Q_3 = 1230$	$a_3 = 3.6 \cdot 10^{-15}$

Table 3: Values used for the different sensitivity tests for three activation energies.

In order to more quantitatively assess the robustness of the proposed parameterization in Table 1, we confront in Figure 7 the measured and modelled $\delta^{15}\text{N}$ differences between the LGM and EH at the 4 Greenland and Antarctic sites selected above. For this comparison, we use not only the parameterization of Table 1 but also sensitivity tests performed with different parameterizations of the temperature dependency of activation energy and impurity effects (details on Table 3).

When using the parameterization of Table 1 (“new model”), Figure 7 shows strong improvement of the simulation of the $\delta^{15}\text{N}$ difference between EH and LGM. Indeed, the modelled EH-LGM difference now has the correct sign at very cold sites of East Antarctica (Figure 7) when compared with $\delta^{15}\text{N}$ measurements.

We present some sensitivity tests to illustrate the choice of our final parameterization (i.e. the new model) through influences on the creep parameters and LGM vs EH $\delta^{15}\text{N}$ changes. As displayed in Figure 8, test A has a higher creep parameter than the old model throughout the whole temperature range. Compared to the output of the old model, the LGM vs EH $\delta^{15}\text{N}$ change simulated with test A is slightly higher but the sign of the $\delta^{15}\text{N}$ change over the last deglaciation is still wrong at Dome C and EDML. This test shows that it is not the mean value of the creep parameter that needs to be changed, but the dependency to temperature. Test B has a higher creep parameter above -35°C , but a lower creep parameter than the old model below -35°C , which starts flattening and hence reaching values higher than the old model creep parameter below -65°C . The LGM vs EH $\delta^{15}\text{N}$ change simulated with test B is still comparable with data at WAIS-Divide. However, the model – data comparison deteriorates at NGRIP and EDML compared to the model-data comparison with the old version of the model. Moreover, it does not solve the model – data mismatch at Dome C. This shows that the change in the creep parameter at intermediate temperature is too steep. Strong differences occur

at high temperature (above -30°C) but it does not affect the modelled $\delta^{15}\text{N}$ change between LGM and EH for our 4 sites. On the contrary, the slightly lower creep parameter at low temperature leads to a worse agreement between model and data for the Dome C deglaciation than when using the “new model”. Test C has been designed so that the activation energy at low temperature corresponds to estimates of activation energy for ice surface diffusion (Jung et al., 2004; Nie et al., 2009), a mechanism that is expected to be important at low temperature (Ashby, 1974). Using such a parameterization leads to a fair agreement between the modelled and the measured $\delta^{15}\text{N}$ change over the last deglaciation for the different sites. At Dome C, the correct sign for the $\delta^{15}\text{N}$ evolution between LGM and the Holocene is predicted by the model. However, the modelled $\delta^{15}\text{N}$ increase is still too small compared to the data and the $\delta^{15}\text{N}$ calculated by the “new model”. This is probably due to a too high creep parameter at low temperature.

Summarizing, the best agreement between data and model for Dome C is obtained for the parameters given on Table 1: the creep parameter of “new model” flattens below -50°C and is thus not very different for the LGM or the EH at Dome C. As a result, the modelled LID and hence $\delta^{15}\text{N}$ are less sensitive to temperature, and the sign of the EH-LGM difference can be inverted, and brought closer to the observations. It should be noted that despite many sensitivity tests we could not find a parameterization able to reproduce the EH-LGM $\delta^{15}\text{N}$ changes for all 4 sites. In the “new model” without impurity effect, it is not possible to reproduce the measured EDML $\delta^{15}\text{N}$ change over the last deglaciation even when taking into account the uncertainty in the input parameters (temperature and accumulation rate, Supplementary Figure S9).

3.2.4 Impurity softening

The dust content in LGM ice is much larger than in Holocene ice (Figure 6), and impurity inclusions in ice have an impact on the grain structure, allowing it to deform more easily (Alley, 1987; Fujita et al., 2014). We incorporated dust softening using the parameterization of Freitag et al (2013) as detailed in Section 2.2.2. We compared two expressions for the impurity softening (tuned to be applied to the Herron and Langway model, or Pimienta and Barnola model), but found that the differences between the two parameterisations were minor (Figure 7). We use the Herron and Langway parameters in the following.

Figure 8 shows the effect of impurities on the creep parameter: densification is enhanced over the whole temperature range. At all sites, incorporating impurity softening reduces the firn thickness during periods characterized by high impurity concentration in the ice (LGM). It thus leads to an increase of the EH-LGM LID difference (Figure 7).

This effect clearly helps to bring in agreement modelled and measured $\delta^{15}\text{N}$ at Dome C, Vostok and EDML (Figures 6, 7 and Supplementary Figure S8): for these sites, the model incorporating the parameterization of activation energy depicted in Table 1 and the impurity effects is able to reproduce the $\delta^{15}\text{N}$ increase over the last deglaciation. Note that short-lived peaks in impurities, likely triggered by volcanic events, have no visible effect on bulk firn thickness (Figure 6). Contrary to the improved situation in cold Antarctic sites, we observe that, at the warmer sites like NGRIP and WAIS-Divide, incorporating impurity softening deteriorates the model data fit, which was already good in the older version of the model, and also good with other firn densification models (Kindler et al, 2014; Buizert et al, 2015). It produces almost no change in firn thickness between the LGM and the EH at NGRIP, which contradicts $\delta^{15}\text{N}$ observations. The same mismatch is observed at WAIS-Divide using a different model, as already noted by Buizert et al. (2015). We tested the sensitivity to the dust parameterization by implementing the Freitag parameterization adapted to the Pimienta-Barnola model instead of the parameters for the Herron and Langway model used with our improved model (cf Section 2.2.2). The two different parameterizations of the impurity effect lead to very comparable LGM to EH $\delta^{15}\text{N}$ changes over the last deglaciation on the 4 sites discussed here.

The model – data mismatch observed when incorporating the dust effect may be partially due to the fact that we did not readjust a_i and Q_i after implementation of the impurity effect. To explore this possibility, sensitivity test D has been designed with a re-parameterization of the a_i and Q_i values after implementation of the impurity effect. To do so, we calculated the optimal creep parameter A for each mean EH and LGM condition at each site, and adjusted sequentially a_3 , a_2 , a_1 , Q_3 , Q_2 , and Q_1 to minimize the model-data mismatch. Only a_3 , a_2 and Q_3 needed adjustments, and their values can be found in Table 3. We did not perform the adjustment on modern density profiles, because these are only weakly sensitive to the dust parameterization, Ca^{2+} concentrations being low.

Impurity concentration is very high at NGRIP during the glacial period. As a consequence, even if our new parameterization of a_i and Q_i (new model) properly reproduces the Greenland $\delta^{15}\text{N}$ level at LGM, this glacial modelled Greenland $\delta^{15}\text{N}$ level is too low when including the impurity effect. The re-parameterization of a_i and Q_i proposed as sensitivity test D enables an improvement of the agreement between model and data for glacial $\delta^{15}\text{N}$ at WAIS-Divide, maintain the results at Dome-C and EDML, but can still not produce reasonable results at NGRIP (Figure 7).

The mismatch observed for the $\delta^{15}\text{N}$ simulations at WAIS-Divide and NGRIP when incorporating the impurity effect suggests that the parameterization presented in Equations (8) and (9) is not appropriate to be used on bulk $[\text{Ca}^{2+}]$ concentration and/or for LGM simulation. Actually, the proposed parameterization by Freitag et al. (2013) was tuned to density variability in present-day firn, and may not be valid for LGM when $[\text{Ca}^{2+}]$ concentrations were 10-100 times larger than present-day. It is also possible that the dust effect saturates at

high concentration, and is no longer sensitive above a certain threshold. To further improve the model – data agreement with the dust parameterization, a possibility is to add simple thresholds on a minimum and maximum effect of calcium as proposed in supplementary material (Supplementary Text S2 and Figure S10). Implementing threshold values on calcium reduces the large inconsistencies between model results and $\delta^{15}\text{N}$ data, in particular at NGRIP (through the threshold at high calcium concentration) and at WAIS (through the threshold at low calcium concentration).

It is also possible that impurity influence, like temperature, acts differently depending on the dominant mechanism for firn deformation, and that the impurity effect is more important at colder temperature. The mechanisms by which impurities influence firn deformation are still poorly understood. Dust particles do not always influence densification on the same way: dissolved particles soften firn and ice while the softening or hardening effect of non-dissolved impurities is less clear (Fujita et al., 2016; Alley et al., 1987). More work is thus needed before the correct “impurity effect” component and the mechanisms by which it acts on densification are identified (e.g. Fujita et al., 2014, 2016). Here, we have shown that a simple parameterization as a function of $[\text{Ca}^{2+}]$ concentration does not provide uniformly good results, and seems only suitable for sites on the Antarctic Plateau.

To sum up, the new parameterization of the creep parameter has been designed to preserve good agreement between the old model outputs and data at sites that were already well simulated (WAIS-Divide, NGRIP, Talos Dome). In addition, this parameterization improves the simulation of the deglaciation at cold Antarctic Sites (Dome C, Vostok). However, the EH-LGM $\delta^{15}\text{N}$ change at Dome C and EDML cannot be reproduced using only the temperature dependency of activation energy. The inclusion of impurity effect following the Freitag parameterization improves the situation for cold sites but leads to inconsistent $\delta^{15}\text{N}$ evolutions over the deglaciation at WAIS-Divide and NGRIP unless threshold effects are implemented.

4. Conclusion and perspectives

In this study, we have presented a revision of the LGGE firn densification model. We have summarized the physical basis and parameterization choices of this firn model that would explain a large part of the disagreement between modelled and measured $\delta^{15}\text{N}$ evolution over the last deglaciation for extremely cold sites of East Antarctica. Based on analogy with ceramic sintering at hot temperature and recent observations of the impurity effect on firn density, we have improved the LGGE densification model by incorporating new parameterizations for the evolution of the creep parameter with temperature and impurity contents within the firn densification module. We follow previous studies evidencing different dominant firn sintering

mechanisms for different temperature ranges that support a temperature dependency of the creep activation energy. We showed that these new parameterizations improve the agreement between model and data at low temperature (below -30°C), and retain the good agreement at warmer temperature. In particular, the improved LGGE firn density model is now able to reproduce the $\delta^{15}\text{N}$ increase over deglaciations at cold sites such as Dome C and Vostok.

The new parameterization implies a more rapid firn densification at lower temperature and high impurity load than in classical firnification models. This result obtained with our associated appropriate parameterization is in agreement with the study of Parrenin et al. (2012) showing that the classical firn densification model overestimates LID during the last glacial period at EDC. With our revised model, the simulated Δage is also significantly decreased for the glacial periods at low accumulation and temperature sites of the East Antarctic plateau (Dome C, Vostok and Dome Fuji). This has important consequences for building air vs ice timescales in Antarctica and hence for the studies of the relationships between temporal evolutions of atmospheric composition vs. Antarctic temperature. At EDC 21 ka (ice age), the modelled Δage decreases from 4840 years (old model) to 4270 years (new model) or 4200 years (new model including impurity effect). At Vostok 21 ka (ice age), the modelled Δage decreases from 5630 years (old model) to 5030 years (new model) or 4900 years (new model including impurity effect). The latest results are in good agreement with the recent determination of Δage within the AICC2012 timescale: 3920 years for EDC 21 ka (ice age) and 5100 years for Vostok 21 ka (ice age). This is not unexpected since the EDC LID in the construction of the AICC2012 timescale is deduced from the EDC $\delta^{15}\text{N}$ scenario, a hypothesis supported by the available gas and ice stratigraphic markers over the last deglaciation (Parrenin et al., 2012).

Our finding is however associated with several limitations so that this new model does not propose a definite re-evaluation of the formulation of the activation energy but better proposes some ways to be further tested and explored to improve firn densification models especially for applications on paleoclimate reconstructions. Our approach remains empirical and we could not identify separately the different mechanisms involved. The problem of $\delta^{15}\text{N}$ data-model mismatch in low temperature and accumulation rate sites of East Antarctica is thus not definitively solved. Still, we showed that revising the temperature and impurity dependence of firn densification rate can potentially strongly reduce the $\delta^{15}\text{N}$ data-model mismatch and proposed preliminary parameterizations easy to implement in any firn densification model.

Finally, the new parameterization proposed here ~~hence~~ calls for further studies. First, laboratory or field studies of firn densification at very cold controlled conditions are needed to check the predominance of one mechanism over another at low temperature such as the predominance of the boundary diffusion over grain boundary mechanism around -60°C ; this is a real challenge because of the slow speed of deformation.

Second, we have suggested that the current parameterization of impurity on firn softening should be revised, especially for very high impurity load (Greenland) using for example thresholds on impurity concentrations. Third, the separate effects of impurities and temperature on firn densification and hence $\delta^{15}\text{N}$ evolution should be tested on periods other than the last deglaciation. Sequences of events associated with non-synchronous changes in surface temperature, accumulation rate and impurity content would be particularly valuable for this objective. Finally, additional constraints on the firn modelling can also be obtained through the use of cross-dating on new ice core with high resolution signals as already used by Parrenin et al. (2012).

Acknowledgements: We thank Anders Svensson, Rob Arthern, Hans Christian Steen-Larsen and Xiao Cunde for data sharing and Sarah Guilbaud for her work during her final internship study. Thanks to Pierre Badel for insightful discussions about densification mechanisms. Thanks to Myriam Guillevic for her work on the densification model and helpful discussions. This work is supported by INSU/CNRS LEFE project NEVE-CLIMAT and the ERC COMBINISO 306045.

References

Alley, R. B.: Firn densification by grain-boundary sliding: a first model, *J. Phys. Colloq.*, 48(C1), C1-249-C1-256, doi:10.1051/jphyscol:1987135, 1987.

Altnau, S., Schlosser, E., Isaksson, E. and Divine, D., Climatic signals from 76 shallow firn cores in Dronning Maud Land, East Antarctica, *The Cryosphere Discussions*, Volume 8, Issue 6, pp. 5961-6005, 2014.

Anderson, D. L. and Benson, C. S.: The densification and diagenesis of snow, in *Ice and Snow: Properties, Processes and Applications*, pp. 391–411, MIT Press., 1963.

Arnaud, L.: Modélisation de la transformation de la neige en glace à la surface des calottes polaires; Etude du transport des gaz dans ces milieux poreux, PhD Thesis, Université Joseph Fournier - Grenoble 1, 294 pp, 1997.

Arnaud, L., Barnola, J. M. and Duval, P.: Physical modeling of the densification of snow/firn and ice in, *Phys. Ice Core Rec.*, 26, 39–44, 2000.

Arthern, R. J., Vaughan, D. G., Rankin, A. M., Mulvaney, R. and Thomas, E. R.: In situ measurements of Antarctic snow compaction compared with predictions of models, *J. Geophys. Res.*, 115(F3), doi:10.1029/2009JF001306, 2010.

Arzt, E.: The influence of an increasing particle coordination on the densification of spherical powders, *Acta Metall.*, 30(10), 1883–1890, 1982.

Arzt, E., Ashby, M. F. and Easterling, K. E.: Practical applications of hot-isostatic pressing diagrams: four case studies, *Metall. Trans. A*, 14(1), 211–221, 1983.

Ashby M. F., A first report on sintering diagrams, *Acta Metallurgica*, vol. 22, 1974.

Barnes, P., Tabor, D. and Walker, J. C. F.: The friction and creep of polycrystalline ice, in *Proceedings of the Royal Society of London A: Mathematical, Physical and Engineering Sciences*, vol. 324, pp. 127–155, The Royal Society, 1971.

Barnola, J.-M., Pimienta, P., Raynaud, D. and Korotkevich, Y. S.: CO₂-climate relationship as deduced from the Vostok ice core: a re-examination based on new measurements and on a re-evaluation of the air dating, *Tellus B*, 43(2), 83–90, 1991.

Bazin, L., Landais, A., Lemieux-Dudon, B., Toyé Mahamadou Kele, H., Veres, D., Parrenin, F., Martinerie, P., Ritz, C., Capron, E., Lipenkov, V., Loutre, M-F., Vinther, B., Svensson, A., Rasmussen, S. O., Severi, M., Blunier, T., Leuenberger, M., Fischer, H., Masson-Delmotte, V., Chappellaz, J., and Wolff E.: An optimized multi-proxy, multi-site Antarctic ice and gas orbital chronology (AICC2012): 120-800 ka, *Clim. Past*, 9(4), 1715–1731, 2013.

Bender M. L., Sowers T., Barnola J.-M. and Chappellaz J., Changes in the O₂/N₂ ratio of the atmosphere during recent decades reflected in the composition of air in the firn at Vostok Station, Antarctica, *Geophysical Research Letters*, vol. 21, N. 3, 189-192, 1994.

Bender, M. L., Floch, G., Chappellaz, J., Suwa, M., Barnola, J.-M., Blunier, T., Dreyfus, G., Jouzel, J. and Parrenin, F.: Gas age–ice age differences and the chronology of the Vostok ice core, 0–100 ka, *J. Geophys. Res.*, 111(D21), doi:10.1029/2005JD006488, 2006.

Benson, C. S.: Stratigraphic studies in the snow and firn of the Greenland ice sheet, PhD Thesis, California Institute of Technology, pp 228, 1960.

Blackford, J. R.: Sintering and microstructure of ice: a review, *J. Phys. Appl. Phys.*, 40(21), R355–R385, doi:10.1088/0022-3727/40/21/R02, 2007.

Buizert, C., Sowers, T. and Blunier, T.: Assessment of diffusive isotopic fractionation in polar firn, and application to ice core trace gas records, *Earth Planet. Sci. Lett.*, 361, 110–119, doi:10.1016/j.epsl.2012.11.039, 2013.

Buizert, C., Gkinis, V., Severinghaus, J. P., He, F., Lecavalier, B. S., Kindler, P., Leuenberger, M., Carlson, A. E., Vinther, B., Masson-Delmotte, V., White, J. W. C., Liu, Z., Otto-Bliesner, B. and Brook, E. J.: Greenland temperature response to climate forcing during the last deglaciation, *Science*, 345(6201), 1177–1180, doi:10.1126/science.1254961, 2014.

Buizert, C., Cuffey, K. M., Severinghaus, J. P., Baggenstos, D., Fudge, T. J., Steig, E. J., Markle, B. R., Winstrup, M., Rhodes, R. H., Brook, E. J., Sowers, T. A., Clow, G. D., Cheng, H., Edwards, R. L., Sigl, M., McConnell, J. R. and Taylor, K. C.: The WAIS Divide deep ice core WD2014 chronology-Part 1: Methane synchronization (68–31 ka BP) and the gas age–ice age difference, *Clim. Past*, 11(2), 153–173, doi:10.5194/cp-11-153-2015, 2015.

Capron, E., Landais, A., Buiron, D., Cauquoin, A., Chappellaz, J., Debret, M., Jouzel, J., Leuenberger, M., Martinerie, P., Masson-Delmotte, V., Mulvaney, R., Parrenin, F. and Prié, F.: Glacial–interglacial dynamics of Antarctic firn columns: comparison between simulations and ice core air- $\delta^{15}\text{N}$ measurements, *Clim. Past*, 9(3), 983–999, doi:10.5194/cp-9-983-2013, 2013.

Cauquoin, A., Landais, A., Raisbeck, G. M., Jouzel, J., Bazin, L., Kageyama, M., Peterschmitt, J.-Y., Werner, M., Bard, E. and ASTER Team, Comparing past accumulation rate reconstructions in East Antarctic ice cores using ^{10}Be , water isotopes and CMIP5-PMIP3 models, *Climate of the Past*, 11, 355–367, 2015.

Colbeck, S. C.: Theory of metamorphism of dry snow, *J. Geophys. Res. Oceans*, 88(C9), 5475–5482, 1983.

Craig, H., Horibe, Y. and Sowers, T.: Gravitational separation of gases and isotopes in polar ice caps, *Science*, 242(4886), 1675–1678, 1988.

Cuffey, K. M. and Clow, G. D.: Temperature, accumulation, and ice sheet elevation in central Greenland through the last deglacial transition, *J. Geophys. Res. Oceans*, 102(C12), 26383–26396, 1997.

Cuffey, K. M., Clow, G. D., Steig, E. J., Buizert, C., Fudge, T. J., Koutnik, M., Waddington E. D., Alley, R. B. and Severinghaus, J. P., Deglacial temperature history of West Antarctica, *PNAS*, vol 11, no. 50, 14249–14254, 2016.

Dahl-Jensen, D.: Past Temperatures Directly from the Greenland Ice Sheet, *Science*, 282(5387), 268–271, doi:10.1126/science.282.5387.268, 1998.

Dee, D. P., Uppala, S. M., Simmons, A. J., Berrisford, P., Poli, P., Kobayashi, S., Andrae, U., Balmaseda, M. A., Balsamo, G., Bauer, P., Bechtold, P., Beljaars, A. C. M., van de Berg, L., Bidlot, J., Bormann, N., Delsol, C., Dragani, R., Fuentes, M., Geer, A. J., Haimberger, L., Healy, S. B., Hersbach, H., Hólm, E. V., Isaksen, L., Kállberg, P., Köhler, M., Matricardi, M., McNally, A. P., Monge-Sanz, B. M., Morcrette, J.-J., Park, B.-K., Peubey, C., de Rosnay, P., Tavolato, C., Thépaut, J.-N. and Vitart, F.: The ERA-Interim reanalysis: configuration and performance of the data assimilation system, *Q. J. R. Meteorol. Soc.*, 137(656), 553–597, doi:10.1002/qj.828, 2011.

Dreyfus, G. B., Jouzel, J., Bender, M. L., Landais, A., Masson-Delmotte, V. and Leuenberger, M.: Firn processes and $\delta^{15}\text{N}$: potential for a gas-phase climate proxy, *Quat. Sci. Rev.*, 29(1–2), 28–42, doi:10.1016/j.quascirev.2009.10.012, 2010.

Ebinuma, T. and Maeno, N.: Particle rearrangement and dislocation creep in a snow-densification process, *J. Phys. Colloq.*, 48(C1), C1-263-C1-269, doi:10.1051/jphyscol:1987137, 1987.

EPICA community members: Eight glacial cycles from an Antarctic ice core, *Nature*, 429(6992), 623–628, 2004.

Freitag, J., Kipfstuhl, S., Laepple, T. and Wilhelms, F.: Impurity-controlled densification: a new model for stratified polar firn, *J. Glaciol.*, 59(218), 1163–1169, doi:10.3189/2013JoG13J042, 2013.

Frieler, K., Clark, P. U., He, F., Buizert, C., Reese, R., Ligtenberg, S. R. M., van den Broeke, M. R., Winkelmann, R. and Levermann, A.: Consistent evidence of increasing Antarctic accumulation with warming, *Nat. Clim. Change*, 5(4), 348–352, doi:10.1038/nclimate2574, 2015.

Fujita, S., Hirabayashi, M., Goto-Azuma, K., Dallmayr, R., Satow, K., Zheng, J. and Dahl-Jensen, D.: Densification of layered firn of the ice sheet at NEEM, Greenland, *J. Glaciol.*, 60(223), 905–921, doi:10.3189/2014JoG14J006, 2014.

Fujita, S., Goto-Azuma, K., Hirabayashi, M., Hori, A., Iizuka, Y., Motizuki, Y., Motoyama, H. and Takahashi, K.: Densification of layered firn in the ice sheet at Dome Fuji, Antarctica, *J. Glaciol.*, 62(231), 103–123, doi:10.1017/jog.2016.16, 2016.

Goujon, C., Barnola, J.-M. and Ritz, C.: Modeling the densification of polar firn including heat diffusion: Application to close-off characteristics and gas isotopic fractionation for Antarctica and Greenland sites, *J. Geophys. Res. Atmospheres*, 108(D24), 2003.

Gow, A. J.: Deep core studies of the accumulation and densification of snow at Byrd station and Little America V, Antarctica, CRREL Research Report 197, 1968.

Grachev A. M. and Severinghaus J. P., Determining the thermal diffusion factor for Ar-40/Ar-36 in air to aid paleoreconstruction of abrupt climate change, *The Journal of Physical Chemistry*, 107(23), pp 4636-4642, 2003.

Guillevic, M., Bazin, L., Landais, A., Kindler, P., Orsi, A., Masson-Delmotte, V., Blunier, T., Buchardt, S. L., Capron, E., Leuenberger, M., Martinerie, P., Prié, F. and Vinther, B. M.: Spatial gradients of temperature, accumulation and $\delta^{18}\text{O}$ -ice in Greenland over a series of Dansgaard-Oeschger events, *Clim. Past*, 9(3), 1029–1051, doi:10.5194/cp-9-1029-2013, 2013.

Hagenmuller, P., Chambon, G. and Naaim, M.: Microstructure-based modeling of snow mechanics: a discrete element approach, *The Cryosphere*, 9(5), 1969–1982, doi:10.5194/tc-9-1969-2015, 2015.

Helsen, M. M., van den Broeke, M. R., van de Wal, R. S. W., van de Berg, W. J., van Meijgaard, E., Davis, C. H., Li, Y. and Goodwin, I.: Elevation Changes in Antarctica Mainly Determined by Accumulation Variability, *Science*, 320(5883), 1626–1629, doi:10.1126/science.1153894, 2008.

Herron, M. M. and Langway, C. C.: Firn densification: an empirical model, *J. Glaciol.*, 25(93), 373–385, 1980.

Hörhold, M. W., Laepple, T., Freitag, J., Bigler, M., Fischer, H. and Kipfstuhl, S.: On the impact of impurities on the densification of polar firn, *Earth Planet. Sci. Lett.*, 325, 93–99, 2012.

Jacka, T. H. and Li, J.: The steady-state crystal size of deforming ice, *Ann. Glaciol.*, 20(1), 13–18, 1994.

Jouzel, J.: Magnitude of isotope/temperature scaling for interpretation of central Antarctic ice cores, *J. Geophys. Res.*, 108(D12), doi:10.1029/2002JD002677, 2003.

Jouzel, J., Masson-Delmotte, V., Cattani, O., Dreyfus, G., Falourd, S., Hoffmann, G., Minster, B., Nouet, J., Barnola, J. M., Chappellaz, J., Fischer, H., Gallet, J. C., Johnsen, S., Leuenberger, M., Loulergue, L., Luethi, D., Oerter, H., Parrenin, F., Raisbeck, G., Raynaud, D., Schilt, A., Schwander, J., Selmo, E., Souchez, R., Spahni, R., Stauffer, B., Steffensen, J. P., Stenni, B., Stocker, T. F., Tison, J. L., Werner, M. and Wolff, E. W.: Orbital and Millennial Antarctic Climate Variability over the Past 800,000 Years, *Science*, 317(5839), 793–796, doi:10.1126/science.1141038, 2007.

Jung K.-H., Park, S.-C., Kim, J.-H. and Kang, H., Vertical diffusion of water molecules near the surface of ice, *Journal of Chemical Physics*, vol. 121, No. 6, DOI: 10.1063/1.1770518, 2004.

Kapsner, W. R., Alley, R. B., Shuman, C. A., Anandakrishnan, S. and Grootes, P. M.: Dominant influence of atmospheric circulation on snow accumulation in Greenland over the past 18,000 years, *Nature*, 373(6509), 52–54, 1995.

Kawamura K., Severinghaus J. P., Ishidoya S., Sugawara S., Hashida G., Motoyama H., Fujii Y., Aoki S. and Nakazawa T., Convective mixing of air in firn at four polar sites, *Earth and Planetary Science Letters*, 244, 672-682, 2006.

Kindler, P., Guillevic, M., Baumgartner, M., Schwander, J., Landais, A., Leuenberger, M., Spahni, R., Capron, E. and Chappellaz, J.: Temperature reconstruction from 10 to 120 kyr b2k from the NGRIP ice core, *Clim. Past*, 10(2), 887–902, doi:10.5194/cp-10-887-2014, 2014.

Köhler, P., Knorr, G., Buiron, D., Lourantou, A., & Chappellaz, J., Abrupt rise in atmospheric CO₂ at the onset of the Bølling/Allerød: in-situ ice core data versus true atmospheric signal, *Climate of the Past*, 7(2), 473-486, 2011.

Kojima, K.: *Densification of seasonal snow cover*, *Phys. Snow Ice Proc. HUSCAP*, 1(2), 929–952, 1967.

Landais, A., Barnola, J. M., Kawamura, K., Caillon, N., Delmotte, M., Van Ommen, T., Dreyfus, G., Jouzel, J., Masson-Delmotte, V., Minster, B., Freitag, J., Leuenberger, M., Schwander, J., Huber, C., Etheridge, D. and Morgan, V.: *Firn-air δ¹⁵N in modern polar sites and glacial–interglacial ice: a model-data mismatch during glacial periods in Antarctica?*, *Quat. Sci. Rev.*, 25(1–2), 49–62, doi:10.1016/j.quascirev.2005.06.007, 2006.

Landais, A., Dreyfus, G., Capron, E., Jouzel, J., Masson-Delmotte, V., Roche, D. M., Prié, F., Caillon, N., Chappellaz, J., Leuenberger, M., Lourantou, A., Parrenin, F., Raynaud, D. and Teste, G.: *Two-phase change in CO₂, Antarctic temperature and global climate during Termination II*, *Nat. Geosci.*, 6(12), 1062–1065, doi:10.1038/ngeo1985, 2013.

Li, J. and Zwally, H. J.: *Modeling the density variation in the shallow firn layer*, *Ann. Glaciol.*, 38(1), 309–313, 2004.

Ligtenberg, S. R. M., Medley, B., Van Den Broeke, M. R. and Munneke, P. K.: *Antarctic firn compaction rates from repeat-track airborne radar data: II. Firn model evaluation*, *Ann. Glaciol.*, 56(70), 167–174, doi:10.3189/2015AoG70A204, 2015.

Lipenkov, V. Y., Barkov, N. I., Duval, P. and Pimienta, P.: *Crystalline texture of the 2083 m ice core at Vostok Station, Antarctica*, *J. Glaciol.*, 35(121), 392–398, 1989.

Loulergue, L., Parrenin, F., Blunier, T., Barnola, J.-M., Spahni, R., Schilt, A., Raisbeck, G. and Chappellaz, J.: *New constraints on the gas age-ice age difference along the EPICA ice cores, 0-50 kyr*, *Clim. Past*, 3, 527–540, 2007.

Loulergue, L., Schilt, A., Spahni, R., Masson-Delmotte, V., Blunier, T., Lemieux, B., Barnola, J.-M., Raynaud, D., Stocker, T. F. and Chappellaz, J.: *Orbital and millennial-scale features of atmospheric CH₄ over the past 800,000 years*, *Nature*, 453(7193), 383–386, doi:10.1038/nature06950, 2008.

Lundin, J., Stevens, C., Arthern, R., Buizert, C., Orsi, A., Ligtenberg, S., Waddington, E., *Firn Model Intercomparison Experiment (FirnMICE)*, *Journal of Glaciology*, 1-22. doi:10.1017/jog.2016.114, 2017.

Lüthi, D., Le Floch, M., Bereiter, B., Blunier, T., Barnola, J.-M., Siegenthaler, U., Raynaud, D., Jouzel, J., Fischer, H., Kawamura, K. and Stocker, T. F.: *High-resolution carbon dioxide concentration record 650,000–800,000 years before present*, *Nature*, 453(7193), 379–382, doi:10.1038/nature06949, 2008.

Maeno, N. and Ebinuma, T.: *Pressure sintering of ice and its implication to the densification of snow at polar glaciers and ice sheets*, *J. Phys. Chem.*, 87(21), 4103–4110, 1983.

Marcott, S. A., Bauska, T. K., Buizert, C., Steig, E. J., Rosen, J. L., Cuffey, K. M., Fudge, T. J., Severinghaus, J. P., Ahn, J., Kalk, M. L., McConnell, J. R., Sowers, T., Taylor, K. C., White, J. W. C. and Brook, E. J.: *Centennial-scale changes in the global carbon cycle during the last deglaciation*, *Nature*, 514(7524), 616–619, doi:10.1038/nature13799, 2014.

Martinerie, P., Raynaud, D., Etheridge, D. M., Barnola, J.-M. and Mazaudier, D.: *Physical and climatic parameters which influence the air content in polar ice*, *Earth Planet. Sci. Lett.*, 112(1–4), 1–13, 1992.

Martinerie, P., Lipenkov, V. Y., Raynaud, D., Chappellaz, J., Barkov, N. I. and Lorius, C.: *Air content paleo record in the Vostok ice core (Antarctica): A mixed record of climatic and glaciological parameters*, *J. Geophys. Res. Atmospheres*, 99(D5), 10565–10576, 1994.

Mellor, M.: *Properties of snow*, CRREL Monograph, Section III-A1., 1964.

Miller, D. A., Adams, E. E. and Brown, R. L.: *A microstructural approach to predict dry snow metamorphism in generalized thermal conditions*, *Cold Reg. Sci. Technol.*, 37(3), 213–226, doi:10.1016/j.coldregions.2003.07.001, 2003.

Morgan, V. I., *High-temperature ice creep tests*, *Cold Regions Science and Technology*, 19, 295-300, 1991.

Nie S., Bartelt, N. C. and Thürmer, K., Observation of Surface Self-Diffusion on Ice, *Physical Review Letters*, PRL 102, 136101, DOI: 10.1103/PhysRevLett.102.136101, 2009.

Orsi, A. J., Cornuelle, B. D., & Severinghaus, J. P., Magnitude and temporal evolution of Dansgaard–Oeschger event 8 abrupt temperature change inferred from nitrogen and argon isotopes in GISP2 ice using a new least-squares inversion, *Earth and Planetary Science Letters*, 395, 81–90, 2014.

Overly, T. B., Hawley, R. L., Helm, V., Morris, E. M. and Chaudhary, R. N.: Greenland annual accumulation along the EGIG line, 1959–2004, from ASIRAS airborne radar and detailed neutron-probe density measurements, *Cryosphere Discuss.*, 9(6), 6791–6828, doi:10.5194/tcd-9-6791-2015, 2015.

Parrenin, F., Dreyfus, G., Durand, G., Fujita, S., Gagliardini, O., Gillet, F., Jouzel, J., Kawamura, K., Lhomme, N., Masson-Delmotte, V., Ritz, C., Schwander, J., Shoji, H., Uemura, R., Watanabe, O., and Yoshida, N.: 1-D-ice flow modelling at EPICA Dome C and Dome Fuji, East Antarctica, *Clim. Past*, 3(2), 243–259, 2007.

Parrenin, F., Petit, J.-R., Masson-Delmotte, V., Wolff, E., Basile-Doelsch, I., Jouzel, J., Lipenkov, V., Rasmussen, S. O., Schwander, J., Severi, M., Udisti, R., Veres, D. and Vinther, B. M.: Volcanic synchronisation between the EPICA Dome C and Vostok ice cores (Antarctica) 0–145 kyr BP, *Clim. Past*, 8(3), 1031–1045, doi:10.5194/cp-8-1031-2012, 2012.

Parrenin, F., Masson-Delmotte, V., Köhler, P., Raynaud, D., Paillard, D., Schwander, J., Barbante, C., Landais, A., Wegner, A., Jouzel, J.: Synchronous change of atmospheric CO₂ and Antarctic temperature during the last deglacial warming, *Science*, vol. 339, 1060–1063, 2013.

Pimienta, P.: Etude du comportement mécanique des glaces polycristallines aux faibles contraintes: applications aux glaces des calottes polaires, PhD Thesis, Université Scientifique Technologique et Médicale de Grenoble., 166 pp, 1987.

Pimienta, P. and Duval, P.: Rate controlling processes in the creep of the polar glacier ice, *J. Phys. Colloq.*, 48(C1), C1-243–C1-248, doi:10.1051/jphyscol:1987134, 1987.

Proksch, M., Rutter, N., Fierz, C. and Schneebeli, M.: Intercomparison of snow density measurements: bias, precision, and vertical resolution, *The Cryosphere*, 10(1), 371–384, doi:10.5194/tc-10-371-2016, 2016.

Ramseier, R. O.: Self-diffusion in ice monocrystals, CRREL Research Report no 232, 1967.

Rasmussen, S. O., Andersen, K. K., Svensson, A. M., Steffensen, J. P., Vinther, B. M., Clausen, H. B., Siggaard-Andersen, M.-L., Johnsen, S. J., Larsen, L. B., Dahl-Jensen, D., Bigler, M., Röthlisberger, R., Fischer, H., Goto-Azuma, K., Hansson, M. E. and Ruth, U.: A new Greenland ice core chronology for the last glacial termination, *J. Geophys. Res.*, 111(D6), doi:10.1029/2005JD006079, 2006.

Rhodes, R. H., Brook, E. J., Chiang, J. C., Blunier, T., Maselli, O. J., McConnell, J. R., Romanini, D. and Severinghaus, J. P.: Enhanced tropical methane production in response to iceberg discharge in the North Atlantic, *Science*, 348(6238), 1016–1019, 2015.

Salamatin, A. N., Lipenkov, V. Y., Barnola, J. M., Hori, A., Duval, P. and Hondoh, T.: Snow/firn densification in polar ice sheets, *Phys. Ice Core Rec. - II*, 68(Supplement), 195–222, 2009.

Schwander, J.: The transformation of snow to ice and the occlusion of gases, *Environ. Rec. Glaciers Ice Sheets*, 53–67, 1989.

Schwander, J., Barnola, J. M., Andrié, C., Leuenberger, M., Ludin, A., Raynaud, D., & Stauffer, B., The age of the air in the firn and the ice at Summit, Greenland. *Journal of Geophysical Research: Atmospheres*, 98(D2), 2831–2838, 1993.

Schwander, J., Sowers, T., Barnola, J.-M., Blunier, T., Fuchs, A. and Malaizé, B.: Age scale of the air in the summit ice: Implication for glacial-interglacial temperature change, *J. Geophys. Res. Atmospheres*, 102(D16), 19483–19493, 1997.

Severinghaus, J. P., Sowers, T., Brook, E. J., Alley, R. B. and Bender, M. L.: Timing of abrupt climate change at the end of the Younger Dryas interval from thermally fractionated gases in polar ice, *Nature*, 391(6663), 141–146, 1998.

Sime, L. C., Wolff, E. W., Oliver, K. I. C. and Tindall, J. C., Evidence for warmer interglacials in East Antarctic ice cores, *Nature*, vol. 462, 2009.

Sowers, T., Bender, M. and Raynaud, D.: Elemental and isotopic composition of occluded O₂ and N₂ in polar ice, *J. Geophys. Res. Atmospheres*, 94(D4), 5137–5150, 1989.

Sowers, T., Bender, M. and Korotkevich, Y.: $\delta^{15}\text{N}$ of N₂ in Air Trapped in Polar ice, *J. Geophys. Res.*, 97(D14), 15–683, 1992.

Veres, D., Bazin, L., Landais, A., Toyé Mahamadou Kele, H., Lemieux-Dudon, B., Parrenin, F., Martinerie, P., Blayo, E., Blunier, T., Capron, E., Chappellaz, J., Rasmussen, S. O., Seeri, M., Svensson, A., Vinther, B., and Wolff, E. W.: The Antarctic ice core chronology (AICC2012): an optimized multi-parameter and multi-site dating approach for the last 120 thousand years, *Clim. Past*, 9(4), 1733–1748, 2013.

WAIS Divide Project Members: Onset of deglacial warming in West Antarctica driven by local orbital forcing, *Nature*, 500(7463), 440–444, doi:10.1038/nature12376, 2013.

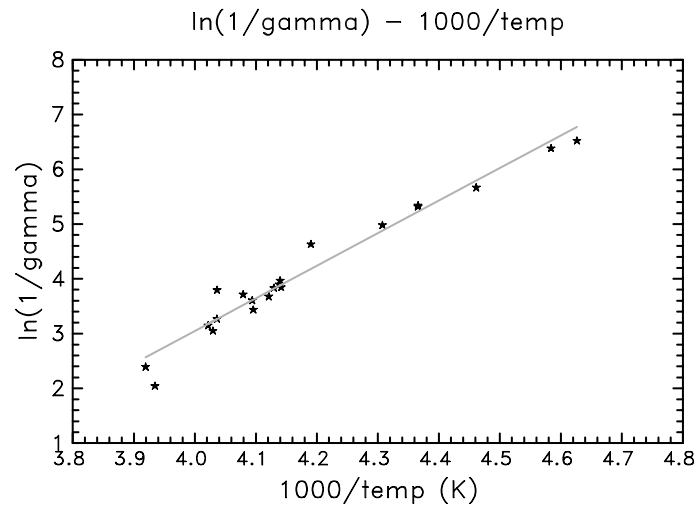
WAIS Divide Project Members: Precise inter-polar phasing of abrupt climate change during the last ice age, *Nature*, 520(7549), 661–665, 2015.

Wilkinson, D. S. and Ashby, M. F.: Pressure sintering by power law creep, *Acta Metall.*, 23(11), 1277–1285, 1975.

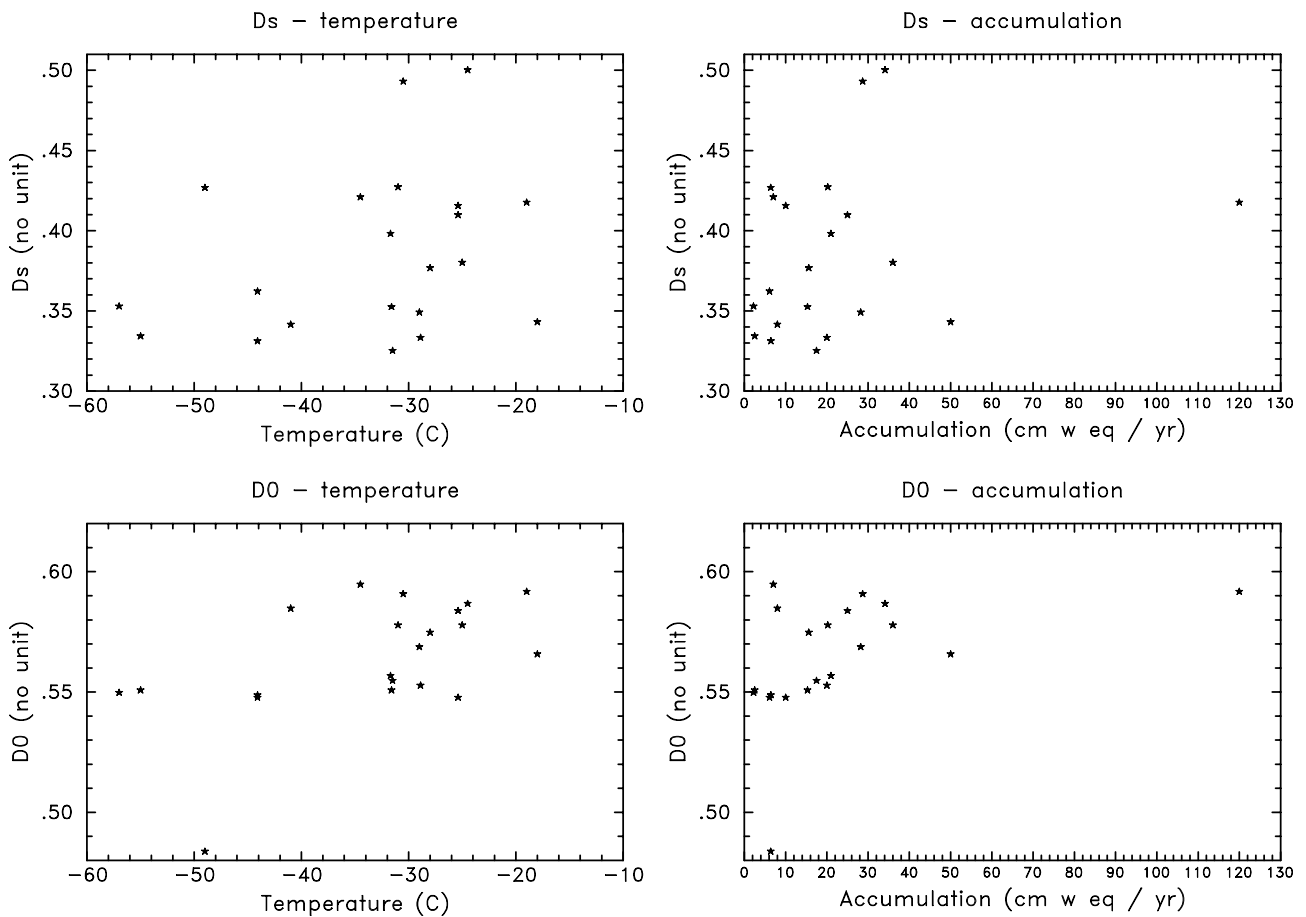
Witrant, E., Martinerie, P., Hogan, C., Laube, J. C., Kawamura, K., Capron, E., Montzka, S. A., Dlugokencky, E. J., Etheridge, D., Blunier, T. and Sturges, W. T.: A new multi-gas constrained model of trace gas non-homogeneous transport in firn: evaluation and behaviour at eleven polar sites, *Atmospheric Chem. Phys.*, 12(23), 11465–11483, doi:10.5194/acp-12-11465-2012, 2012.

Zwally, H. J. and Li, J.: Seasonal and interannual variations of firn densification and ice-sheet surface elevation at the Greenland summit, *J. Glaciol.*, 48(161), 199–207, 2002.

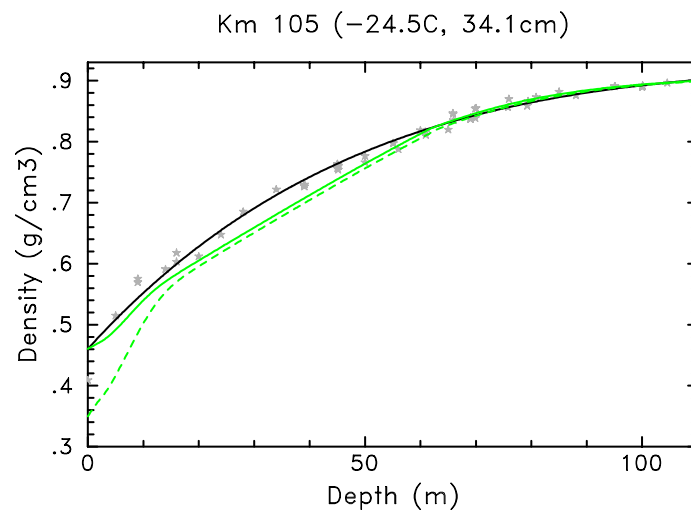
Supplementary material



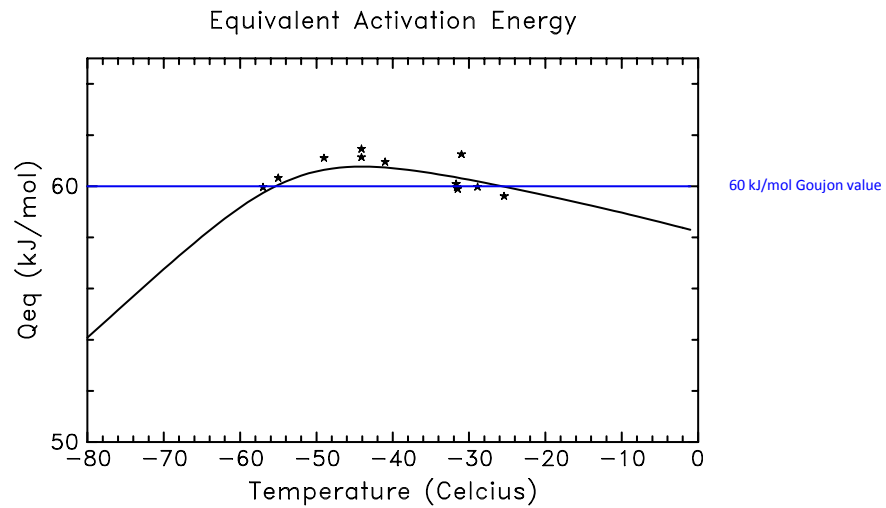
Supplementary Figure S1: Logarithmic representation of γ coefficient in Equation (4) as a function of the site temperature. The stars represent the γ coefficient calculated by the model for each site, the grey line represents a linear regression. Its slope allows evaluation of the activation energy relative to the snow densification mechanism in the model: 49.5 kJ/mol.



Supplementary Figure S2: Variations of the surface (D_s) and critical (D_0) relative densities with site temperature and accumulation. D_s is the value of the polynomial fit to density data represented on Figures S3 and S7 at the surface. D_0 is adjusted to minimize the root mean square deviations between model results and the polynomial fit to density data between the surface and the depth at which a density of 840 kg/m^3 is reached. No correlation between D_s or D_0 with temperature or accumulation could be found. Although the variability of D_s and D_0 are large, their impact on the LID is relatively small as illustrated on Figure S3.

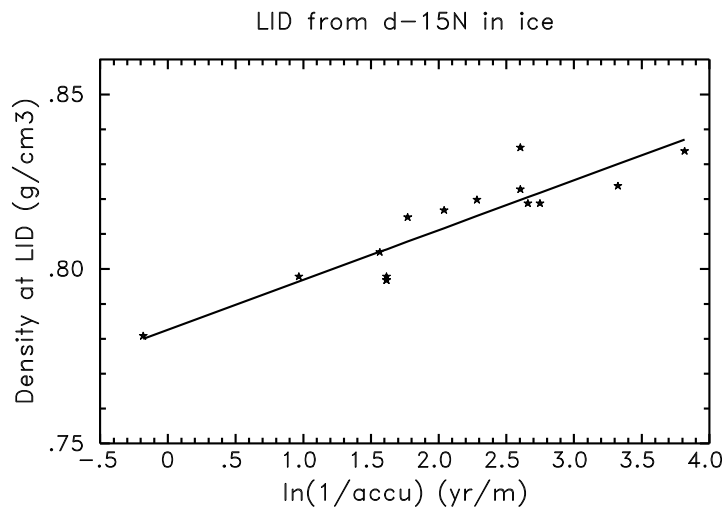


Supplementary Figure S3: Impact of the surface density value (D_s) on model results at Km 105 site. Grey stars represent measured densities, the black line represents a polynomial fit to density data. The two green curves represent model results obtained with two largely different values of the surface density. Lower values of D_s lead to faster modelled densification rates. While the difference between the two densification curves is important at the surface, the two curves are almost similar in the deep firn. The difference on D_s thus does not have much importance for the determination of the LID.



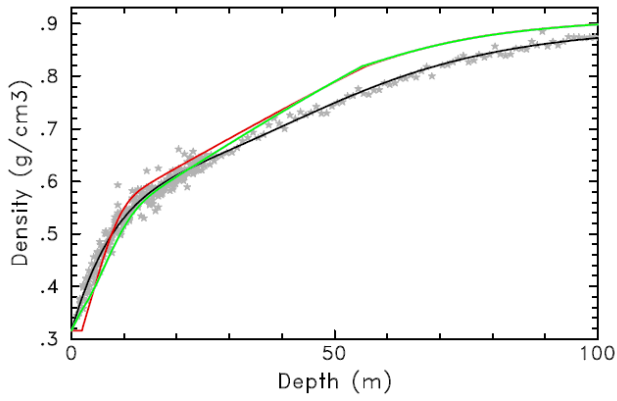
Supplementary Figure S4: Equivalent activation energies calculated for our model (without impurity effect, black line; with impurity effect for present day sites with available calcium concentrations, black stars). The blue line represents the value of 60kJ/mol used in Goujon et al. (2003).

For our model, the equivalent activation energy Q_{eq} is calculated by solving: $e^{\frac{-Q_{eq}}{RT}} = a_1 \times e^{\frac{-Q_1}{RT}} + a_2 \times e^{\frac{-Q_2}{RT}} + a_3 \times e^{\frac{-Q_3}{RT}}$.

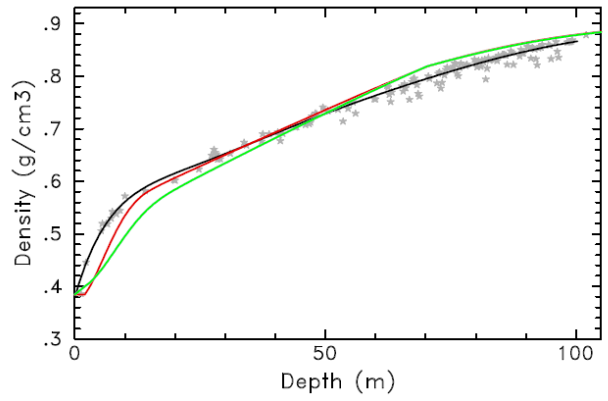


Supplementary Figure S5: Calculated density at LID with the Witrant et al. (2012) model of gas transport in firn (see main text, Section 2.4) as a function of the logarithm of the inverse of the accumulation rate (in m w. eq./yr). The stars show the results at individual firn air pumping sites (12 sites, 15 boreholes), and the line shows the regression presented in Equation (10) of the main text. The correlation coefficient is 0.9.

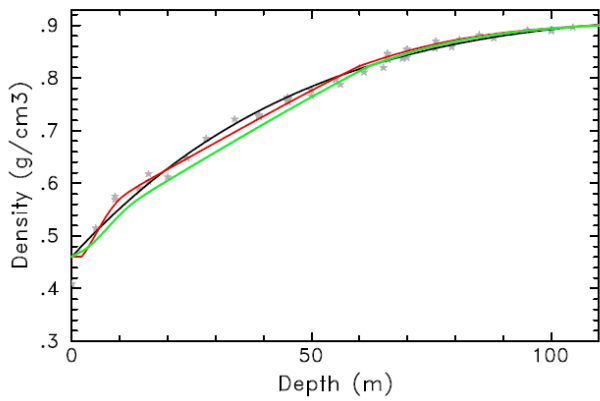
Dye 3 (-18C, 50cm)



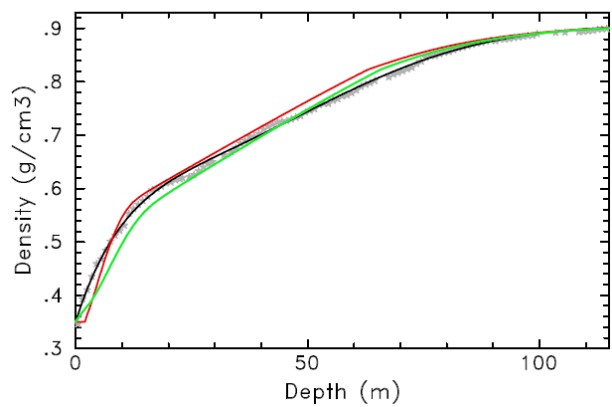
DE08 (-19C, 120cm)



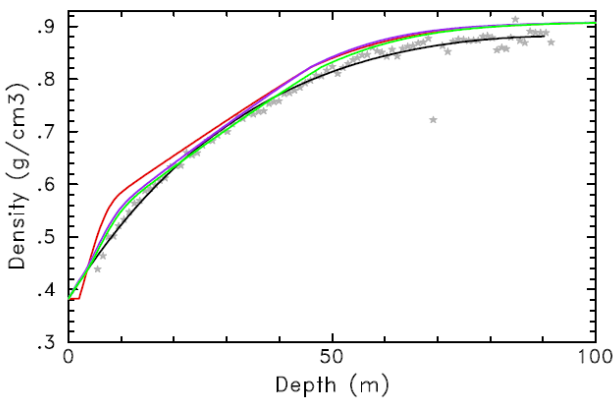
Km 105 (-24.5C, 34.1cm)



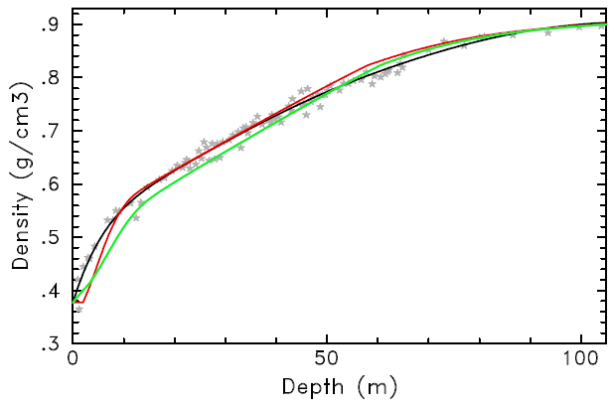
Site 2 (-25C, 36cm)



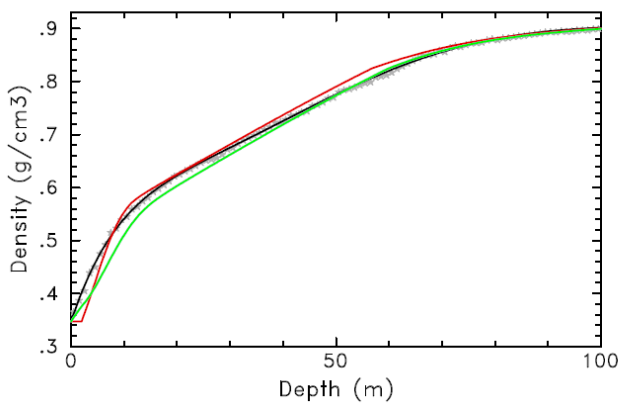
Siple Dome (-25.4C, 10cm)



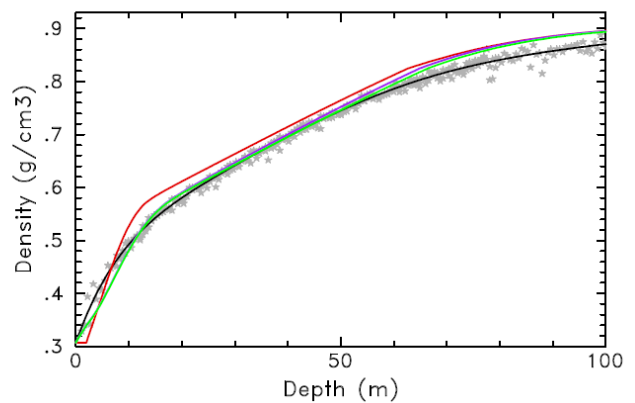
D-47 (-25.4, 25cm)



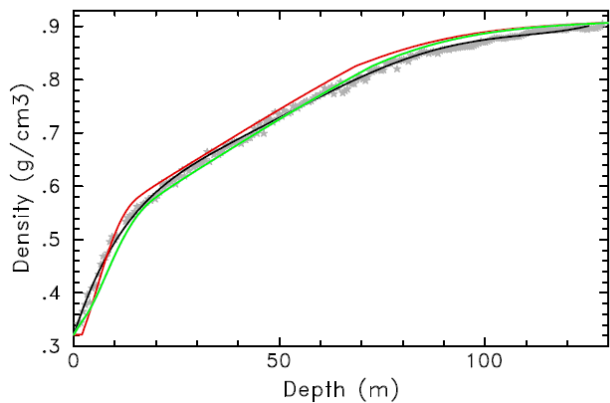
Byrd (-28C, 15.6cm)



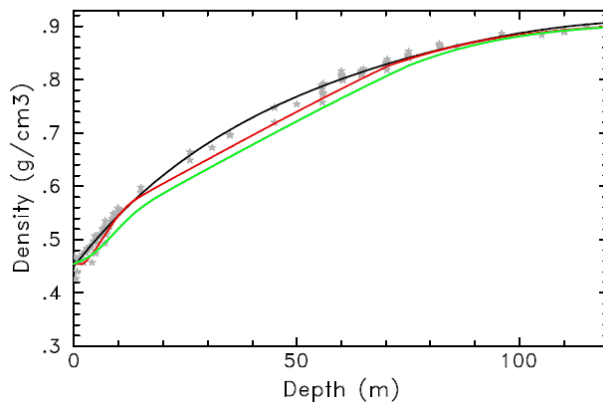
NEEM (-28.9, 20cm)



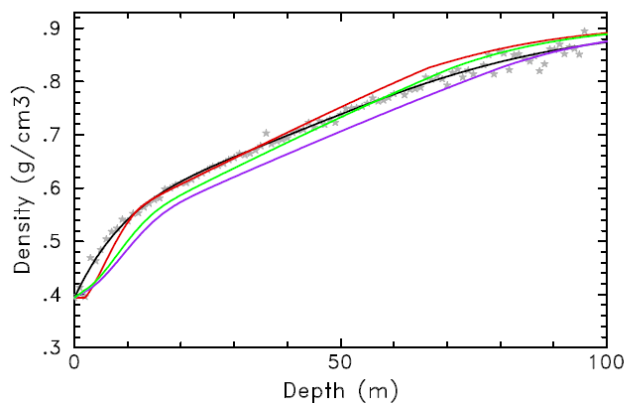
Crete (-29C, 28.2cm)



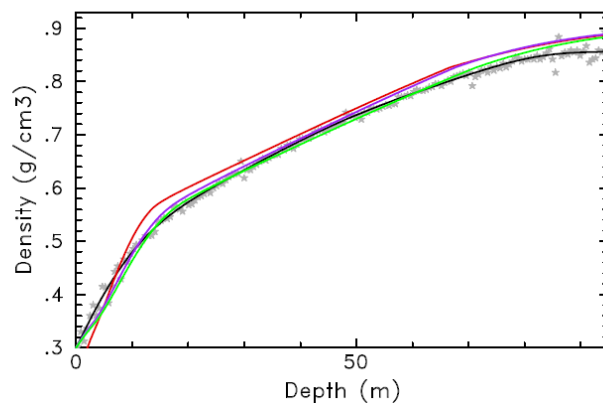
Km 200 (-30.5C, 28.7cm)



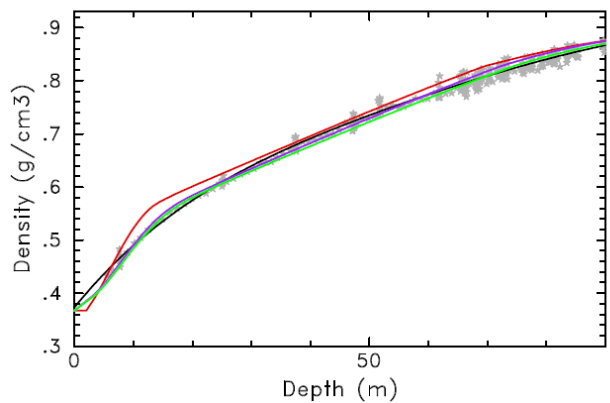
WAIS Divide (-31C, 20.2cm)



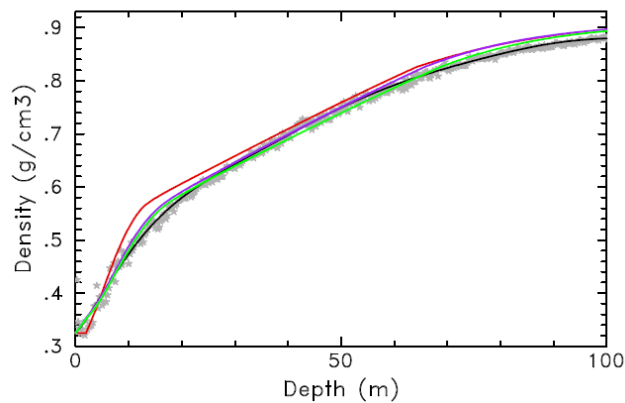
NGRIP (-31.5, 17.5cm)



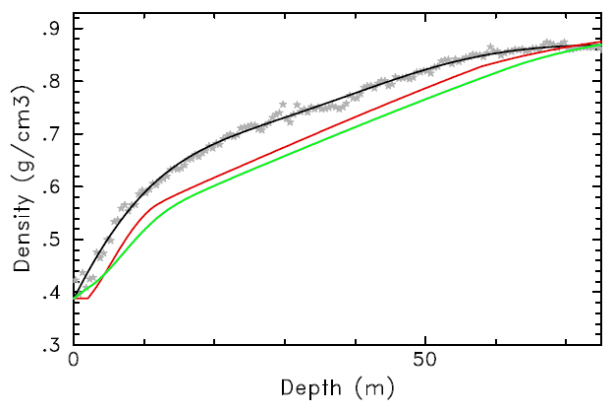
GRIP (-31.7C, 21cm)



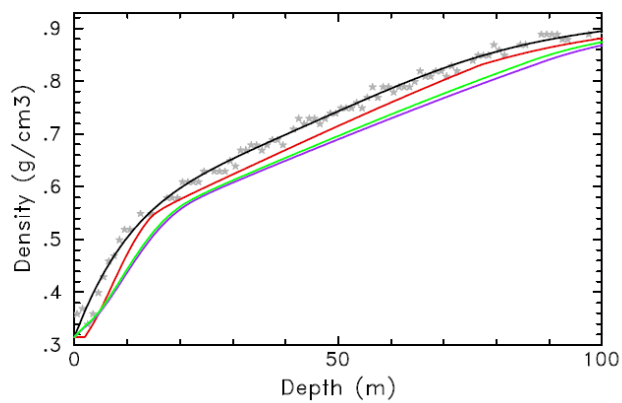
B29 (-31.6, 15.3cm)

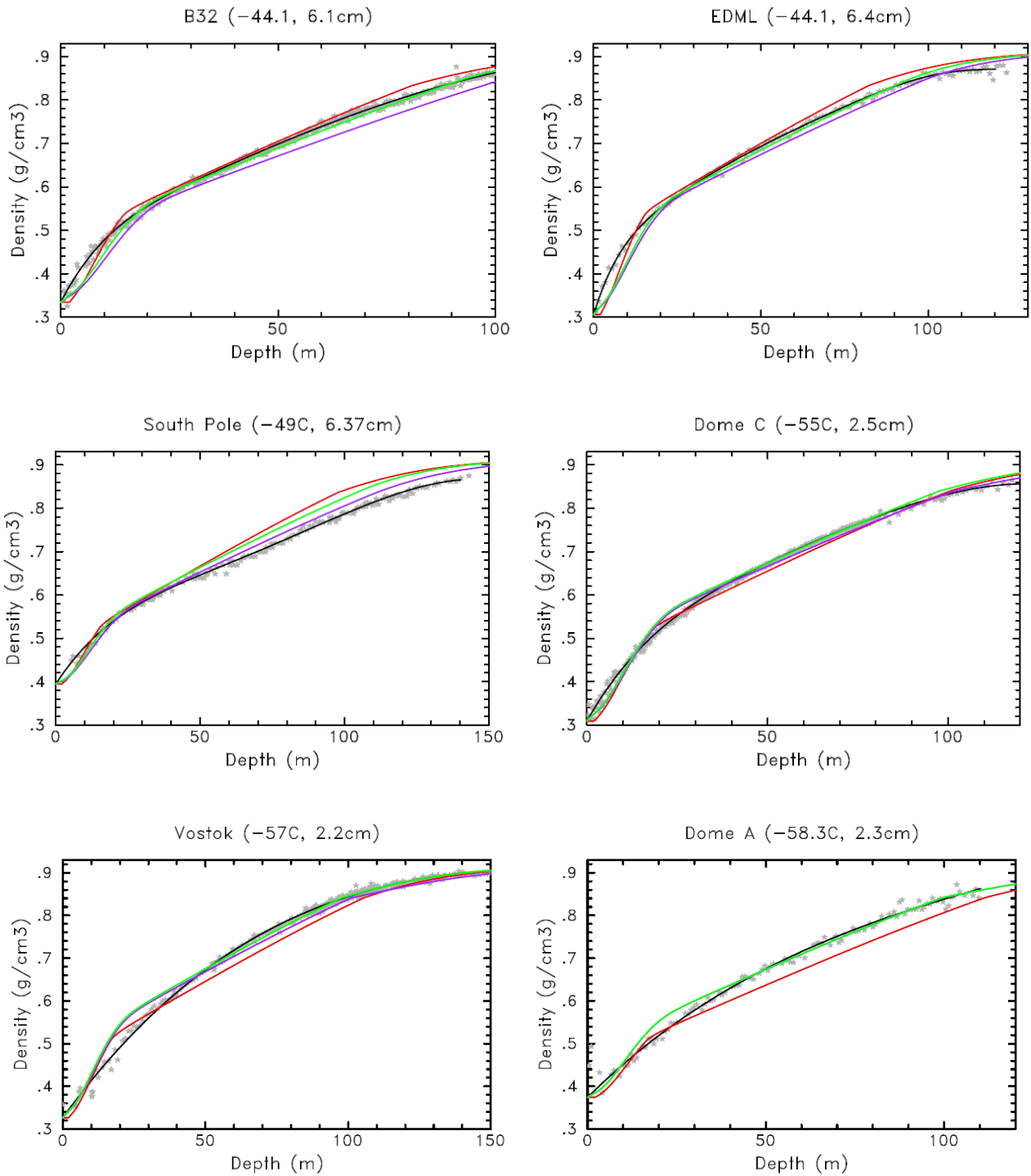


Mizuho station (-34.5C, 7cm)

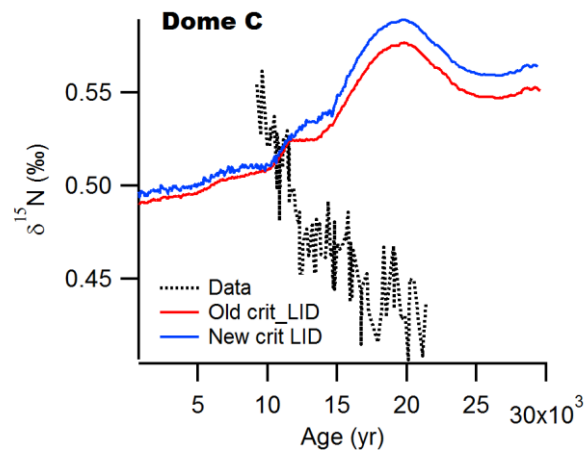


Talos (-41C, 8cm)

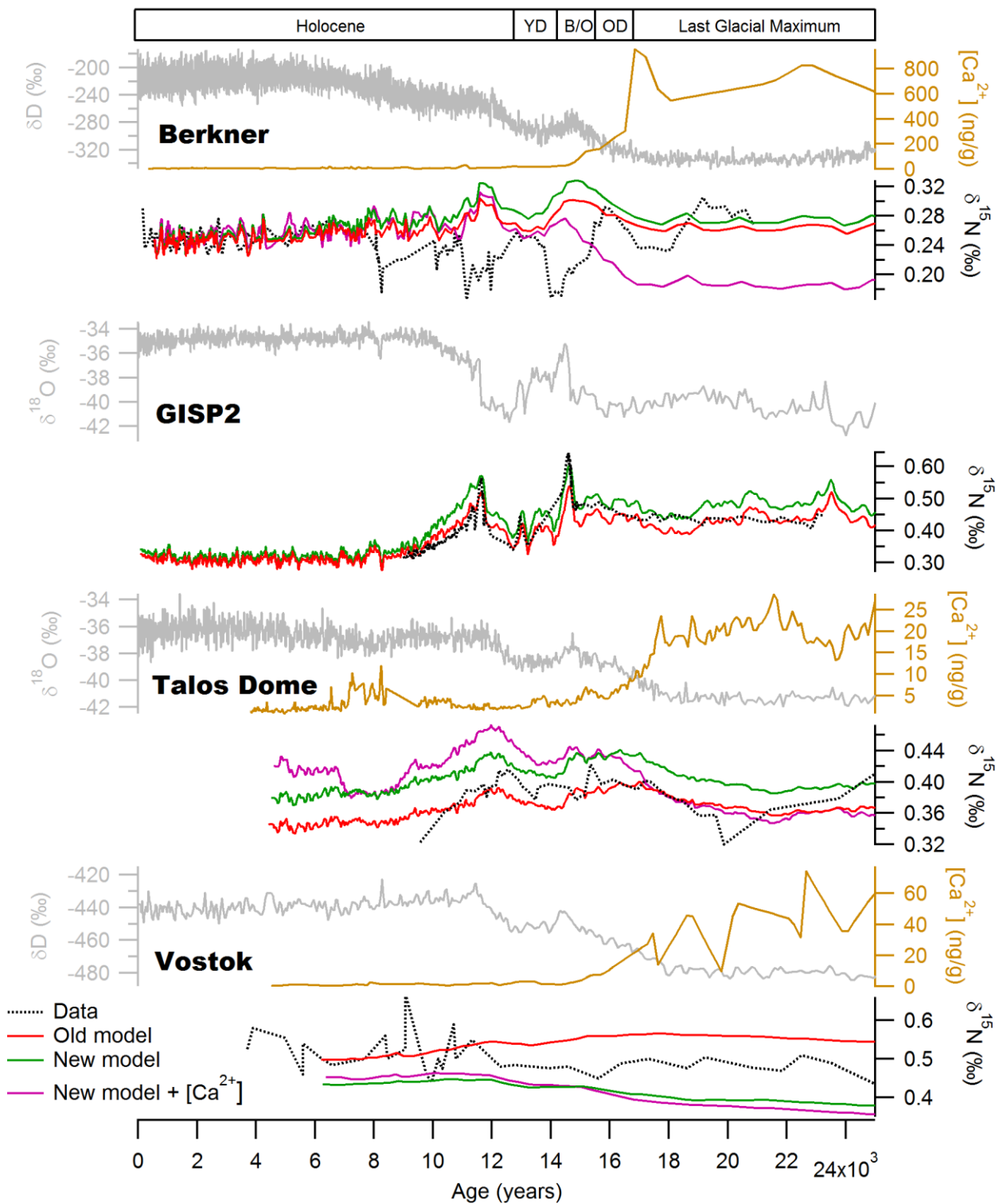




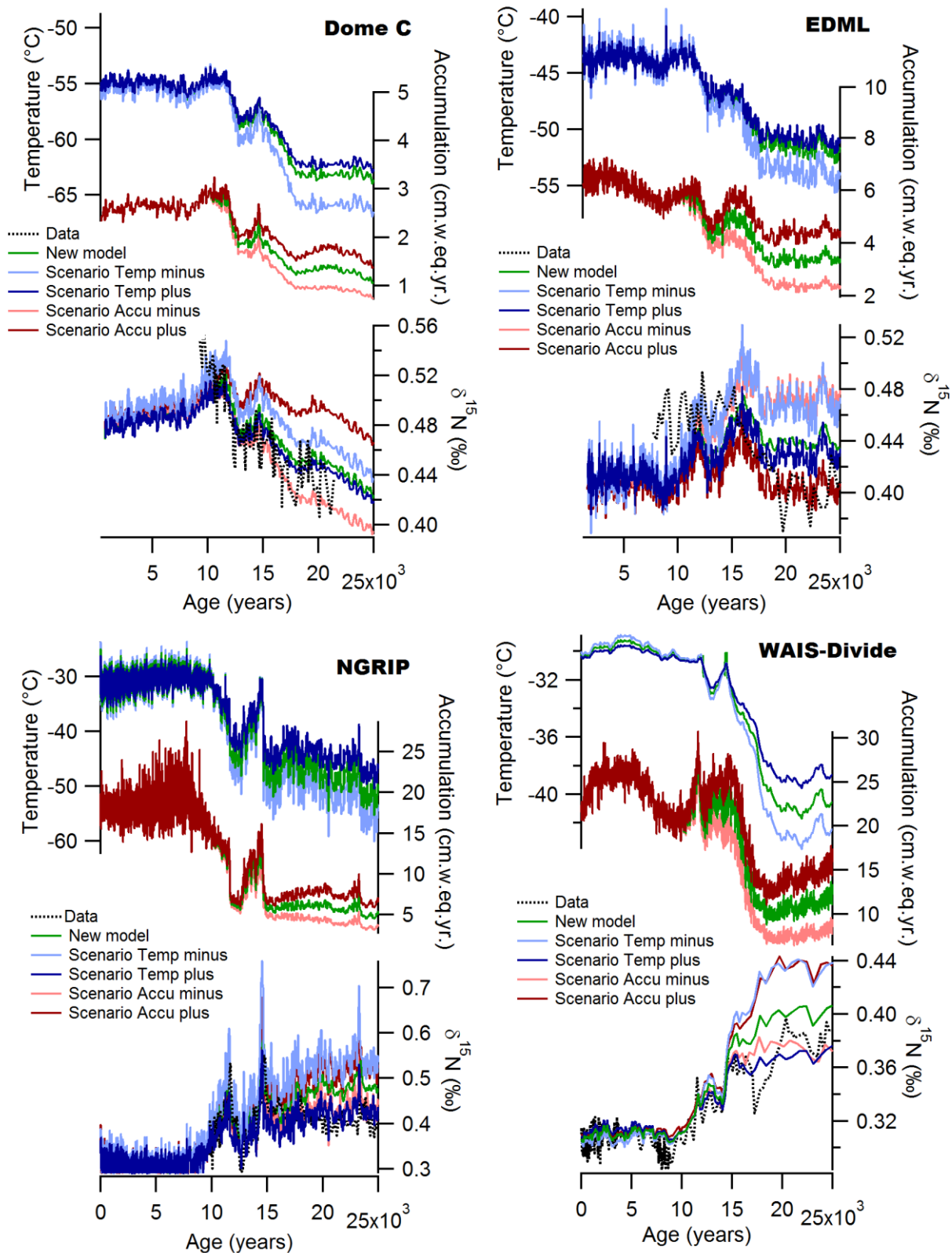
Supplementary Figures S6: Measured and modelled density profiles for 22 sites, the grey stars correspond to the data, the polynomial fit to the data is in black, the density profile simulated with the old version of the LGGE model is in red, the density profile simulated with the new version of the LGGE model is in green and the density profile simulated with the new version of the LGGE model with the dust effect in purple.



Supplementary Figure S7: Comparison of the measured (in black) and the old modelled $\delta^{15}\text{N}$ at Dome C. The simulated $\delta^{15}\text{N}$ using the old gas trapping criterion is in red and the simulated $\delta^{15}\text{N}$ using the new gas trapping criterion is in blue.



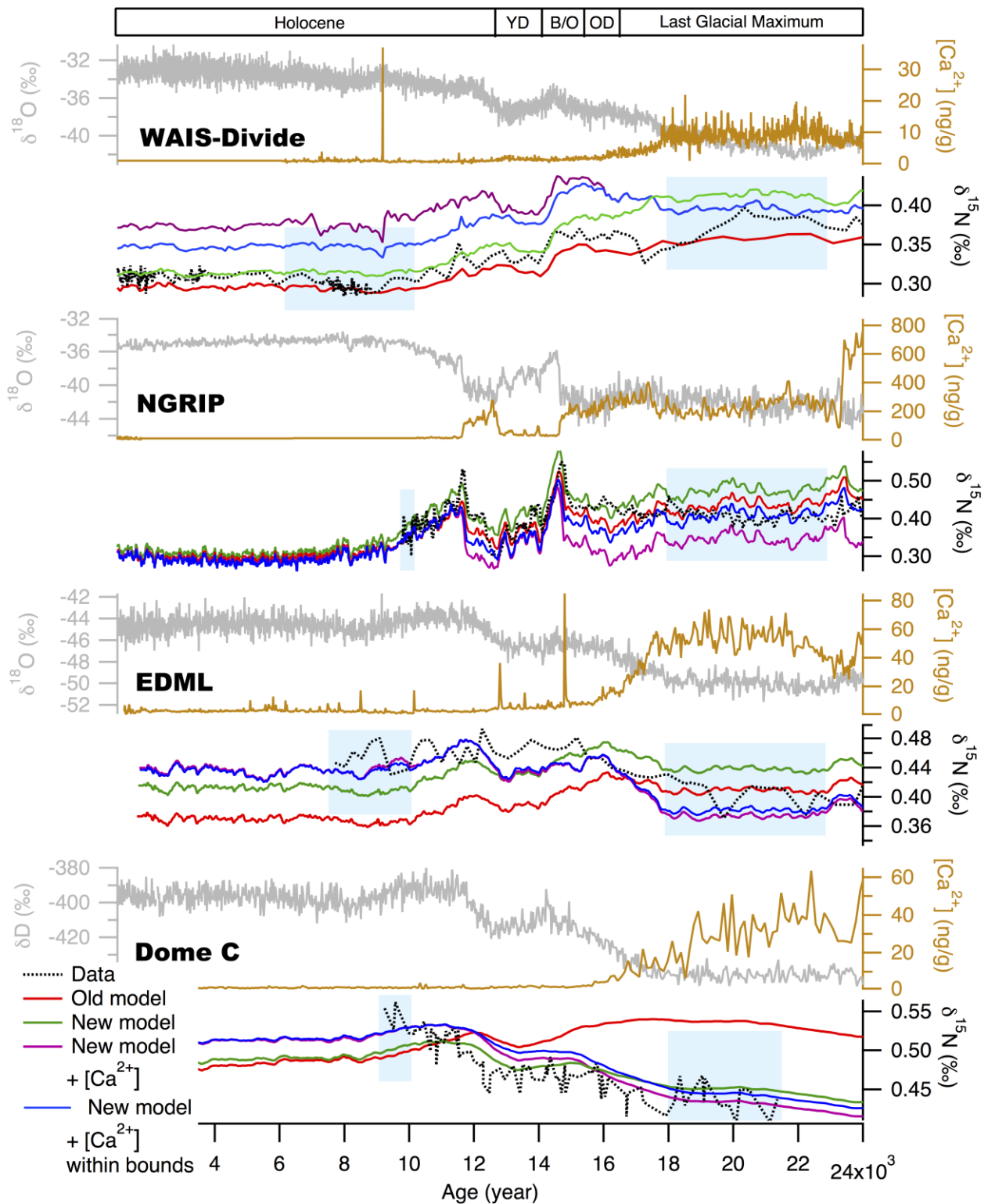
Supplementary Figure S8: Comparison of the measured $\delta^{15}\text{N}$ (black) and the modeled $\delta^{15}\text{N}$ (old (red), new version (green) and new version with impurity (purple)) of the LGGE model for Berkner, GISP2, Talos Dome and Vostok. The water $\delta^{18}\text{O}$ or δD profiles are displayed in grey and the calcium concentration profile in gold.



Supplementary Figure S9: Comparison of the measured (black) and modelled $\delta^{15}\text{N}$ at Dome C, EDML, NGRIP and WAIS-Divide over the last deglaciation with our new model without impurity effect, using five different temperature and accumulation rate scenarios. The standard scenarios (Table S2) and corresponding $\delta^{15}\text{N}$ model outputs are in green. For building the Accu minus/plus and Temp minus/plus scenarios displayed on the two upper panels for each sites, we took the uncertainties mentioned in the main text: Accu minus

correspond to a LGM accumulation rate of -30% (-20%) in Antarctica (Greenland) compared to the standard run; Accu plus corresponds to a LGM accumulation rate of +30% (+20%) in Antarctica (Greenland) compared to the standard run. In Antarctica, Temp plus corresponds to a decrease by 10% of the temperature increase over the last deglaciation (i.e. warmer LGM temperature); Temp minus corresponds to an increase by 30% of the temperature increase over the last deglaciation (i.e. lower LGM temperature). In Greenland, Temp minus and Temp plus are scenarios where the temperature of the LGM is changed by +3 and -3°C.

Within the uncertainty range of the model inputs, it is possible to match the measured $\delta^{15}\text{N}$ with the model except for EDML where the modelled $\delta^{15}\text{N}$ LGM to EH change is always too small even with the scenario Accu plus. Note that the same figures can be obtained with the old version of the LGGE model with similar amplitude for the differences in simulated LGM $\delta^{15}\text{N}$ level between the different scenarios.



Supplementary Figure S10: Comparison of the measured $\delta^{18}\text{O}$ or δD (grey), the calcium concentration (gold), the measured $\delta^{15}\text{N}$ (black) and the modelled $\delta^{15}\text{N}$ (old (red), new version (green), new version with impurity following Freitag parameterization (purple) and new version with impurity (blue) using a parameterization with threshold for high and low values of the calcium concentration) of the LGGE model for WAIS-Divide, NGRIP, EDML and Dome C. Blue boxes for each sites indicate the periods over which the $\delta^{15}\text{N}$ average for the LGM and EH have been estimated for the calculation of the amplitude of the $\delta^{15}\text{N}$ change over the deglaciation

Sites	Location (Latitude ; Longitude)	Temperature (°C)	Accumulation (cm.w.eq.yr)	[Ca ²⁺] (ng/g)	Surface density (kg/m ³)	$\sigma_{\text{fit-data}}$ (kg/m ³)	$\sigma_{\text{old model-fit}}$ (kg/m ³)	$\sigma_{\text{new model-fit}}$ (kg/m ³)	$\sigma_{\text{new model with dust-fit}}$ (kg/m ³)
Dye 3 ^[1]	65°11'N ; 43°50'W	-18.0	50.0	X	357	13.8	32.7	30.8	X
DE08 ^[2]	66°43'19"S ; 113°11'58"E	-19.0	120.0	X	384.2	10.3	20.9	29.8	X
Km105 ^[4]	67°58'S ; 93°70'E	-24.5	34.1	X	460.5	14.0	10.7	21.1	X
Site 2 ^[5]	76°59'N ; 56°04'W	-25.0	36.0	X	350.1	5.8	18.3	19.2	X
Siple Dome ^[3]	81°39'3"S ; 148°47'66"W	-25.4	10.0	8.0	382.7	8.9	29.4	13.2	19.5
D-47 ^[6]	67°23'S ; 138°43'E	-25.4	25.0	X	377.4	12.5	15.9	21.8	X
Byrd ^[7]	80°S ; 120°W	-28.0	15.6	X	347.1	3.8	15.9	18.6	X
NEEM ^[8]	77.45°N ; 51.06°W	-28.9	20.0	7.4	307.2	8.0	27.2	13.5	15.8
Crête (site A) ^[9]	70°38'5.68"N ; 324°10'48"E	-29.0	28.2	X	321.7	7.0	18.7	14.0	X
Km200 ^[10]	68°15'S ; 94°05'E	-30.5	28.7	X	454.4	10.5	21.8	37.7	X
WAIS divide ^[11]	79°28'S ; 112°05'W	-31.0	20.2	1.58	393.7	8.7	18.2	21.3	35.1
Ngrip ^[12]	75°10'N ; 42°32'W	-31.2	17.5	10.0	299.9	6.9	22.2	9.9	13.4
Grip ^[13]	72°34'N ; 37°37'W	-31.7	21.0	7.8	367.0	6.7	18.9	10.3	8.8
B29 ^[14]	76°00'N ; 43°29'E	-31.6	15.3	9.2	325	10.1	22.7	7.2	10.2
Mizuho ^[15]	70°41'53"S ; 44°19'54"E	-34.5	7.0	X	421	9.8	50.0	66.5	X
Talos Dome ^[16]	72°49'S ; 159°11'E	-41.0	8.0	4.0	315.3	12.1	29.6	46.0	51.9

B32 ^[17]	75°00'S ; 0°00'E	-44.1	6.1	1.7	334.5	6.2	15.6	13.3	28.7
EDML ^[18]	75°S ; 0°04'E	-44.1	6.4	3.0	305.9	5.3	19.4	16.9	23.6
South Pole ^[19]	90°S	-49.0	6.37	2.0	394.4	6.4	35.5	26.7	15.2
Dôme C ^[20]	75°06'S ; 123°21'E	-55.0	2.5	1.8	309.2	6.2	15.3	11.0	11.0
Vostok ^[21]	78°28'S ; 106°48'E	-57.0	2.2	1.6	326.5	8.0	28.0	23.5	23.0
Dome A ^[22]	80°22'01.6"S 77°22'22.3E	-58.3	2.3	X	374	9.8	32	13.4	X

References below were used for the following data: ^a location, ^b density, ^c temperature, ^d accumulation, ^e calcium concentration

Best efforts were made to find information about the methodologies used for density measurements. The following Greek letters are used to indicate the method used, the use of several letters for the same site implies that several data series were used.

α : volume and weight measurements on whole cores or bags. The precision of such measurements is dependent on the regularity of the core shape.

β : volume and weight measurements in firn, and high precision hydrostatic weighing measurements in ice

γ : volume and weight measurements on machined samples (regular volume, samples are often small)

δ : gamma ray beam attenuation through the ice core (very high resolution)

ϵ : camera assisted volume measurements, and weight measurements (high resolution)

[1] ^{a, c, d} Robin, 1983; ^b http://gcmd.nasa.gov/r/d/LSSU_and_PSU_Firn_data Spencer et al., 2001

[2] ^{a, b, c, d} Etheridge and Wookey, 1989; ^b Arnaud et al., 1998, 2000, γ density measurement method

[3] ^{a, b} <https://nsidc.org/data/waiscores/corec.html>, ^c Butler et al., 1999; Jones et al., 2014; Kreutz et al., 1999, 2000, α density measurement method

[4] ^{a, b, c, d} Salamatin et al., 2009, γ density measurement method

[5] ^{a, c} Robin, 1983; ^b http://gcmd.nasa.gov/r/d/LSSU_PSU_Firn_data Spencer et al., 2001 originally from Langway, 1967 with β density measurement method

[6] ^{a, b, c, d} Arnaud et al., 1998 with β density measurement method

[7] ^{a, b, c, d} http://gcmd.nasa.gov/r/d/LSSU_PSU_Firn_data Spencer et al., 2001, originally from Gow, 1968 with β density measurement method

[8] ^{a, b, c} Buizert et al., 2012; ^b Steen-Larsen et al., 2011 ; ^e Gfeller et al., 2014, α density measurement method

[9] ^{a, b, c, d} http://gcmd.nasa.gov/r/d/LSSU_PSU_Firn_data and Spencer et al., 2001 ; ^b originally from Clausen et al., 1988

[10] ^{a, b, c, d} Salamatin et al., 2009; ^b Arnaud et al., 1998, γ density measurement method

[11] ^{a, b, c, d} Fitzpatrick et al., 2014 ; ^e Cole-Dai et al., 2013

[12] ^{a, c, d} Ngrip community members, 2004, ^b H.C. Steen-Larsen Pers. Comm., ^e Svensson pers. Comm., 2016, α density measurement method

[13] ^{a, b, c, d} http://gcmd.nasa.gov/r/d/LSSU_PSU_Firn_data and Schwander et al., 1997; ^e Izuka et al., 2008, α and γ density measurement methods

[14] Freitag et al., 2013; Hörhold et al., 2011, δ density measurement method

[15] a, c, d (Nishio et al., 1979) ; b (Narita and Maeno, 1978), γ density measurement method

[16] a, c www.taldice.org/project/site ; b www.taldice.org/data (data from F. Parrenin) ; d Stenni et al., 2002 e Schüpbach et al., 2013

[17] Freitag et al., 2013; Hörhold et al., 2011, δ density measurement method

[18] a, b Kipfstuhl et al., 2009 ; c Freitag et al., 2013; d Oerter et al., 2004; e Fischer et al., 2007, α density measurement method

[19] a, b, c http://gcmd.nasa.gov/r/d/LSSU_PSU_Firn_data and Spencer et al., 2001 ; d Mosley-Thompson et al., 1995; e Ferris et al., 2011

[20] a, d Gautier et al., 2016, b R. Mulvaney pers. com. and Leduc-Leballeur et al., 2015; c Arnaud et al., 2000 ; e Lambert et al., 2012, α and ϵ density measurement methods

[21] a, c, d Arnaud et al., 2000 ; b http://gcmd.nasa.gov/r/d/LSSU_PSU_Firn_data and Spencer et al., 2001 and J.-M. Barnola, unpublished (using γ density measurement method); e De Angelis et al., 1997

[22] a, b, c Cunde et al., 2008 ; Cunde pers. com. 2016 ; d: Hou et al., 2007 and Ding et al., 2016, α density measurement method

*Supplementary Table S1: Standard deviation between modeled and measured density profiles for **22** polar sites, for the old LGGE model and the new LGGE model (with three different activation energies in the firn densification module noted “new model” and with three different activation energies depending on Ca^{2+} concentration in the firn densification module noted “new model with dust”). The values in bold indicate the lowest standard deviation between modeled and fitted density profiles for each site.*

Δ age	Data	Old	New	New + dust
Dye 3	78	68.4	61.8	-
DE08	35.5	36.8	31.3	-
km105	104.4	111.7	106.4	-
Site2	112.2	109.2	103.3	-
Siple Dome	329	287.9	296.9	284.9
D-47	152	145.3	141.7	-
Byrd	238.9	225	226.9	-
NEEM	209.4	187.4	191.9	187.4
Crete	156.1	150	145.7	-
km200	137.9	156.7	152.6	-
WAIS divide	225	206.5	206.5	233.3
North GRIP	248.4	226.2	236.5	224.5
GRIP	209.9	205.7	205.7	200
B29	270.3	251	264.7	252.9
Mizuho	483.7	518.4	557	-
Talos	554.1	592.6	637.7	656.4
B32	896.8	816.1	889.9	978.4
EDML	874.5	787.3	852.9	899.7
SP	1160.9	965.2	1002.8	1068.7
DC	2639.1	2473	2461	2557
Vostok	2814.3	2960.4	2810.4	2919.5
Dome A	2812.7	3024.8	2764	-

Supplementary Table S2: Comparison of Δ age at the bottom of the firn for the different sites studied here. The main features already observed for the comparison of the standard deviation between modeled and measured density profiles (Table S1) are also observed here. This is the case for the worsened agreement between model and data at Talos and Mizuho when using the new parameterization or the improved model vs data agreement at low temperature and low accumulation sites of the bottom of the table (B32, EDML, South Pole, Dome C, Vostok, Dome A).

Sites	Temperature scenario	Accumulation rate scenario	Calcium scenario
NGRIP	Dahl-Jensen et al., 1998 ; Kindler et al., 2014	Bazin et al., 2013	Svensson (comm. pers.) and Seierstad et al., 2014
Dome C	Stenni et al., 2010	Bazin et al., 2013	Fischer et al., 2007 and Lambert et al., 2012
EDML	Stenni et al., 2010	Bazin et al., 2013	Fischer et al., 2007
WAIS-Divide	Buizert et al., 2015 and WAIS Divide Project Members, 2013	Fudge et al., 2016	Buizert et al., 2015
Berkner Island	Capron et al., 2013	Capron et al., 2013	Capron et al., 2013
GISP2	Cuffey and Clow, 1997	Cuffey and Clow 1997	X
Talos Dome	Buiron et al., 2011	Bazin et al., 2013	Schüpbach et al., 2013
Vostok	Cuffey and Vimeux, 2001	Bazin et al., 2013	Legrand et al., 1988

Supplementary Table S3: References of the temperature, accumulation rate and calcium scenarios over the last deglaciation for NGRIP, Dome C, EDML, WAIS-Divide, Berkner Island, GISP2, Talos Dome and Vostok. The temperature (T) scenario for NGRIP has been built so that its temporal evolution reflects the $\delta^{18}O$ temporal evolution ($T=a\delta^{18}O+b$) with an adjustment of a and b to reflect the $\sim 20^{\circ}C$ temperature change between LGM and Holocene (Dahl-Jensen et al., 1998) as well as abrupt change of temperature of $\sim 12.5^{\circ}C$ and $\sim 10.5^{\circ}C$ at the onset of the Bølling-Allerød and end of Younger Dryas as given by Kindler et al. (2014)

EH – LGM (‰)	Dome C	EDML	NGRIP	WAIS-D
Measured	0.1051	0.0538	-0.0986	-0.0780
Old	-0.0404	-0.0446	-0.1080	-0.0639
Old + dust	0.0904	0.0545	-0.0088	-0.0078
New parameterization (Table 1)	0.0519	-0.0313	-0.112	-0.0909
New parameterization + dust	0.0930	0.0651	-0.00937	-0.0129
Test A	-0.0183	-0.0331	-0.0842	-0.0648
Test A + dust	0.0714	0.0474	-0.00282	-0.00658
Test B	-0.0336	-0.0644	-0.147	-0.10
Test B + dust	0.106	0.0604	-0.0272	-0.0225
New parameterization + dust following Freitag parameterization for the Pimienta – Barnola model	0.0915	0.0646	-0.00717	-0.0092

Supplementary Table S4: Results of the difference between the average of the Early Holocene (EH) and the average of the Last Glacial Maximum (LGM) for the sensitivity tests displayed on Figure 7 for the 4 sites described in the main text.

NGRIP	Δ age (old version)	Δ age (new version)	Δ age (new version + dust)	DATA
Bølling /Allerød	870 years	920 years	740 years	1040±100 years
End of Younger Dryas	760 years	820 years	640 years	800±100 years

Supplementary Table S5: Comparison of measured and modelled Δ age with different parameterizations of the model at two different points of the last deglaciation at NGRIP. The only way to compare Δ age model output with data is actually on the abrupt warming recorded very clearly both in the $\delta^{18}\text{O}$ in the ice phase and $\delta^{15}\text{N}$ in the gas phase on the NGRIP ice core because we have an accurate associated timescale (GICC05). The agreement between data and model is slightly better when using the new version but the addition of dust leads to a strong deterioration as observed on the $\delta^{15}\text{N}$ profiles.

NB: the uncertainty on the Δ age from the data is mainly linked to the resolution of the $\delta^{15}\text{N}$ signal.

1
2
3
4
5
6
7
8
9
10
11
12
13
14
15
16
17
18
19
20
21
22
23
24
25
26
27
28
29
30
31
32
33

Supplementary Text S1: Model input files and running conditions

For paleoclimate applications, we have one input file for each site. The file has 5 columns: depth, age, difference of temperature with respect to present-day surface temperature, accumulation rate and calcium concentration. Except for WAIS-D, the spatial resolution is constant from the top to the bottom of each ice core and varies between sites between 1 and 2 m. Such resolution is largely sufficient to depict the temporal variability of temperature and accumulation over the last deglaciation (the lowest temporal resolution is 200 years at Vostok for the LGM; at NGRIP, the temporal resolution corresponding to 1 m spatial resolution in the input file is about 50 years at LGM). For WAIS-D, the input files were designed so that the temporal resolution is constant to 10 years all along the ice core.

The model running conditions are very similar to those described in Goujon et al. (2003). For density calculation, the depth step is 0.25 m down to 150 m depth, 2.5 m depth down to 550 m depth and 25 m depth below. We only simplified the boundary between the 2.5 m and 25 m grids to guarantee that the change occurs at a grid node (Goujon et al. (2003) used a criterion based on the difference between pure ice density and the modelled density). Relative coordinates z/H (H being the ice thickness) are used for solving the ice sheet vertical velocity equation as in Goujon et al. (2003).

In this study, we modified the time step: Goujon et al. (2003) used a one year time step for all sites, whereas we adjusted the time step in link with the maximum accumulation rate in the input file. Indeed the accumulation rate defines the firn sinking speed. Stable results are obtained with a time step of $0.3/\max(Ac)$ where Ac is the accumulation rate in $m\ w.eq.yr^{-1}$. Thus our time step is shorter than one year only at very high accumulation rate sites ($Ac > 0.3m\ w.eq./yr$). Numerical tests showed that with the above depth and time grid, Eulerian and Lagrangian calculations of the density profiles lead to consistent results. However, for gas age calculations, a lagrangian tracking of firn layers is necessary to simulate the detailed shape of $\delta^{15}N$ anomalies during Dansgaard-Oeschger events in Greenland.

As in Goujon et al. (2003), a limitation of our model is that the ice sheet thickness and lower boundary condition do not vary with time. Two parameters are imposed at the boundary between the ice and bedrock: the temperature and vertical speed. Basal temperature is inferred from borehole measurements. If it is colder than the melting temperature estimated as a function of hydrostatic pressure (equation 8 in Goujon et al., 2008), the basal vertical speed is nul. Otherwise, the melting temperature is used and the basal vertical speed (melting rate) needs to be specified in input.

Supplementary Text S2:

34 The major discrepancies between our model results with dust and $\delta^{15}\text{N}$ data with dust occur outside the
35 range of calcium concentrations at modern sites. We hence illustrate here how the addition of simple
36 thresholds on a minimum and maximum effect of calcium can strongly reduce the main discrepancies
37 between our model results with dust and $\delta^{15}\text{N}$ data. We have thus adjusted the dust parameterization
38 proposed by Freitag with two threshold (Ca_{min} and Ca_{max}) such as:

- 39 - If $\text{Ca} < \text{Ca}_{\text{min}}$: use the Freitag parameterization with $\text{Ca} = \text{Ca}_{\text{min}}$
- 40 - If $\text{Ca} > \text{Ca}_{\text{max}}$: use the Freitag parameterization with $\text{Ca} = \text{Ca}_{\text{max}}$
- 41 - If $\text{Ca}_{\text{min}} < \text{Ca} < \text{Ca}_{\text{max}}$, use the original Freitag parameterization

42 In this study, we have chosen values of 2ng/g and 50ng/g for respectively Ca_{min} and Ca_{max} .

43 Implementing threshold values on calcium (blue lines on the Figure S10) reduces the largest inconsistencies
44 between model results and $\delta^{15}\text{N}$ data, in particular at NGRIP (through the threshold at high calcium
45 concentration) and at WAIS (through the threshold at low calcium concentration).

46

47 References

48

49 Arnaud, L., Lipenkov, V., Barnola, J.-M., Gay, M. and Duval, P.: Modelling of the densification of polar
50 firn: characterization of the snow-firn transition, in *Annals of Glaciology*, vol. 26, pp. 39–44., 1998.

51 Arnaud, L., Barnola, J. M. and Duval, P.: Physical modeling of the densification of snow/firn and ice
52 in, *Phys. Ice Ore Rec.*, 26, 39–44, 2000.

53 Bazin, L., Landais, A., Lemieux-Dudon, B., Toyé Mahamadou Kele, H., Veres, D., Parrenin, F.,
54 Martinerie, P., Ritz, C., Capron, E., Lipenkov, V., Loutre, M. F., Raynaud, D., Vinther, B. M., Svensson,
55 A., Rasmussen, S. O., Severi, M., Blunier, T., Leuenberger, M., Fisher, H., Masson-Delmotte, V.,
56 Chappellaz, J. and Wolff, E.: An optimized multi-proxy, multi-site Antarctic ice and gas orbital
57 chronology (AICC2012): 120-800 ka, *Clim. Past*, 9(4), 1715–1731, 2013.

58 Buiron, D., Chappellaz, J., Stenni, B., Frezzotti, M., Baumgartner, M., Capron, E., Landais, A., Lemieux-
59 Dudon, B., Masson-Delmotte, V., Montagnat, M., Parrenin, F. and Schilt, A.: TALDICE-1 age scale of
60 the Talos Dome deep ice core, East Antarctica, *Clim. Past*, 7(1), 1–16, doi:10.5194/cp-7-1-2011,
61 2011.

62 Buizert, C., Martinerie, P., Petrenko, V. V., Severinghaus, J. P., Trudinger, C. M., Witrant, E., Rosen,
63 J. L., Orsi, A. J., Rubino, M., Etheridge, D. M., Steele, L. P., Hogan, C., Laube, J. C., Sturges, W. T.,
64 Levchenko, V. A., Smith, A. M., Levin, I., Conway, T. J., Dlugokencky, E. J., Lang, P. M., Kawamura, K.,
65 Jenk, T. M., White, J. W. C., Sowers, T., Schwander, J. and Blunier, T.: Gas transport in firn: multiple-
66 tracer characterisation and model intercomparison for NEEM, Northern Greenland, *Atmospheric*
67 *Chem. Phys.*, 12(9), 4259–4277, doi:10.5194/acp-12-4259-2012, 2012.

68 Buizert, C., Cuffey, K. M., Severinghaus, J. P., Baggenstos, D., Fudge, T. J., Steig, E. J., Markle, B. R.,
69 Winstrup, M., Rhodes, R. H., Brook, E. J., Sowers, T. A., Clow, G. D., Cheng, H., Edwards, R. L., Sigl,
70 M., McConnell, J. R. and Taylor, K. C.: The WAIS Divide deep ice core WD2014 chronology-Part 1:
71 Methane synchronization (68–31 ka BP) and the gas age–ice age difference, *Clim. Past*, 11(2), 153–
72 173, doi:10.5194/cp-11-153-2015, 2015.

73 Butler, J. H., Battle, M., Bender, M. L., Montzka, S. A., Clarke, A. D., Saltzman, E. S., Sucher, C. M.,
74 Severinghaus, J. P. and Elkins, J. W.: A record of atmospheric halocarbons during the twentieth
75 century from polar firn air, *Nature*, 399(6738), 749–755, 1999.

76 Capron, E., Landais, A., Buiron, D., Cauquoin, A., Chappellaz, J., Debret, M., Jouzel, J., Leuenberger,
77 M., Martinerie, P., Masson-Delmotte, V., Mulvaney, R., Parrenin, F. and Prié, F.: Glacial–interglacial
78 dynamics of Antarctic firn columns: comparison between simulations and ice core air- $\delta^{15}\text{N}$
79 measurements, *Clim. Past*, 9(3), 983–999, doi:10.5194/cp-9-983-2013, 2013.

80 Clausen, H. B., Gundestrup, N. S., Johnsen, S. J., Bindshadler, R. and Zwally, J.: Glaciological
81 investigations in the Crete area, central Greenland: A search for a new deep-drilling site, *Ann Glaciol*,
82 10, 10–15, 1988.

83 Cole-Dai, J., Ferris, D. G., Lanciki, A. L., Savarino, J., Thiemens, M. H. and McConnell, J. R.: Two likely
84 stratospheric volcanic eruptions in the 1450s CE found in a bipolar, subannually dated 800 year ice
85 core record, *J. Geophys. Res. Atmospheres*, 118(14), 7459–7466, 2013.

- 86 Cuffey, K. M. and Clow, G. D.: Temperature, accumulation, and ice sheet elevation in central
87 Greenland through the last deglacial transition, *J. Geophys. Res. Oceans*, 102(C12), 26383–26396,
88 1997.
- 89 Cuffey, K. M. and Vimeux, F.: Covariation of carbon dioxide and temperature from the Vostok ice
90 core after deuterium-excess correction, *Nature*, 523–526, 2001.
- 91 De Angelis, M., Steffensen, J. P., Legrand, M., Clausen, H. and Hammer, C.: Primary aerosol (sea salt
92 and soil dust) deposited in Greenland ice during the last climatic cycle: Comparison with east
93 Antarctic records, *J. Geophys. Res. Oceans*, 102(C12), 26681–26698, 1997.
- 94 Ding, M., Xiao, C., Yang, Y., Wang, Y., Li, C., Yuan, N., Shi, G., Sun, W. and Ming, J., “Re-assessment
95 of recent (2008 2013) surface mass balance over Dome Argus, Antarctica,” vol. 1, no. 2008 2013,
96 pp. 1–8, 2016.
- 97 Etheridge, D. M. and Wooley, C. W.: Ice core drilling at a high accumulation area of Law Dome,
98 Antarctica. 1987, *Ice Core Drill.*, 10–14, 1988.
- 99 Ferris, D. G., Cole-Dai, J., Reyes, A. R. and Budner, D. M.: South Pole ice core record of explosive
100 volcanic eruptions in the first and second millennia A.D. and evidence of a large eruption in the
101 tropics around 535 A.D., *J. Geophys. Res.*, 116(D17), doi:10.1029/2011JD015916, 2011.
- 102 Fischer, H., Fundel, F., Ruth, U., Twarloh, B., Wegner, A., Udisti, R., Becagli, S., Castellano, E.,
103 Morganti, A., Severi, M., Wolff, E., Littot, G., Röthlisberger, R., Mulvaney, R., Hutterli, M. A.,
104 Kaufmann, P., Federer, U., Lambert, F., Bigler, M., Hansson, M., Jonsell, U., de Angelis, M., Boutron,
105 C., Siggaard-Andersen, M.-L., Steffensen, J. P., Barbante, C., Gaspari, V., Gabrielli, P. and Wagenbach,
106 D.: Reconstruction of millennial changes in dust emission, transport and regional sea ice coverage
107 using the deep EPICA ice cores from the Atlantic and Indian Ocean sector of Antarctica, *Earth Planet.*
108 *Sci. Lett.*, 260(1–2), 340–354, doi:10.1016/j.epsl.2007.06.014, 2007.
- 109 Fitzpatrick, J. J., Voigt, D. E., Fegyveresi, J. M., Stevens, N. T., Spencer, M. K., Cole-Dai, J., Alley, R. B.,
110 Jardine, G. E., Cravens, E. D., Wilen, L. A., Fudge, T. J. and McConnell, J. R.: Physical properties of the
111 WAIS Divide ice core, *J. Glaciol.*, 60(224), 1181–1198, doi:10.3189/2014JoG14J100, 2014.
- 112 Freitag, J., Kipfstuhl, S., Laepple, T. and Wilhelms, F.: Impurity-controlled densification: a new model
113 for stratified polar firn, *J. Glaciol.*, 59(218), 1163–1169, doi:10.3189/2013JoG13J042, 2013.
- 114 Fudge, T. J., Markle, B. R., Cuffey, K. M., Buizert, C., Taylor, K. C., Steig, E. J., Waddington, E. D.,
115 Conway, H. and Koutnik, M.: Variable relationship between accumulation and temperature in West
116 Antarctica for the past 31,000 years: wdc temperature and accumulation, *Geophys. Res. Lett.*, 43(8),
117 3795–3803, doi:10.1002/2016GL068356, 2016.
- 118 Gautier, E., Savarino, J., Erbland, J., Lanciki, A. and Possenti, P.: Variability of sulfate signal in ice core
119 records based on five replicate cores, *Clim. Past*, 12(1), 103–113, doi:10.5194/cp-12-103-2016,
120 2016.
- 121 Gfeller, G., Fischer, H., Bigler, M., Schüpbach, S., Leuenberger, D. and Mini, O.: Representativeness
122 and seasonality of major ion records derived from NEEM firn cores, *The Cryosphere*, 8(5), 1855–
123 1870, doi:10.5194/tc-8-1855-2014, 2014.

- 124 Goujon, C., Barnola, J.-M. and Ritz, C.: Modeling the densification of polar firn including heat
125 diffusion: Application to close-off characteristics and gas isotopic fractionation for Antarctica and
126 Greenland sites, *J. Geophys. Res. Atmospheres*, 108(D24), 2003.
- 127 Gow, A. J.: Deep core studies of the accumulation and densification of snow at Byrd station and
128 Little America V, Antarctica, CRREL., 1968.
- 129 Hörhold, M. W., Kipfstuhl, S., Wilhelms, F., Freitag, J. and Frenzel, A.: The densification of layered
130 polar firn, *J. Geophys. Res. Earth Surf.*, 116(F1), 2011.
- 131 Iizuka, Y., Horikawa, S., Sakurai, T., Johnson, S., Dahl-Jensen, D., Steffensen, J. P. and Hondoh, T.: A
132 relationship between ion balance and the chemical compounds of salt inclusions found in the
133 Greenland Ice Core Project and Dome Fuji ice cores, *J. Geophys. Res.*, 113(D7),
134 doi:10.1029/2007JD009018, 2008.
- 135 Jones, T. R., White, J. W. C. and Popp, T.: Siple Dome shallow ice cores: a study in coastal dome
136 microclimatology, *Clim. Past*, 10(3), 1253–1267, doi:10.5194/cp-10-1253-2014, 2014.
- 137 Kindler, P., Guillevic, M., Baumgartner, M., Schwander, J., Landais, A., Leuenberger, M., Spahni, R.,
138 Capron, E. and Chappellaz, J.: Temperature reconstruction from 10 to 120 kyr b2k from the NGRIP
139 ice core, *Clim. Past*, 10(2), 887–902, doi:10.5194/cp-10-887-2014, 2014.
- 140 Kipfstuhl, S., Faria, S. H., Azuma, N., Freitag, J., Hamann, I., Kaufmann, P., Miller, H., Weiler, K. and
141 Wilhelms, F.: Evidence of dynamic recrystallization in polar firn, *J. Geophys. Res.*, 114(B5),
142 doi:10.1029/2008JB005583, 2009.
- 143 Kreutz, K. J., Mayewski, P. A., Twickler, M. S., Whitlow, S. I., White, J. W. C., Shuman, C. A., Raymond,
144 C. F., Conway, H. and McConnell, J. R.: Seasonal variations of glaciochemical, isotopic and
145 stratigraphic properties in Siple Dome (Antarctica) surface snow, *Ann. Glaciol.*, 29(1), 38–44, 1999.
- 146 Kreutz, K. J., Mayewski, P. A., Meeker, L. D., Twickler, M. S. and Whitlow, S. I.: The effect of spatial
147 and temporal accumulation rate variability in West Antarctica on soluble ion deposition, *Geophys.*
148 *Res. Lett.*, 27(16), 2517, 2000.
- 149 Lambert, F., Bigler, M., Steffensen, J. P., Hutterli, M. and Fischer, H.: Centennial mineral dust
150 variability in high-resolution ice core data from Dome C, Antarctica, *Clim. Past*, 8(2), 609–623,
151 doi:10.5194/cp-8-609-2012, 2012.
- 152 Langway, C. C. J.: Stratigraphic analysis of a deep ice core from Greenland, CRREL Res. Rep. 77, pp
153 130, 1967.
- 154 Leduc-Leballeur, M., Picard, G., Mialon, A., Arnaud, L., Lefebvre, E., Possenti, P. and Kerr, Y.:
155 Modeling L-band brightness temperature at Dome C in Antarctica and comparison with SMOS
156 observations, *IEEE Trans. Geosci. Remote Sens.*, 53(7), 4022–4032, 2015.
- 157 Legrand, M. R., Lorius, C., Barkov, N. I. and Petrov, V. N.: Vostok (Antarctica) ice core: atmospheric
158 chemistry changes over the last climatic cycle (160,000 years), *Atmospheric Environ.* 1967, 22(2),
159 317–331, 1988.
- 160 Mosley-Thompson, E., Thompson, L. G., Paskievitch, J. F., Pourchet, M., Gow, A. J., Davis, M. E. and
161 Kleinman, J.: Recent increase in South Pole snow accumulation, *Ann. Glaciol.*, 21(1), 131–138, 1995.

- 162 Narita, H. and Maeno, N.: II. Compiled Density Data from Cores Drilled at Mizuho Station (Appendix:
163 Miscellaneous Compiled Data), Mem. Natl. Inst. Polar Res. Spec. Issue, 10, 136–158, 1978.
- 164 Ngrip community members: High-resolution record of Northern Hemisphere climate extending into
165 the last interglacial period, *Nature*, 431(7005), 147–151, 2004.
- 166 Nishio, F., Fuji, Y. and Kusunoki, K.: Measured and computed temperature profiles at Mizuho station,
167 East Antarctica, *Sea Level Lee Clim. Change*, 239–246, 1979.
- 168 Oerter, H., Graf, W., Meyer, H. and Wilhelms, F.: The EPICA ice core from Dronning Maud Land: first
169 results from stable-isotope measurements, *Ann. Glaciol.*, 39(1), 307–312, 2004.
- 170 Robin, G. de Q.: Profile data, Greenland region, *Clim. Rec. Polar Ice Sheets Camb. Univ. Press Camb.*,
171 98–111, 1983.
- 172 Salamatin, A. N., Lipenkov, V. Y., Barnola, J. M., Hori, A., Duval, P. and Hondoh, T.: Snow/firn
173 densification in polar ice sheets, *Phys. Ice Core Rec. - II*, 68(Supplement), 195–222, 2009.
- 174 Schüpbach, S., Federer, U., Kaufmann, P. R., Albani, S., Barbante, C., Stocker, T. F. and Fischer, H.:
175 High-resolution mineral dust and sea ice proxy records from the Talos Dome ice core, *Clim. Past*,
176 9(6), 2789–2807, doi:10.5194/cp-9-2789-2013, 2013.
- 177 Schwander, J., Sowers, T., Barnola, J.-M., Blunier, T., Fuchs, A. and Malaizé, B.: Age scale of the air
178 in the summit ice: Implication for glacial-interglacial temperature change, *J. Geophys. Res.*
179 *Atmospheres*, 102(D16), 19483–19493, 1997.
- 180 Seierstad, I. K., Abbott, P. M., Bigler, M., Blunier, T., Bourne, A. J., Brook, E., Buchardt, S. L., Buizert,
181 C., Clausen, H. B., Cook, E., Dahl-Jensen, D., Davies, S. M., Guillevic, M., Johnsen, S. J., Pedersen, D.
182 S., Popp, T. J., Rasmussen, S. O., Severinghaus, J. P., Svensson, A. and Vinther, B. M.: Consistently
183 dated records from the Greenland GRIP, GISP2 and NGRIP ice cores for the past 104 ka reveal
184 regional millennial-scale $\delta^{18}O$ gradients with possible Heinrich event imprint, *Quat. Sci. Rev.*, 106,
185 29–46, doi:10.1016/j.quascirev.2014.10.032, 2014.
- 186 Shugui, H., Yuansheng, H., Cunde, X. L.Y. and Jiawen, R. E. N., “Recent accumulation rate at Dome A
187 , Antarctica,” vol. 52, no. 40576001, 2007.
- 188 Spencer, M. K., Alley, R. B. and Creyts, T. T.: Preliminary firn-densification model with 38-site dataset,
189 *J. Glaciol.*, 47(159), 671–676, 2001.
- 190 Steen-Larsen, H. C., Masson-Delmotte, V., Sjolte, J., Johnsen, S. J., Vinther, B. M., Bréon, F.-M.,
191 Clausen, H. B., Dahl-Jensen, D., Falourd, S., Fettweis, X., Gallée, H., Jouzel, J., Kageyama, M., Lerche,
192 H., Minster, B., Picard, G., Punge, H. J., Risi, C., Salas, D., Schwander, J., Steffen, K., Sveinbjörnsdóttir,
193 A. E., Svensson, A. and White, J.: Understanding the climatic signal in the water stable isotope
194 records from the NEEM shallow firn/ice cores in northwest Greenland, *J. Geophys. Res.*, 116(D6),
195 doi:10.1029/2010JD014311, 2011.
- 196 Stenni, B., Proposito, M., Gragnani, R., Flora, O., Jouzel, J., Falourd, S. and Frezzotti, M.: Eight
197 centuries of volcanic signal and climate change at Talos Dome (East Antarctica), *J. Geophys. Res.*
198 *Atmospheres*, 107(D9), 2002.
- 199 Stenni, B., Masson-Delmotte, V., Selmo, E., Oerter, H., Meyer, H., Röthlisberger, R., Jouzel, J.,
200 Cattani, O., Falourd, S., Fischer, H., Hoffmann, G., Iacumin, P., Johnsen, S. J., Minster, B. and Udisti,

- 201 R.: The deuterium excess records of EPICA Dome C and Dronning Maud Land ice cores (East
202 Antarctica), *Quat. Sci. Rev.*, 29(1–2), 146–159, doi:10.1016/j.quascirev.2009.10.009, 2010.
- 203 WAIS Divide Project Members: Onset of deglacial warming in West Antarctica driven by local orbital
204 forcing, *Nature*, 500(7463), 440–444, doi:10.1038/nature12376, 2013.
- 205 Witrant, E., Martinerie, P., Hogan, C., Laube, J. C., Kawamura, K., Capron, E., Montzka, S. A.,
206 Dlugokencky, E. J., Etheridge, D., Blunier, T. and Sturges, W. T.: A new multi-gas constrained model
207 of trace gas non-homogeneous transport in firn: evaluation and behaviour at eleven polar sites,
208 *Atmospheric Chem. Phys.*, 12(23), 11465–11483, doi:10.5194/acp-12-11465-2012, 2012.
- 209 Xiao, C., I. Allison, Y. Li, Hou, S., Dreyfus, G. B., Barnola, J.-M., Jiawen, R. E. N., Lingen, B., Shenkai, Z.,
210 and Kameda, T., “Surface characteristics at Dome A, Antarctica: first measurements and a guide to
211 future ice-coring sites,” *Ann. Glaciol.*, pp. 82–87, 2008.
- 212

